# PATH-LOSS PREDICTION MODELS FOR CELLULAR NETWORKS IN OKENE, KOGI STATE, NIGERIA

**BY**

**ONIPE, John Asuva**

**MEng/SEET/2017/7497**

**DEPARTMENT OF TELECOMMUNICATION ENGINEERING,**

**SCHOOL OF ELECTRICAL ENGINEERING AND TECHNOLOGY,**

**FEDERAL UNIVERSITY OF TECHNOLOGY,**

**MINNA**

**JULY, 2021**

# ABSTRACT

Signal path-loss in Radio communication results in low signal power at the receiver antenna of telecommunication systems. It drastically affects network performance negatively. Path-loss is found to be very high in mountainous environments such as Okene in Kogi State, Nigeria, which is the case study of this research. The result is poor network service despite the fair distribution of network infrastructure. A suitable and accurate path-loss model to predict the path-loss of this environment is necessary to enable network operators make plans for network optimization by deciding the appropriate capacity of equipment, suitable base transceiver station location and efficient network coverage design. The method of modeling in this research is the modification of selected path-loss models which have history of adaptability to various environments and frequencies. The models selected are the Free Space model, the COST-231 model, the Hata model, the Egli model and the ECC-33 model. The predictions by these models were compared with the measured path-loss in three environments – urban Okene central area, suburban Okengwe area and Rural Agasa/Upogoro area. The networks used are 3G UMTS and 2G EDGE of 9mobile, MTN, Glo and Airtel. The average root mean square errors (RMSE) of the predicted path-loss were used to modify the selected models. New path-loss predictions were made using the modified models. The modified models that gave the least average RMSE were selected as the optimal models for that environment at that frequency. The result of the study showed that the optimal models for the urban and suburban environments were developed from COST-231 model for 2G and 3G while optimal models for the rural environment were developed from the Hata model. The average RMSE of the optimal models were 9.39dBm for 3G and 12.88dBm for 2G Networks in the urban area, 11.28dBm for 3G and 11.60dBm for 2G Networks in the suburban area and 10.34dBm for 2G Network in the rural area. However, for 3G in the rural environment, the original Hata model maintained the least average RMSE of 10.02dBm after the modifications process. Hence, no new model was developed for 3G network in the rural area. The optimized models showed various percentages of improvement over the reference models. The range of deviations acceptable for suitability of a model is 0 to 12dBm. The signal power received from the field measurement confirmed that the high signal path-loss was caused by the mountainous terrain. These optimized models are recommended for network operators as a guide to making decisions on network optimization in Okene mountainous area and for planning to upgrade to 4G.

# TABLE OF CONTENTS

**CONTENTS** **PAGE**


**DECLARATION** i

**CERTIFICATION** ii

**ACKNOWLDGEMENT** iii

**ABSTRACT** v

**TABLE OF CONTENTS** vi

**LIST OF TABLES** ix

**LIST OF FIGURES** x

**CHAPTER ONE** 1

**1.0 INTRODUCTION** 1

1.1 Background to the Study 1

1.2 Research Motivation 6

1.3 Statement of the Research Problem 6

1.4 Aim 7

1.5 Objectives 7

1.6 Justification of the Research 7

1.7 Significance of the Research 8

1.8 Organization of Thesis 9

**CHAPTER TWO** 10

**2.0 LITERATURE REVIEW** 10

2.1 Basic Propagation Mechanisms 10

2.2 Path-loss in Radio Signal Propagation 11

2.3 Free Space Loss 15

2.4 Radio Link Budget 16

2.5 Radio Frequency Path-loss Models 17

2.5.1 Durkin's Model 18

2.5.2 Okumura Model 19

2.5.3 Hata Model 21

2.5.4 COST-231 (Extension to Hata) Model 22

2.5.5 Walfisch Model (also known as Walfisch-Bertoni or Walfisch-Ikegami Model) 22

2.5.6 ECC-33 Model (Electronic Communication Committee) 23

2.5.7 Egli Model 24

2.6 Review of Related Works 24

CHAPTER THREE 28
3.0 RESEARCH METHODOLOGY 28
3.1 RESEARCH PROCEDURE 28
3.2 Description of Investigated Area and Network 30
3.1.1 Selected Environments 32
3.1.2 Selected Networks 32
3.2 Materials and Tools 33
3.2.1 Network Analyzer software: 33
3.2.2 GPS measurement software: Virtual Maze GPS tool 34
3.3 Measurement 35
3.4 Transmitter-Receiver distance calculation 36
3.5 Presentation of Results 37
3.6 Data Analysis 46
3.7 RMSE of Calculated Path-loss 48
CHAPTER FOUR 49
4.0 RESULTS AND DISCUSSION 49
4.1 Measured Received Signal Strength Indicator (RSSI) 49
4.1.1 3G RSSI Variation in the Urban environment 49
4.1.2 3G RSSI Variation in the Suburban environment 50
4.1.3 3G RSSI Variation in the Rural environment 51
4.1.4 2G RSSI Variation in the Urban environment 52
4.1.5 2G RSSI Variation in the Suburban environment 53
4.1.6 2G RSSI Variation in the Rural environment 54
4.2 Measured and Calculated Path-loss 55
4.2.1 3G Networks Signal Path-loss in the Urban Area 55
4.2.2 3G Networks Signal Path-loss in the Suburban Area 57
4.2.3 3G Networks Signal Path-loss in the Rural Area 59
4.2.4 2G Networks Signal Path-loss in the Urban Area 61
4.2.5 2G Networks Signal Path-loss in the Suburban Area 63
4.2.6 2G Networks Signal Path-loss in the Rural Area 65
4.3 Validation of Calculated Path-loss/RMSE Values 67
4.3.1 RMSE Values of Path Loss Models for Urban Environment 67
4.3.2 RMSE Values of Path Loss Models for Suburban Environment 69
4.3.3 RMSE Values of Path Loss Models for Rural Environment 70
4.3.4 Summary of average RMSE Values for all Environments 71
4.4 Modeling 71
4.4.1 The Modification Process 72
4.4.2 Modification Results 73

4.4.3 Path-loss Model Optimization for 3G 2100MHz: 73
4.4.4 Path-loss Model Optimization for 2G (1800MHz) 76
4.5 Summary of Optimized Path-loss models: 79
4.6 Performance evaluation 80
4.6.1. Urban environment Optimized model performance 81
4.6.2 Suburban environment optimal models performance 82
4.6.3 Rural environment optimal model performance 83
4.6.4 Performance evaluation summary 84
4.7 Findings 85
**CHAPTER FIVE** **Error! Bookmark not defined.**
**5.0 CONCLUSION AND RECOMMENDATIONS Error! Bookmark not defined.**
5.1 Conclusion **Error! Bookmark not defined.**
5.2 Recommendations **Error! Bookmark not defined.**
**REFERENCES** 86
**APPENDICES** 92

# LIST OF TABLES

**Table** **Page**


3.1 Selected Areas Investigated ... 32
3.2 Average RSSI(dBm) of 3G Networks in Okene Central Urban Area ... 38
3.3 Average RSSI(dBm) of 2G Networks in Okene Central Urban Area ... 39
3.4 Average RSSI (dBm) of 3G Networks in Okengwe Suburban Environment ... 41
3.5 Average RSSI (dBm) of 2G Networks in Okengwe Suburban Environment ... 42
3.6 Average RSSI (dBm) of 3G Networks in Agasa/Upogoro Rural Environment ... 44
3.7 Average RSSI (dBm) of 2G Networks in Agasa/Upogoro Rural Environment ... 45
3.8 Network Parameters Used ... 45
4.1 RMSE Values of Path Loss Models for 3G Networks Urban Environment ... 68
4.2 RMSE Values of Path Loss Models for 2G Networks in Urban Environment ... 68
4.3 RMSE Values of Path Loss Models for 3G Networks Suburban Environment ... 69
4.4 RMSE Values of Path Loss Models for 2G Networks in Suburban Environment ... 69
4.5 RMSE Values of Path Loss Models for 3G Networks in Rural Environment ... 70
4.6 RMSE Values of Path Loss Models for 2G Networks in Rural Environment ... 70
4.7 Average RMSE for 3G Network ... 71
4.8 Average RMSE for 2G Networks ... 71
4.9 Percentage Improvement of the Optimal Models over the Reference Models ... 85

# LIST OF FIGURES


**Figure** **Page**

2.1 Path Loss in a Wireless Communication System....................11
2.2 Multipath Propagation....................13
2.3 Median Attenuation Relative to Free Space (*Amu*(*f,d*))....................21
3.1 Research Procedure....................28
3.2 Okene Hilly Terrain Map....................31
3.3 A Landscape Picture of Okengwe in Okene, Kogi State Nigeria....................31
3.4 Screenshots of Cellmapper and Network Cell Info Lite....................34
3.5 Virtual Maze GPS tool....................35
3.6 Drive Test Routes in Okene Central Urban Environment....................37
3.7 Drive Test Routes in Okengwe Suburban Environment....................40
3.8 Drive Test Routes in Agasa/Upogoro Rural Environment....................43
4.1 RSSI Variation with Distance for 3G UMTS in the Urban Area....................49
4.2 RSSI Variation with Distance for 3G UMTS in the Suburban Area....................50
4.3 RSSI Variation with Distance for 3G UMTS in the Rural Area....................51
4.4 RSSI Variation with Distance for 2G EDGE in the Urban Area....................52
4.5 RSSI Variation with Distance for 2G EDGE in the Suburban Area....................53
4.6 RSSI Variation with Distance for 2G EDGE in the Rural Area....................54
4.7 Measured and Calculated Path-loss for 3G Networks in the Urban Area....................56
4.8 Measured and Calculated Path-loss for 3G Network in the Suburban Area....................58
4.9 Measured and Calculated Path-loss for 3G Networks in the Rural Area....................60
4.10 Measured and Calculated Path-loss for 2G Networks in the Urban Area....................62
4.11 Measured and Calculated Path-loss for 2G Networks in the Suburban Area....................64
4.12 Measured and Calculated Path-loss for 2G Network in the Rural Area....................66
4.13 Urban 3G UMTS Model RMSE....................74
4.14 Suburban 3G UMTS Model RMSE....................75
4.15 Rural 3G UMTS Model RMSE....................76
4.16 Urban 2G UMTS Model RMSE....................77
4.17 Suburban 2G UMTS Model RMSE....................78
4.18 Rural 2G UMTS Model RMSE....................79
4.19 Optimized Model Compared with Reference Models for Urban Area....................81
4.20 Optimal Models Compared with Reference Models for Suburban Area....................82
4.21 Optimal Models Compared with Reference Models for Rural Area....................84

# CHAPTER ONE

## 1.0 INTRODUCTION

### 1.1 Background to the Study

Wireless communication refers to the transmission of information from one point to another without material medium between the source and the destination. This implies that the medium of transfer is the air or space. It has evolved over the years from analogue (voice, texts, images, and videos) to digital (data) communication. Wireless communication, in this age, has proved to be a universal solution to almost every known world problem relating to individuals, corporate bodies and the government. Every area of human existence is impacted positively by wireless transfer of information - voice and data – from one point to the other (Elechi and Otasowie, 2016). Under the regulation of the Nigerian Communication Commission (NCC), several wireless communication network providers rolled out voice and data transfer services with effective service for customer satisfaction as a major aim (Musefiu *et al.*, 2017). Unfortunately, the process of transmitting the voice and data signals from the network providers' base transceiver station (BTS) to the mobile receivers of the subscribers is characterized by signal power impairment at the air interface between the transmitting antenna and the receiving antenna (Segun I. Popoola *et al.*, 2018). These impairments cause signal propagation path-loss which grossly undermine the efficiency of the operators to provide satisfactory services. Path-loss is the degradation of or reduction in the power of the transmitted signal as it travels within the air interface from the transmitting antenna to the receiving antenna over a specified distance (Abiodun *et al.*, 2017). The determination of path-loss using some mathematical models is important to the network service providers while planning to set up the service in a new environment or optimizing an existing service (Imoize and Oseni, 2019).

Regular radio frequency planning and management are required to ensure continuous optimal performance of mobile telecommunication services provided for subscribers within an area. It is necessitated by the need to always maintain effectiveness and efficiency in the supply of mobile telecommunication services of voice and data (Onuu and Usanga, 2017). Usually, the quality of service is estimated from the link budget which is used to predict the received signal power from the transmitted signal power and the gains and losses from the transmitter to the receiver (Popoola *et al.*, 2017). The losses along the transmission path (or path-loss) greatly affect the quality of service. Hence it becomes very important to determine the path-loss from time to time and optimize the system when and where necessary. Path-loss models, which are mathematical representations of the path loss, are normally developed for this purpose (Worgu *et al.*, 2017).

Several efforts have been made over the years of wireless communication and are still being made, especially in mobile systems, to develop models that can be used to evaluate the path-loss in different types of environments at various frequencies (Akujobi *et al*, 2016). Existing popular path-loss models include the Longley-rice model, Okumura model, Hata model, Egli model, ECC-33 model and COST-231 (Extended Hata) model (Hoomod *et al.*, 2018). Each of the models has its limitations such that it may not be applicable in every environment and for every transmit antenna height and range of frequency (Rappaport, 2005).

Path-loss models and link budget required for effective radio frequency planning are site-specific. Site-specific models are path-loss models designed for a particular environment or geographical environment to accurately predict the path-loss behavior of that environment (Imoize and Oseni, 2019). When a model is designed using data from a particular environment, the model will perform well for that area. The prediction of that same model in another area will be poorer than its prediction in the area of origin. Generalized path-loss models usually do not accurately capture the path-loss behavior for every area under consideration without some modification or adjustment. This is because of differences in the quality and quantity of the various factors that affect the losses in radio signal propagation in different areas (Worgu *et al*., 2017). Such factors include weather, topography, terrain, buildings, geographical distribution (or demography) and population size. Two places with similar terrain may not be modeled equally by a general model developed for that terrain because one could be an urban area while the other is a rural area. Hence, for the same network type (1800MHz EDGE, 2100MHz UMTS) for instance, the model that correctly predicts the path-loss for a city with its characteristic tall buildings and heavy traffic and population may not accurately predict the path-loss of a rural area with low population and low traffic.

The Nigerian Communication Commission is saddled with the responsibility of regulating the operation of telecommunication services in the Country and has made certain standards of best practices available which the service providers need to comply with for satisfactory service delivery (Musefiu *et al*., 2017). Such standards along with various radio frequency propagation models must be properly understood and explored for an environment under consideration for propagation path-loss modeling and network coverage design. Factors that come under consideration in addition to mobile radio environment impairment elements of reflection, diffraction and scattering include topography, population density, and vegetation, building types, rainfall and town planning (Tarkaa *et al*., 2017).

The popularity and spread of mobile communication began with the advent of the Global System for Mobile communications (GSM) technology which is the second-generation (2G) of global digital communication standard (Okoro and Iwuji, 2019). It marks the advent of digital cellular networks. It operates in the 900 MHz frequency band. According to Tarkaa *et al*. (2017), GSM expanded over time to 2.5G General Packet Radio Service (GPRS), and later to 2.75G Enhanced Data for GSM Evolution (EDGE 1800MHz) data communications. Subsequently, the Third-Generation Partnership Project (3GPP) developed the third-generation (3G) 2100MHz Universal Mobile Telecommunication System (UMTS) standards, followed by 4G Long Term Evolution Advanced (LTE-A) standards (Ebhota *et al.*, 2018). According to Bakare *et al.* (2017), the GSM system was introduced into the Nigerian market and society precisely on 6th August, 2001.

When the GSM network was initially introduced in Okene area of Kogi State by MTN in 2002, few numbers of base stations were scantily deployed and located on top of hills. The reception was good in some areas but very poor in some others as a result of the irregular hilly terrain (Omorogiuwa and Edeko, 2009). With the deregulation in the mobile communication industry, more network providers also deployed their infrastructure. The reception improved a little. The strength of mobile radio signal received by users in the area depends on the location of the receiver and the base transceiver station (BTS) relative to the hills and mountains (Lee and Park, 2018). Path-loss models for this area are, therefore, needed to enable network providers study the signal losses caused majorly by the irregular terrain and discover the need for network optimization to get network services to the parts that are obstructed by the hills and rocks.

This work was carried out by taking network signal measurements in three areas to represent the three different environments (urban, suburban and rural) in Okene land. According to Dijkstra *et al.*, (2019), urban environments refer to high population areas (typically 1000 per $km^2$) used both as offices and residences. They have all the resources needed by the outlying suburban and rural areas. Suburban areas have less population than urban and are majorly used as residences. They are usually the surrounding areas of the urban and have limited resources. The rural environment is an area with a smaller population compared to the suburban. It is also described as an open area where the inhabitants' means of livelihood is dependent on the natural resources of the land such as farming and fishery. They depend on the resources and amenities made available in the urban areas. These three environments – urban, suburban and rural – are always present within a large area (Ebhota *et al.*, 2018). Locally, we refer to rural areas as villages, suburban areas as small towns and urban areas as large towns, cities or metropolises.

The urban environment in this research is represented by Okene Central area which describes the part of the land that is relatively flat and has the urban features of being a commercial and administrative centre and a Local Government headquarter.

The suburban environment selected is Okengwe which is a typical small residential town outlying the Local Government headquarters.

The rural environment selected for investigation is Agasa/Upogoro area which represents the areas with less population and little or no amenities.

Generally all the selected areas are characterized by series of mountains and valleys close to one another.

As at the time of this research, the Network providers whose services are available in Okene area are the 9mobile, MTN, Glo, and Airtel. The network types are the 2G 1800MHz EDGE and the 3G 2100MHz UMTS. The 2G 900MHz GSM has almost been phased out. The two network types for the four service providers are considered in the modeling process to obtain generalized models for each environment based on data from the four networks.

## 1.2 Research Motivation

Radio frequency planning and management need to be carried out quite often in any particular area to sustain the provision of high quality mobile network services. Path-loss models required for effective radio frequency planning are site-specific, implying that the suitable path-loss model can be developed using only the signal strength measurements taken from that particular site (location). This is because the path-loss in two areas having similar environmental descriptions may not be accurately predicted by a generalized model. There are variations in quality and quantity of the various factors responsible for the signal power losses experienced by radio waves in different areas. The need to develop a site-specific path-loss model, using measured data from Okene area, to more accurately predict, evaluate and consequently improve network service performance in Okene area, is the motivation for this research. Also, there is no known published literature to indicate that the path-loss of Okene area has been developed in recent times.

## 1.3 Statement of the Research Problem

There are several path-loss prediction models in literature for urban, suburban and rural environments developed for various places (Akujobi *et al.*, 2016; Ebhota *et al.*, 2018; Okoro and Iwuji, 2019; Shoewu *et al.*, 2016). However, mobile network services performance in many areas of Okene in Kogi State, Nigeria, is relatively poor despite the fair spread of base stations belonging to MTN, Airtel, Globacom, and 9mobile network service providers. It is observed that a mobile station just a few metres away from a base station in some directions could experience very low or almost zero signal power reception. This has been a serious problem to date since there are no known specific solutions designed for these areas. Therefore, it becomes necessary to develop path-loss prediction models for this area which could guide the network providers in re-planning their networks for optimal performance.

## 1.4 Aim

This research aims to develop path-loss prediction models for cellular networks in Okene area of Kogi State, Nigeria.

## 1.5 Objectives

The objectives of this research are to:

i. Obtain geographical location of base stations locations and technical data in order to determine the RSS for the various networks;

ii. Develop the optimal pathloss models on the basis of (i);

iii. Validate the optimal models by evaluating their performances in comparison with Free Space, Hata, COST-231, Egli and ECC-33 models using linear regression metrics.

## 1.6 Justification of the Research

After some years, the RF propagation path-loss behavior of an environment changes, at least slightly, as environmental variables change. This explains why path-loss modeling needs to be a regular exercise. The available published research in Okene area that is similar to this work was carried out far back in 2007-2008 by Omorogiuwa and Edeko (2009), who modeled the received power at 1800MHz in mountainous terrain. This work is based on the two currently available network types (EDGE 1800MHz and UMTS 2100MHz). The services provided by all the available networks (9mobile, MTN, Globacom, and Airtel) are considered in this study as compared with only MTN Network used by Omorogiuwa and Edeko (2009). Secondly, their work considered a part of the area which is not an adequate representation of the mountainous nature of the environment. They also did not effectively capture the three representative environments which are urban, suburban, and rural. In this work, the three selected areas are good representations of all three possible environments (rural, suburban and urban) in Okene area. The path-loss propagation model developed for these three areas will predict accurately the path-loss of any similar environment in any other part of the land. Thirdly, the authors' model for power received was developed from MTN 2G (1800MHz) Network signals only. This work utilized the 2G (1800MHz) and 3G (2100MHz) signals of four different networks (MTN, 9mobile, Globacom and Airtel) to model the path-loss of the area.

## 1.7 Significance of the Research

The site-specific path-loss models developed for the various types of environment in the investigated mountainous area will give the Network providers an accurate and true idea of their various network performances in every environment in the area. The models serve as tools for Network providers to evaluate the effect of the environmental features, especially mountainous terrain, on transmitted signals. Based on the results of the evaluation, they will be able to determine the capacity of the various infrastructures, the appropriate cell-planning scheme and the optimal base transceiver station locations for improved network performance.

This work presents a better method of path-loss modeling to researchers by using measurements from four different networks. Since the BTSs of the various networks are distributed within the environments and operate within the same frequency range, better path-loss behavior is captured from the contributions of all the cells than what can be gotten from a single network.

The path-loss pattern of this mountainous area for the 2G and 3G networks provides the future researchers with an idea of the likely path-loss behavior of the soon-to-be- deployed 4G network in the area. The optimal models will serve as guides for estimating the expected path-loss at 4G frequencies during initial network design and planning.

The network subscribers in the Okene area will also benefit from the research work if the results and recommendations of this work are keyed into by the Network providers and utilized to optimize network performance in the area.

### 1.8 Organization of Thesis

The thesis opens with the Introduction Chapter which gives a general overview of the research work. Chapter Two contains the theoretical background and review of some published literature related to this work. The methods and materials used in achieving the research objectives are presented in Chapter Three. In Chapter Four, the results of the research work were presented and analyzed. The optimized models were developed from three existing models and then evaluated. Chapter Five is the Conclusion and Recommendations for future research.

# CHAPTER TWO

## 2.0 LITERATURE REVIEW

### 2.1 Basic Propagation Mechanisms

Radio wave travels through space as the medium of propagation from the source (transmitter) to the destination (receiver). The transmit antenna radiates the radio signal into space with a certain level of signal power. As the signal travels within its environment of propagation, it experiences degradation in its power either as a result of its distance away from the transmitter or its encounter with obstructions or other environmental effects (Mohamed, 2018). When there are no obstructions between the transmitter and the receiver, signal degradation is mainly due to the distance between the transmitter and the receiver and the frequency of propagation (Eichie *et al.*, 2017). When there are obstructions, the signal experiences absorption of some parts and change of direction of some or the entire signal depending on the nature of the obstruction. This generally describes the mobile radio propagation phenomenon which also contributes to signal path loss in the environment (Lee and Park, 2018).

There are three basic mechanisms that influence radio wave propagation in a mobile communication system. These mechanisms are reflection, diffraction and scattering (Popoola *et al*., 2017).

#### i. Reflection

Reflection occurs when travelling radio wave impinges upon a surface or object whose dimensions are very large relative to the wavelength of the radio wave ((Mohamed, 2018). Examples of such objects or surfaces include the earth surface, buildings and walls.

### ii. Diffraction

When radio wave impinges on a surface or objects with sharp irregular edges, it bends around the obstructing object and thus may still arrive at the receiver even though there is no Line-of-Sight (LOS). This is referred to as diffraction or shadowing (Wang *et l.*, 2017).

### iii. Scattering

Scattering occurs when the radio wave impinges on objects with dimensions smaller than the wavelength of the wave. Scattering in mobile communication systems can be caused by foliage, street signs and lamp posts among others (Ibhaze *et al.*, 2017).

## 2.2 Path-loss in Radio Signal Propagation

As radio signal propagates from the transmitter to the receiver through the environment, it experiences power density reduction due to its path of propagation. Consequently, the received signal power, at any point, is usually lower than the transmitted signal power. A loss has occurred along the path from the transmitter to the receiver. Radio signal path-loss, therefore, is defined as the reduction in power density of an electromagnetic wave or signal as it propagates through the environment (Maloku *et al.*, 2019). Path-loss in wireless communication is illustrated in Figure 2.1.

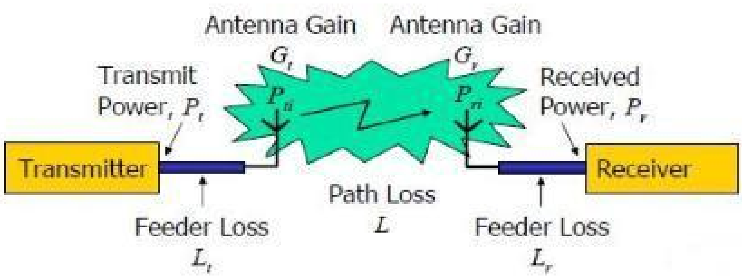


Figure 2. 1 Path Loss in a Wireless Communication System
(Mollel & Kisangiri, 2014)

Path-loss in radio signal propagation is inevitable and a major factor to be considered in wireless communication systems design. The factors responsible for path loss are always present in the environment and are discussed as follows:

**(i) Free Space:** This defines the Line-of-Sight (LOS) propagation environment (Figure 2.1). Radio signals spread out from the transmitting antenna in an ever-increasing sphere. Consequently, the energy of the travelling signal depreciates with increasing distance from the transmitter. Thus, the free space is found to contribute to signal path loss within the environment of propagation (Lasisi *et al.*, 2017).

**(ii) Diffraction and Shadowing:** As already explained in the previous section, diffraction occurs when an object with sharp or rounded edges appears in the path of the signal. As the signal diffracts (bends) around the object, losses occur. How rounded the object is determines how high the loss will be (Tarkaa *et al.*, 2017).

Base station antenna heights are practically much higher than that of the mobile receiver antenna. Therefore, a high buildings or hills lying between the transmitting antenna and the receiving antenna causes the radio signal to undergo diffraction in order to reach the receiving antenna. The mobile receiver is seen to be in the shadow of the signal-obstructing objects; hence the phenomenon is also referred to as shadowing (Anggraeni and Dwiyanti, 2018).

**(iii) Multipath Fading:** Line-of-Sight propagation is desired in radio wave propagation from the transmitter to the receiver in a point-to-point communication system. But in real life, the terrestrial environment is characterised by the presence of various objects which cause signals reflections, diffractions and scattering along the transmission path (Popoola *et al*., 2017). Consequently, the signals reaching the receiver come from a number of different paths (multipath) as shown in Figure 2.2. The signals add up or subtract from each other at the receive end depending on their relative phases to one another. Where some of the signals are out of phase, signal losses (fading) occur. In a mobile receiver system, that is, the receiver is in motion, the overall received signal varies with position. This is caalled Doppler shift which also results in signal power losses (Rappaport, 2005). Mobille receivers such as cellular telecommunicatiions phones will be subject to this multipath efffect which is known as Rayleigh fading (Leee and Park, 2018).

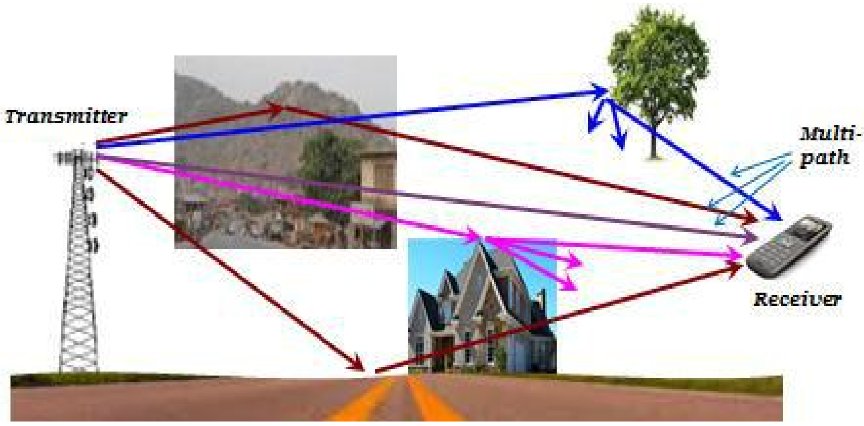


Figure 2. 2 Multipath Propagation

**(iv) Terrain:** Environments with hilly terrain experiences significannt signal power loss as the signal travels over the irregular surface. Hills also create an obstruction to traveling signals and make reception impossible. According to Abiodun *et al*. (2017), at low frequencies, signals experience relatively less attenuation when travelling over marshy or damp terrain while the signal attenuation is higher over the dry sandy teerrains.

**(v) Buildings:** Buildiings in a propagation environment causee signal reflection, diffraction or absorption depending on the building type and nature of its environment. In indoor propagation, signals are often significantly impaired withinn buildings. Signal absorption by buildings ceertainly leads to reduction or degradation in signal strength. The amount of absorption is deependent on the propagation characteristics near the building and on the relative orientation of the building to that of the antenna (Onuu and Usanga, 2017).

**(vi) Vehicle Penetratioon:** When moving vehicles come in-betweenn the transmitter and the receiver, the effect on path-loss is similar to that of buildinggs, except that the penetration is momentary. The signal power goes low momentarily. The loss becomes greater with increased traffic (Tarkaa *et al*., 2017).

**(vii) Foliage Loss:** Jawad *et al*. (2019) explains foliage loss as the loss caused by the propagation of the radio signals over vegetation, most especially forests. Foliage loss varies in magnitude depending on signal frequency, the season, the type of trees, trunks, leaves, branches, and their heights relative to the antenna heights. Wet trees and foliage can attenuate radio signals.

**(viii) Propagation of Signal over Water:** Radio signal might create interference with the frequencies of other cells when propagated over water. Since water surface is a very good reflector of radio waves, there is a possibility of the signal causing interference to the antenna radiation patterns of other cells (Tarkaa *et al*., 2017).

**(ix) Atmosphere:** The atmosphere causes reflection and refraction of signals. In the ionosphere, signals of lower frequencies, especially below 30 - 50MHz, are reflected (or more correctly refracted) back to Earth. At higher frequencies (above 50 MHz), the signals reach the troposphere which refracts them back to earth as a result of changing refractive index (Onuu and Usanga, 2017). This explains how Ultra-High Frequency (UHF) broadcast is able to extend coverage to approximately a third beyond the horizon (Oluwafemi *et al.*, 2018).

**(x) Interference:** Co-channel interference due to signals within the same network, sharing common bandwidth, and adjacent channel interference due to signals from other networks can cause weak signals reception at the receiving antenna. Signals from other man-made objects can also cause interference (Bakare *et al*., 2017). However, the radio resources within the home network of the signals constitute the major source cause of the interference. The losses due to interference are mitigated by accurate frequency planning.

The factors (i) – (x) can also cause either a slow or a rapid fluctuation in the signal level in a radio network. These factors form the basis of cell coverage criteria (Tarkaa *et al.*, 2017).

## 2.3 Free Space Loss

The attenuation of signal power from the transmitter to the receiver in LOS propagation is a function of the transmitter-receiver separation and the operating frequency only. Such type of fading is referred to as free space path-loss and it is a major component of path-loss in wireless communication (Tonga *et al.*, 2019).

Free Space propagation predicts that the received power decays as the negative square root of the distance. Friis' free space equation is given by Orike *et al.*, (2017) as:

$$P_r = \frac{P_t G_t G_r \lambda^2}{(4\pi)^2 d^2 L} \tag{2.1}$$

where $P_r$ is the received power in Watts; $P_t$ is the transmitted power in Watts; $G_t$ is the transmit antenna gain; $G_r$ is the receive antenna gain; $d$ is the transmitter-receiver separation in metres; $L$ is the system loss factor which depends on line attenuation, filter losses and antenna losses and not related with propagation.

The free space path-loss is proportional to the square of $d$ and also to square of the frequency in use. It can be expressed either in terms of frequency or wavelength as:

$P_L = (4\pi d\lambda)^2$ in terms of wavelength (2.2)

and

$P_L = (4\pi dfc)^2$ in terms of frequency. (2.3)

$P_{Lfs}$ = Free space path loss; $d$ = distance from the transmitter to the receiver (m);

$\lambda$ = signal wavelength (m); $f$ = signal frequency (Hz); $c$ = speed of light (m/s).

According to Akujobi *et al*. (2016), the free space path loss ($P_{Lfs}$) in dB for a LOS propagation is given by:

$$P_{Lfs}\ (dB) = 32.44 + 20\log(f_c) + 20\log(d) \tag{2.4}$$

where $P_{Lfs}$ (dB) is the free space path loss in dB, $f_c$ is the signal carrier frequency in MHz and $d$ is the distance between the transmitter and the receiver in km.

## 2.4 Radio Link Budget

During radio network design, it is desirable and important to calculate or predict the expected signal power at the receiver end some distance away from the transmitter based on the transmitted signal power. This calculation is called the Link Budget. It is obtained by adding all the gains together and subtracting all the losses from the transmitted signal power to obtain the received signal power. Radio link budget is defined as a summary of transmitter power levels, communication system losses and gains (Lasisi *et al*., 2017). The link budget equation is summarized as:

$$Received\ Power\ (dBm) = Transmitted\ Power\ (dBm) + Gains\ (dB) + Losses\ (dB) \tag{2.5}$$

With the magnitude of the received signal power from the link budget calculation, the sufficiency of the transmitted power and gains level can be determined. If the received power is lower than desired, then corrective measures are employed to ensure the system performs satisfactorily in terms of signal-to-noise ratio, bit error rate and other key performance indicators.

From the foregoing, the necessity to investigate all likely areas where gains and losses may occur between the transmitter and the receiver is evident. Each link can then be analyzed on its own merits.

A typical link budget is given by Hoomod *et al*. (2018) as:

$$P_r = P_t + G_t + G_r - L_t - L_f - L_r - L_p \tag{2.6}$$

where:

$P_r$ = Received power (dBm)

$P_t$ = Transmitter output power (dBm)

$G_t$ = Transmitter antenna gain (dBi)

$G_t$ = Receiver antenna gain (dBi)

$L_t$ = Transmit feeder and associated losses (feeder and connectors) (dB)

$L_f$ = Free Space loss (dB)

$L_r$ = Receiver feeder and associated losses (feeder and connectors) (dB)

$L_p$ = Miscellaneous signal propagation losses (these include fading margin, polarization mismatch, losses associated with medium through which signal is travelling and other losses) (dB).

### 2.5 Radio Frequency Path-loss Models

When the effects of the various elements responsible for path-loss in mobile communication system is properly understood, we will be able to determine the coverage area of the base station in a location and predict the likely losses from the base station to the mobile station. It also helps in frequency planning and optimization which is a continuous process. It should be remembered, however, that the prediction can only be fairly accurate because we cannot correctly assess the effects of each of the contributing elements. Depending on the method employed in developing the models, three main types of path-loss models can be defined which are suitable for different conditions. According to Cavalcanti *et al*. (2017), the path-loss model types can be stochastic (statistical), deterministic or empirical.

i. **Stochastic (Statistical) models:** Statistical methods use series of random variables to model the propagation environment. It is easier to implement and usually requires the least information and less computational power for the predictions. They are less sensitive to the environment and are the least accurate (Ibhaze *et al.*, 2017).

ii. **Deterministic model:** This method utilizes physical laws of electromagnetic wave propagation to determine the signal path-loss, the coverage and the signal power at a specified position (Surajudeen-Bakinde *et al.*, 2018). Ray tracing is an example of deterministic approach. This method gives more accurate and reliable path-loss compared to the statistical method but it is more expensive in computational effort. Its complexity is caused by the need to consider the details of all the elements within the propagation space, such as buildings, roofs, walls, doors and windows. These different factors cause radio path-loss in a given radio transmission network and make path-loss calculations difficult. However, the radio path loss calculations is important in order to enable equipment to be designed to meet the requirements (Rahul *et al.*, 2019).

**iii. Empirical Models**

Empirical path-loss models are developed strictly from factual observations and measurements taken on the field. It takes into consideration the various factors in the particular environment that cause depreciation of signal strength over different distances away from the transmitter (Oudira *et al.*, 2018). Empirical models do not explain the system's physical characteristic. They are used only to predict path loss. Some of the existing empirical path-loss models are discussed below.

### 2.5.1 Durkin's Model

Durkin's model considers radio signal propagation over irregular terrain. It identifies the obstacles in the radio path and attempts to evaluate the losses due to them. The model reconstructs the ground profile information along the transmitter-receiver path from information obtained from the proposed sites topographic database (Rappaport, 2005).

Durkin's model does not consider multipath as it assumes that the signals get to the receiving antenna only through line-of-sight propagation. It has the advantage of being able to read digital elevation map and produce signal strength contour. The disadvantage is that it does not support multipath communication resulting from foliage, buildings and other manmade structures which also cause significant path-loss.

The Durkin model path loss is given by the simple addition of the free space path loss ($L_f$) and a correction due to plane earth propagation loss ($L_p$) and is given by (Rappaport, 2005) as:

$$PL_{Durkin} = L_f + L_p \tag{2.7}$$

$$L_p = 118.7 - 20log(h_r) - 20log(h_t) + 40log(d) \tag{2.8}$$

where $h_t$ is the transmitter antenna height in $m$;

$h_r$ is receiver antenna height in $m$;

and $d$ is the receiver-transmitter distance in $m$.

### 2.5.2 Okumura Model

Okumura model is one of the most widely quoted and used models of all the available models for signal path-loss prediction in urban areas. Because of its popularity, Okumura model has become a reference for comparing other models. This is possible because the model is designed for use over a wide variety of radio paths encompassing different types of environments and terrain (Lasisi *et al*., 2017). It is based on extensive measurement and its operational frequency is from 150MHz to 1920MHz, with allowance for expansion to about 3000MHz. Distance range is from 1km to 100km and transmitter antenna height is 30m to 1000m (Imoize and Oseni, 2019).

The model is simple and more accurate than other empirical models, but it is slow in response to rapid changes in terrain.

The technique for using the Okumura model is as follows:

– Find free space path loss, $L_F$;

– Determine median attenuation relative to free space $A_{mu}(f,d)$ from curves (Figure 2.3);

– Add other correction factors for antenna heights and terrain

The formula for Okumura Model is expressed by Oudira *et al*. (2018) as:

$$L_m(dB) = L_F + A_{mu}(f,d) - G(h_t) - G(h_r) - G_{AREA} \quad (2.9)$$

where $L_m$ is median of Path-loss;

$L_F$ is free space propagation path-loss;

$A_{mu}(f,d)$ is the median attenuation relative to free space;

$G(h_t)$ is the transmitter (base station) antenna height gain factor;

$G(h_r)$ is receiver (mobile station) antenna height gain factor;

$G_{AREA}$ is gain due to type of environment (suburban, urban or open area)

$$G(h_t) = 20\log(h_t/200), \quad 1000\text{m} > h_t > 30\text{m}; \quad (2.10a)$$

$$G(h_r) = 10\log(h_r/3), \quad h_r \leq 3\text{m} \quad (2.10b)$$

$$G(h_{re}) = 20\log(h_{re}/3), \quad 10\text{m} > h_{re} > 3\text{m} \quad (2.10c)$$

The median attenuation relative to free space, $A_{mu}(f,d)$ and $G_{AREA}$ for a wide range of frequencies are shown in Figure 2.3.

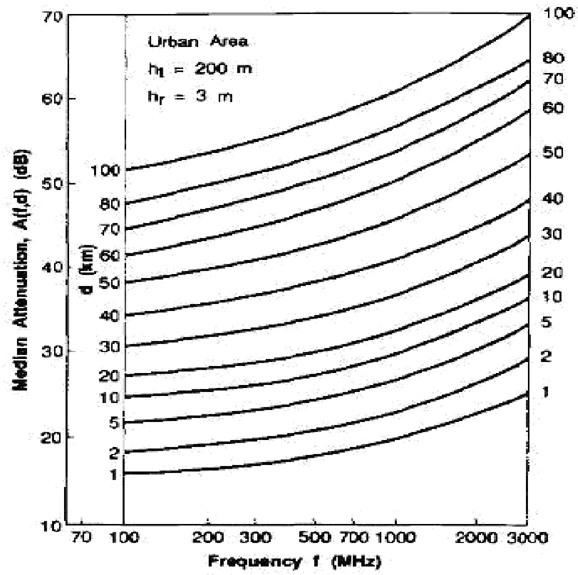


Figure 2. 3 Median Attenuation Relative to Free Space (Amu(f,d)) over a Quasi-Smooth Terrain (Rappaport, 2005)

### 2.5.3 Hata Model

Hata Model is based on the graphical path-loss data provided by Okumura. It presents a standard empirical formula that simplifies the path-loss calculation without the need for Okumura's graph. It is also supplied with correction equations for application to other situations. It is applicable for the same frequency range as Okumura, i.e 150MHz to 1500MHz. The transmitter height ranges from 30m to 200m and receiver height from 1m to 10m and the transmitter-receiver separation is from 1km to 20km.

Hata model standard formula for urban areas is given by Zreikat and Dordevic (2017) as:

$$P_L(\text{dB}) = 69.55 + 26.16 \log f_c - 13.82 \log h_t - a(h_r) + (44.9 - 6.55 \log h_t) \log d \qquad (2.11)$$

where $a(h_r)$ is a correction factor for effective mobile antenna height, and depends on the size of the coverage area.

For a medium sized city, the mobile antenna correction factor is given by

$$a(h_r) = (1.1 \log f_c - 0.7)h_r - (1.56 \log f_c - 0.8) \text{ dB} \qquad (2.12)$$

and for a large city,

$$a(h_r) = 8.29(\log 1.54h_r)^2 - 1.1 \text{ dB} \qquad \text{for } f_c \leq 300 \text{ MHz} \qquad (2.13a)$$

$$a(h_r) = 3.2(\log 1.75h_r)^2 - 4.97 \text{ dB} \qquad \text{for } f_c \geq 300 \text{ MHz} \qquad (2.13b)$$

Although Hata model equations do not include any of the path specific corrections available in the original model, it has, however, greatly improved the practical value of the Okumura model.

### 2.5.4 COST-231 (Extension to Hata) Model

COST (**CO**perationeuropéennedans le domaine de la recherché **S**cientifique et **T**echnique) or European Co-operative for Scientific and Technical research (Euro-COST) developed this model to extend the Hata model to frequencies up to 2GHz (Anggraeni and Dwiyanti, 2018).

The Cost-231 model is expressed in terms of the following parameters:

Carrier frequency, $f_c$: 1500 – 2000 MHz;

Transmitter (Base station) Antenna height, $h_t$: 30 – 200m;

Receiver (Mobile station) Antenna height, $h_r$: 1 – 10m;

Transmission Distance, $d$: 1 – 20km.

The path-loss according to Cost-231 – Hata model extension is expressed as:

$$P_L\,(\text{dB}) = 46.3 + 33.9 \log f_c - 13.28 \log (h_t) - a(h_r) + (44.9 - 6.55 \log h_t)\log d + C_M \quad (2.14)$$

where $a(h_r)$ is defined in equations (2.12), (2.13a) and (2.13b) and

$$C_M = \begin{cases} 0\text{dB} & \text{for medium sized city and suburban areas} \\ 3\text{dB} & \text{for metropolitan centers} \end{cases} \quad (2.15)$$

### 2.5.5 Walfisch Model (also known as Walfisch-Bertoni or Walfisch-Ikegami Model)

This model developed by Walfisch and Bertoni in 1988 predicts path-losses in urban environment. The model considers the effects of rooftops and building height by using diffraction to predict average signal strength at street level. The model consists of three components:

i. Free space loss between isotropic antennas, $L_f$;

ii. Rooftop-to-Street loss, $L_{rts}$; ($L_{rts}$ depends on street widths, frequency, height of reflection relative to receive antenna, and angle of incidence relative to street);

iii. Multi-screen diffraction loss due to rows of buildings $L_{ms}$; ($L_{ms}$ depends on distance between buildings, frequency, height of reflection and antennas, and propagation distance)

The Walfisch-Ikegami model path-loss, $P_L$(dB) is given by Ebhota *et al.* (2018) as:

$$P_L = L_f + L_{rts} + L_{ms} \tag{2.16}$$

### 2.5.6 ECC-33 Model (Electronic Communication Committee)

Like Hata model, the ECC-33 model is an extrapolation of the Okumura model for predicting path-loss for frequencies higher than 3GHz up to 3.5GHz. It was developed on the recommendation of the International Telecommunication Union (ITU) by the Electronic Communication Committee (ECC). ECC-33 path-loss model is given by Popoola *et al.* (2018) as:

$$P_L = A_{fs} + A_{bm} - G_t - G_r \tag{2.17}$$

where $A_{fs}$: Free space attenuation (dB)

$A_{bm}$: Basic median path loss (dB)

$G_t$: Transmitter antenna height gain factor

$G_r$: Receiver antenna height gain factor

These factors can be separately described and given as:

$$A_{fs} = 92.4 + 20 \log(d) + 20 \log(f) \tag{2.18}$$

$$A_{bm}: = 20.41 + 9.83\log(d) + 7.894\log(f) + 9.56[\log(f)]^2 \tag{2.19}$$

$$G_t: = \log(h_t)(13.958 + 5.8[\log(d)]^2) \tag{2.20}$$

When dealing with gain for medium cities, the $G_r$ will be expressed in:

$$G_r: = [42.57 + 13.7 \log(f)][\log(h_r) - 0.585] \tag{2.21a}$$

For large city, $G_r: = 0.759h_r - 1.862$ (2.21b)

### 2.5.7 Egli Model

Egli path-loss model was developed for point-to-point or LOS transmission application over an irregular terrain. It is best suited for cellular communication system with one antenna fixed while the other is mobile. Egli path-loss model is given by Okoro and Iwuji (2019) as:

$$PL_{egli} = G_t G_r \left( \left(\frac{h_t h_r}{d^2}\right)^2 \left(\frac{40}{f}\right)^2 \right) \tag{2.22}$$

where:

$G_t$ is the gain of the base station antenna (dimensionless),

$G_r$ is the gain of the mobile station antenna (dimensionless),

$h_t$ is the height of the base station antenna in metres,

$h_r$ is the height of the mobile station antenna in metres,

$d$ is the distance from base station antenna to mobile station antenna in metres, and $f$ is the frequency of transmission in megahertz (MHz).

$G_t$ and $G_r$ are zero in decimal unit. Hence the Egli Path-loss is simplified by Maloku *et al.* (2019) as:

$$PL_{egli} = 40\log(d) - 20\log(h_t) - 20\log(h_r) - 10\log(40/f)^2 \tag{2.23}$$

Further simplification gives:

$$P_{Legli}\,(\text{dB}) = 20 \log f_c + P_0 + 76.3 \tag{2.24}$$

where $P_0 = 40 \log d - 20 \log_{10} h_t + 10 \log_{10} h_r$ (2.25)

### 2.6 Review of Related Works

Shoewu *et al.* (2016) developed path-loss models for 2G and 3G frequencies in four environments in Lagos State by modifying the COST-231-Hata model chosen because of its suitability to various environment types. The investigated environments were dense urban Lagos Island, urban Surulere, sub-urban Lekki-Onirun and non-urban Agbede-

Ikorodu. They developed optimized models called OMODEEN models whose RMSEs are within 6dB and are of less value than the reference COST-231 model and thus give better path-loss predictions than COST-231. They limited their reference model to COST-231 only without trying other models which, after modification, could result into more accurate optimized model than the OMODEEN models.

Isabona *et al.* (2013) compared measured path-loss for 3G UMTS (2100MHz) in Ugbor Avenue, BIU Campus and Gapiona Avenue of GRA, Benin City, Nigeria and compared with the Lee model, COST-231 model, Hata model and Egli model. The study areas are characterized by high-rising buildings with trees sandwiched in-between them. Result shows poor prediction performance by Lee model because it considers the effective base station antenna height which in itself varies with the topology of the environment. The poor performance of the Egli model in rural Gapiona Avenue was attributed to the fact that Egli model was designed for medium city and sub-urban environments. They observed that the duo of Okumura-Hata and COST-231 Hata performed well in all three areas because they are independent of receiver antenna heights. The study simply investigated the suitability of some selected existing models for path-loss determination in the investigated areas. No attempt was made to optimize the models for better prediction capability.

Tarkaa *et al*. (2017) used Stanford University Interim (SUI) model and MATLAB simulations to analyze the performance of Globacom Nigeria 2G 1800MHz GSM network in Makurdi. The result of the study established the theoretical relationship between path-loss and frequency and between path-loss and transmitter-receiver separation. It shows that path-loss increase with increasing transmitter-receiver distance, increasing frequency and decreasing BTS antenna height. However, the authors utilized data obtained from the network provider to simulate the relationship between path-loss, frequency, distance, and BTS antenna height.

Akujobi *et al*. (2016) utilized the Mean Square Error (MSE) approach to analyze the field path-loss measurement from urban GRA Phase II and suburban Aggrey Road areas of Port Harcourt City, Nigeria at 3G 2100MHz frequency. When compared with existing models, results showed better prediction performance of Okumura-Hata model in urban environment while COST-231 performed better in rural environment. Like Isabona *et al.* (2013), they too did not modify any model for optimal performance but, instead, simply compared the relative performance of some selected models in the investigated area.

A study conducted by Famoriji and Olasoji (2013) compared measured signal path-loss at UHF in Idanre Town of Ondo State, Nigeria with path-loss predictions of COST-231, Hata and Egli models to determine the most suitable existing empirical models for the hilly area. The result showed that the COST-231 model performed better than the other two models (Hata and Egli models). As a result, the COST-231 model was modified using MATLAB software to develop a path-loss model whose prediction performance is higher than the reference models for Idanre hilly area. The frequency of consideration here is not mobile network frequency but that of Television transmission, the Ultra High Frequency (UHF).

Musefiu *et al*. (2017) measured the received signal strength of four mobile telecommunication service providers – Etisalat, Airtel, Globacom and MTN – at 900MHz, and compared with the predictions of Okumura-Hata, COST231 and ECC-33 models. They concluded that COST-231 model gave a better performance in the urban area of Kazaure Town and thus recommended it for path-loss prediction in the urban area.

However, they only compared the performance of the selected reference models without modifying any of them for better result.

Omorogiuwa and Edeko (2009) obtained a path-loss exponent of 3.58 on analysis of measured signal power received at 1800MHz in mountainous environments of Igarra (Edo State), Ajaokuta and Okene (both in Kogi State), Nigeria. They developed a model for predicting the power received in the mountainous areas having established the poor performance of GSM services in those areas due to the nature of the environmental terrain. However, they considered only the MTN 2G (1800MHz) and not other networks nor 3G 2100MHz which was not yet deployed by then. Also, the environments selected for investigation in Okene, which is actually a subsection of their research work, was not representative enough of the mountainous terrain.

In this research, however, the three selected environments sufficiently represent the irregular terrain of Okene area. Also, the 2G (1800MHz) and 3G (2100MHz) frequencies were captured. The signals of four different Networks were used for the modeling and five existing models were used as references. The resulting models more perfectly reflect the path-loss situation of the mountainous area.

# CHAPTER THREE

## 3.0 RESEARCH METHODOLOGY

### 3.1 RESEARCH PROCEDURE

The procedure for the research is shown in the block diagram of Figure 3.1.

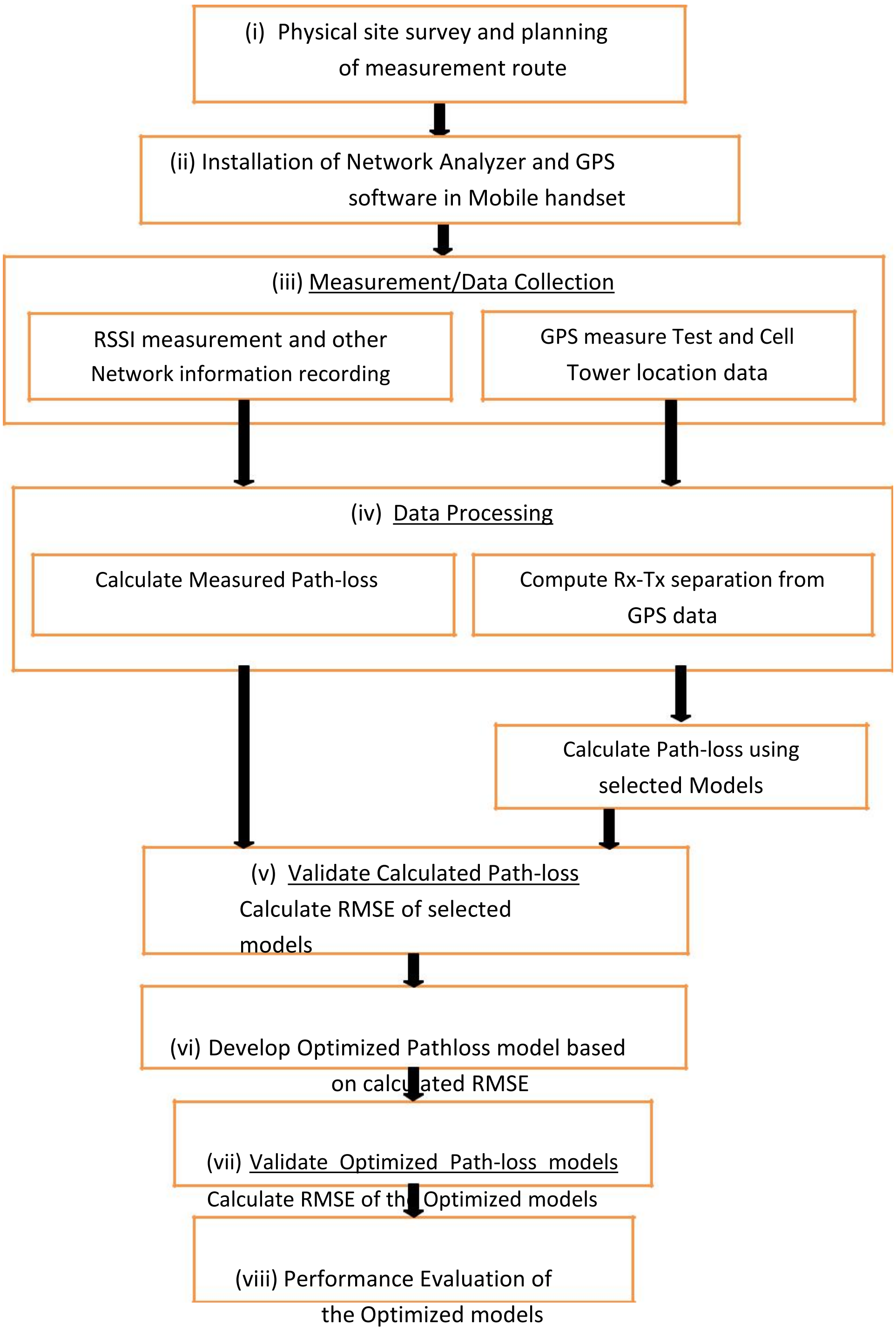


Figure 3.1 Research Procedure

The steps involved are highlighted as follows:

**(i) Physical site survey and planning of drive test routes:**

The three selected environments for investigation were visited and surveyed for the purpose of determining and mapping out the routes for the drive test.

**(ii) Installation of Network Analyzer and GPS software in the Mobile handset:**

The network analyzer software (Cellmapper and Network Cell Info Lite) for received signal data collection and Virtual Maze GPS software for geographical location data collections were installed in the android mobile phone.

**(iii) Drive Test campaign for data collection:**

Drive test campaign was carried out in the three environments for a period of two months, September 23 to November 22, 2019. The first campaign captured the MTN and Glo networks. The second campaign was to capture 9mobile and Airtel networks in all three environments. The third campaign was for verification of the network cells whose Cell Identification Digits (CID) were captured during the signal data measurement campaigns and it lasted for two weeks.

**(iv) Processing of Data:**

Measured path-loss was computed from the measured RSSI. The distance between the serving cells and the receiver at each test point is calculated using the Haversine equation given by Worgu *et al.* (2017) as:

$$d = 2r \sin^{-1}\left(\sqrt{\sin^2\left(\frac{\varnothing_2-\varnothing_1}{2}\right)+\cos(\varnothing_1)\cos(\varnothing_2)\sin^2\left(\frac{\varphi_2-\varphi_1}{2}\right)}\right) \quad (3.1)$$

where $r$ is the radius of earth (= 6371km), $\varnothing_1$, $\varnothing_2$ are latitudes of the two points and $\varphi_1$, $\varphi_2$ is longitude of the two points respectively.

The selected reference models, Free space, COST-231, Hata, Egli and ECC-33, are used to obtain the calculated path-loss.

**(v) Validation of Calculated Path-loss:**

In order to determine the level of deviation of the reference models calculated path-loss from the measured path-loss, their Root Mean Square Errors (RMSEs) were computed. Thereafter, the average RMSE for each reference model was calculated.

**(vi) Optimization of the models:**

The average RMSE of each reference model in each environment is used to modify the reference models to obtain the modification that gives the least deviation (RMSE) either by subtracting or by adding the RMSE to or from the constant term of the model equation. The modified model with the least average RMSE is selected as the optimal model for the environment.

**(vii) Performance evaluation of optimized model:**

The optimal models are used to predict new path-loss values. The new average RMSE of the optimized models are calculated and compared with the average RMSE of the reference models. The percentage improvements in the performance of the optimal models over the reference models are calculated.

### 3.2 Description of Investigated Area and Network

Okene is the headquarter of Okene Local Government Area in the Central Senatorial District of Kogi State, Nigeria. It is located on latitude 7.551220 ($07^{0}$33'N) and longitude 6.235890 ($06^{0}$14'E) and is situated at elevation 384 - 488 meters above sea level. Okene town runs along the A2 highway. It has an area of 328 $km^2$ (127 sq mi) and a population of

479,178 at the 2006 census making it the biggest city in Kogi (Emurotu and Habib, 2019). Figure 3.2 is the satellite map of Okene in Kogi State, showing the hilly terrain.


Figure 3. 2 Okene Hilly Terrain Map
(Source: Google maps; Accessed: 23rd April, 2019)

There are not many high rise buildings. The population in the urban area is dense but moderate both in the suburban and the rural areas. Figure 3.3 is a typical landscape view of all the environments in Okene. It is a hilly area and as a result, radio signal propagation within the environment is greatly impaired.

Figure 3. 3 A Landscape Picture of Okengwe in Okene, Kogi State Nigeria
(Taken: 7th July, 2019)

### 3.1.1 Selected Environments

Based on the description of the urban, suburban and rural areas given in the introductory part of this thesis, the selected environments for investigation within Okene are Okene Central area, Okengwe area and Agasa/Upogoro area.

(i) Okene Central area is an urban environment with dense population. The terrain is representative of areas with a wider stretch of land space between mountains in the area;

(ii) Okengwe is an area which effectively describes suburban environments of the entire Okene area with moderate population used majorly as residences.

(iii) Agasa/Upogoro is a typical rural environment in the mountainous environment. The geographical locations of the three environments are presented in Table 3.1.

Table 3.1 Selected Areas Investigated

| S/N | Environment Type | Location | GPS Coordinates |
|---|---|---|---|
| 1. | Urban | Okene Town | 7° 32' 44" N, 6° 15' 14" E |
| 2. | Sub-urban | Okengwe | 7° 32' 56" N,6° 11' 30" E |
| 3. | Non-urban | Agasa/Upogoro | 7° 36' 01" N, 6° 12' 05" E |

(Source: National Geospatial-Intelligence Agency, Bethesda, MD, USA, 23rd April, 2019)

### 3.1.2 Selected Networks

The Network types available in Okene area, and considered as at the time of this research work, are the 2G EDGE (1800MHz) and 3G UMTS (2100MHz). The 2G GSM (900MHz) is almost non-existent and therefore not considered. The network providers whose services are available are the 9mobile, MTN, Glo and Airtel. The two network types for the four service providers are considered in the modeling process in order to obtain generalized models for each environment based on data measurement from the four networks. This enables the development of models which best describe the path-loss of the environments.

The results of this work give some idea to researchers and service providers of the nature of 4G LTE-A path-loss pattern in the mountainous environment. It can therefore serve as a reference for future network planning during network standard upgrade.

## 3.2 Materials and Tools

Materials and tools used for this work were:

i. An Itel P33 plus android powered Smartphone;

ii. Network Analyzer software: Cellmapper and Network Cell Info Lite;

iii. GPS measurement software: Virtual Maze GPS tool;

iv. 4 Network SIM cards for 9mobile, MTN, Glo and Airtel network services;

v. Booklets for manual recording of the Network Received Signal Strength and GPS data.

vi. A Car for conveying the researchers and the test equipment.

### 3.2.1 Network Analyzer software:

Two Network Analyzer android applications are employed to measure the RSSI and provide other useful network signal information. They are Cellmapper (Lin and Maw, 2018) and Network Cell Info Lite (Okoro and Iwuji, 2019). They are both chosen to complement themselves in terms of other signal information and also to enable comparison between their RSSI readings to ensure correctness. The two software identify the network type (standard), network operator, transmit and receive frequencies in MHz, and signal strength in dBm, Cell Identification Digit (CID) of the serving network cell and Location Area Code (LAC) of the network. These are manually recorded and screenshots of the applications are as shown in Figure 3.4(a) and Figure 3.4(b) for Cellmapper and Network Cell Info Lite respectively.

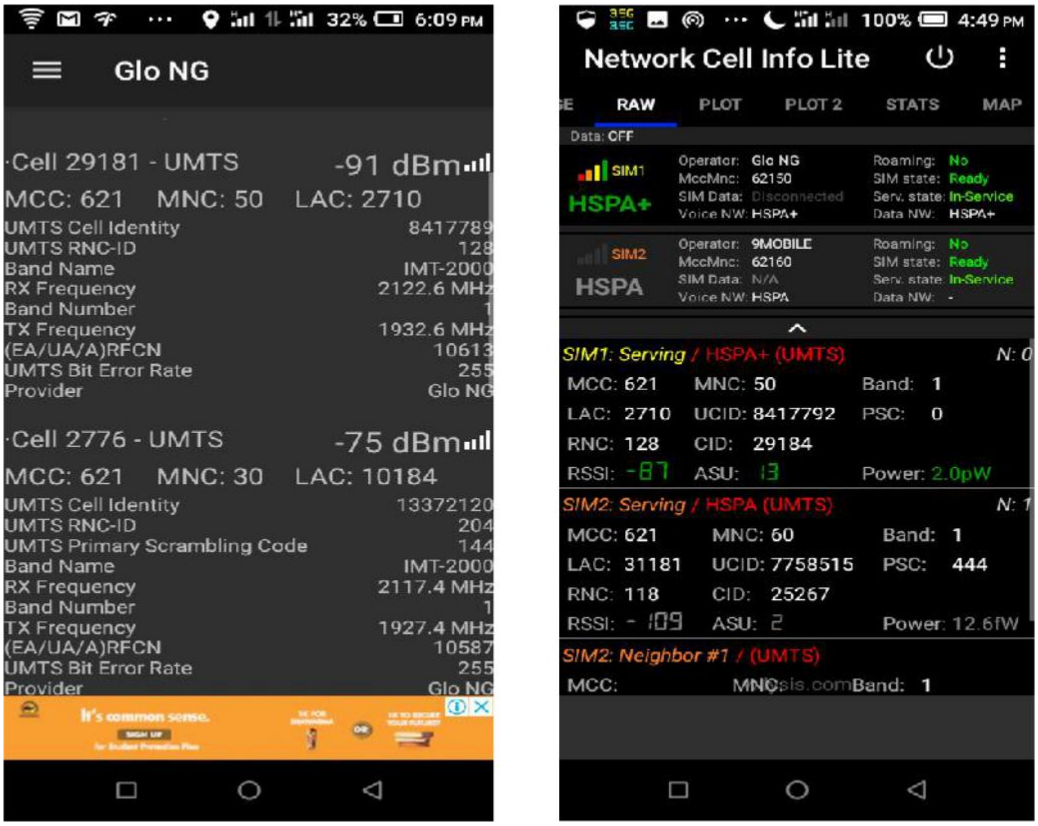


(a) Cellmapper (b) Network Cell Info Lite

Figure 3.4 Screenshots of Cellmapper and Network Cell Info Lite

### 3.2.2 GPS measurement software: Virtual Maze GPS tool

Virtual Maze GPS tool is an android device application that reads the live GPS location of a point. It also takes reading of the altitude of the location. It was used to read the GPS locations (latitude, longitude and altitude) of the measurement positions and the BTS locations. Screenshots of the Virtual Maze GPS Tool in operation are shown in Figure 3.5(a and b).

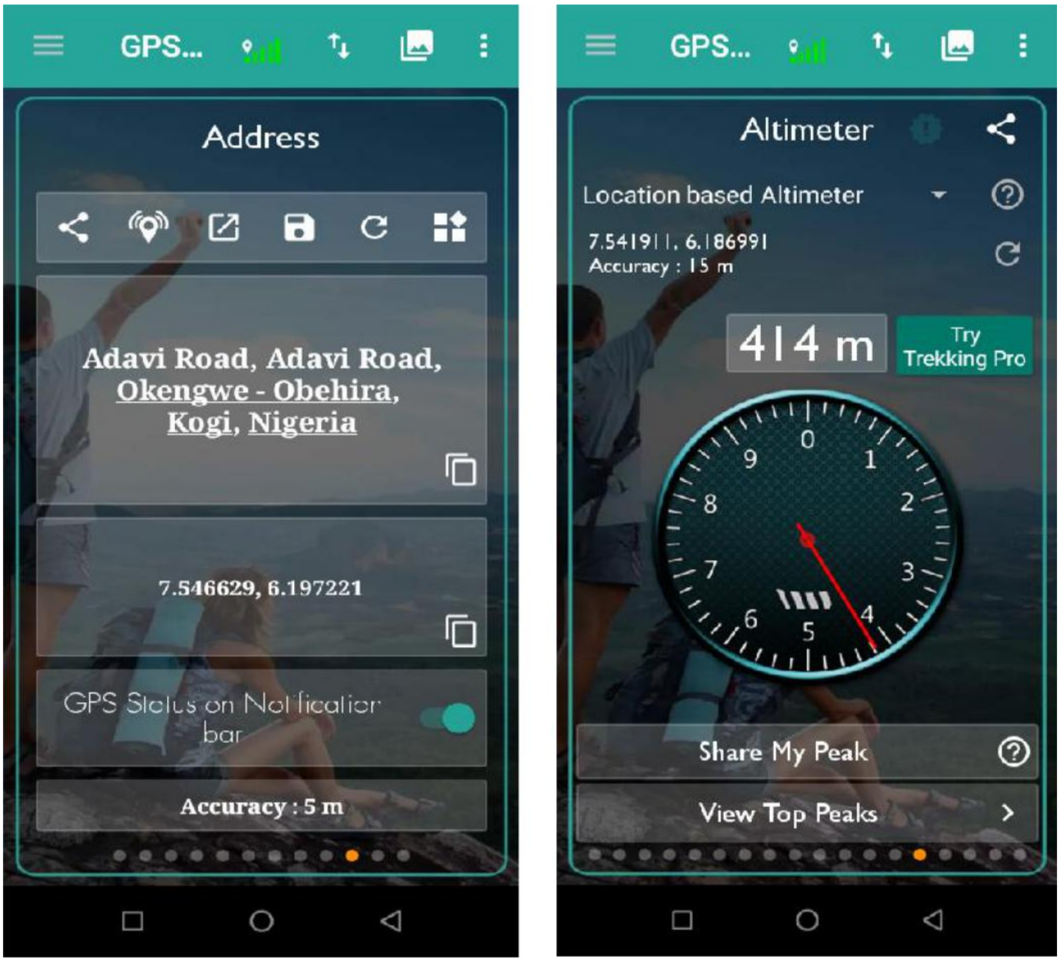


(a) Location Address and Coordinates (b) Altimeter

Figure 3.5 Virtual Maze GPS tool

## 3.3 Measurement

Measurement campaign was carried out in the three areas of Okene town, Okengwe and Agasa/Upogoro from September 23 to November 22, 2019. RF signal analyzers (Network Cell Info Lite and Cellmapper) were installed in an Itel P33 plus smart phone to measure and indicate the received signal power (RSSI), serving cell id, transmit frequency and other network information. The installed GPS tools software reads the location data (latitude, longitude and altitude) of measurement points and that of the cell-towers. The measurement data at each point were recorded on the spot into a recording booklet. The two network signal capture software were carefully selected to compare their readings in order to obtain correct results. The readings of these software were compared with the inbuilt signal strength meter of the Itel P33 plus to ascertain the software's accuracy of reading. The software also complement each other in the other network information they supply. Their performances are satisfactory.

Measurements are taken at about 50m interval along test routes. At each point, measurements of 3G 2100MHz RSSI, transmit frequency and other cell information for each of two networks (MTN and Glo) were recorded. At each location, the RSSI readings were monitored and taken five times within a period of about ten minutes and the average reading was computed. The phone network was then switched to 2G 900/1800MHz network type in order to measure and record the same data for 2G network. The same process was carried out for the other two networks (9mobile and Airtel) in the second drive test campaign. With the aid of the GPS tools software, the latitude, longitude and altitude of the measurement points are also read and recorded.

Physical verification of each serving network Cells whose cell-id was captured during the measurement campaign was carried out in a third campaign to verify and record their exact geographical locations from November 25 to December 3, 2019.

### 3.4 Transmitter-Receiver distance calculation

The separation *d* between the mobile receiver and the fixed BTS at each measurement position was calculated from the recorded GPS data of each position and the serving cell using the Haversine Equation 3.1.

## 3.5 Presentation of Results

The measurement locations in each of the environments are shown in Figures 3.7 to 3.9 with the measurement points tagged with numbers in sequence. The BTS locations of the networks are as shown and labeled.

The average received signal strength indicator (RSSI) in dB as measured on the field for each of the networks in each of the environments are presented in Table 3.2 to Table 3.7. Figure 3.6 shows the measurement points (Appendix A) and BTS locations in Okene Central Urban environment.


Figure 3.6 Drive Test Routes in Okene Central Urban Environment with Measurement Points and BTS Locations (Source: Google maps; Plotted: 10th February, 2020)

The average values of RSSI in dBm measured at each of the points in Figure 3.6 are shown in Table 3.2 for 3G.

Table 3.2 Average RSSI(dBm) of 3G Networks in Okene Central Urban Area

| | 9mobile 3G | | MTN 3G | | Glo 3G | | Airtel 3G | |
|---|---|---|---|---|---|---|---|---|
| **S/N** | **Distance (m)** | **$RSSI_{ave}$ (dBm)** | **Distance (m)** | **$RSSI_{ave}$ (dBm)** | **Distance (m)** | **$RSSI_{ave}$ (dBm)** | **Distance (m)** | **$RSSI_{ave}$ (dBm)** |
| **1** | 461.2 | -65.8 | 869.0 | -88.2 | 604.6 | -74.6 | 978.2 | -55.8 |
| **2** | 987.1 | -66.6 | 715.6 | -83.4 | 241.4 | -88.2 | 877.6 | -54.2 |
| **3** | 580.4 | -65.4 | 1010.2 | -61.4 | 1200.6 | -71 | 498.0 | -57 |
| **4** | 332.8 | -63.8 | 399.5 | -61.4 | 1399.0 | -81.8 | 413.3 | -65.8 |
| **5** | 211.6 | -57.4 | 235.6 | -51 | 1366.8 | -58.2 | 280.2 | -62.6 |
| **6** | 376.0 | -57.8 | 195.6 | -70.2 | 1173.8 | -74.2 | 60.5 | -59.8 |
| **7** | 639.2 | -68.2 | 420.4 | -65.8 | 967.3 | -79.4 | 272.0 | -52.6 |
| **8** | 869.7 | -73.8 | 139.0 | -64.6 | 729.6 | -77.8 | 631.5 | -68.6 |
| **9** | 930.6 | -79.8 | 102.8 | -71.8 | 807.4 | -82.6 | 489.0 | -71.4 |
| **10** | 1138.3 | -60.6 | 139.8 | -85.4 | 852.8 | -74.2 | 661.7 | -56.6 |
| **11** | 1411.9 | -69.8 | 373.2 | -79 | 1292.0 | -73.8 | 635.0 | -61.8 |
| **12** | 1546.8 | -71.8 | 613.6 | -75.4 | 1490.9 | -85.8 | 545.1 | -60.2 |
| **13** | 109.7 | -67.4 | 1633.4 | -80.6 | 1624.2 | -85.4 | 439.2 | -59 |
| **14** | 193.9 | -53 | 1458.1 | -68.6 | 1523.8 | -62.2 | 434.1 | -60.2 |
| **15** | 477.4 | -71.8 | 504.9 | -73.8 | 545.6 | -76.6 | 539.5 | -59.4 |
| **16** | 773.1 | -67.8 | 196.8 | -52.6 | 339.4 | -59.4 | 230.2 | -51.8 |
| **17** | 933.8 | -81 | 39.9 | -51 | 2166.7 | -77.8 | 43.8 | -52.2 |
| **18** | 1327.1 | -75.8 | 293.1 | -64.6 | 627.7 | -79.8 | 557.1 | -56.6 |
| **19** | 710.8 | -65.4 | 712.7 | -65.8 | 667.5 | -85.8 | 552.3 | -67 |
| **20** | 929.4 | -73.8 | 237.0 | -51 | 878.4 | -83.8 | 414.5 | -53.4 |
| **21** | 681.7 | -71.8 | 275.5 | -77.8 | 322.0 | -96.2 | 518.9 | -71.4 |
| **22** | 927.0 | -70.6 | 755.0 | -73.8 | 109.5 | -57 | 394.8 | -62.2 |
| **23** | 1155.7 | -60.2 | 513.6 | -77.8 | 1225.6 | -77 | 428.0 | -66.6 |

Similarly, the average values of RSSI in dBm measured at each of the points in Figure 3.6 for 2G Networks are shown in Table 3.3.

Table 3.3  Average RSSI(dBm) of 2G Networks in Okene Central Urban Area

Table 3.3  Average RSSI(dBm) of 2G Networks in Okene Central Urban Area

| | **9mobile 2G** | | **MTN 2G** | | **Glo 2G** | | **Airtel 2G** | |
|---|---|---|---|---|---|---|---|---|
| **S/N** | **Distance (m)** | **RSSI$_{ave}$ (dBm)** | **Distance (m)** | **RSSI$_{ave}$ (dBm)** | **Distance (m)** | **RSSI$_{ave}$ (dBm)** | **Distance (m)** | **RSSI$_{ave}$ (dBm)** |
| **1** | 1081.4 | -53.8 | 595.5 | -77.8 | 604.6 | -62.2 | 978.2 | -55 |
| **2** | 819.3 | -52.2 | 1007.5 | -71.8 | 241.4 | -69.4 | 665.9 | -51 |
| **3** | 580.4 | -57.8 | 1010.2 | -63.4 | 271.6 | -51 | 498.0 | -51 |
| **4** | 332.8 | -51 | 399.5 | -69.8 | 1399.0 | -63.8 | 413.3 | -57.8 |
| **5** | 211.6 | -51 | 235.6 | -51 | 442.8 | -51 | 716.9 | -57.8 |
| **6** | 376.0 | -51 | 195.6 | -59.8 | 1173.8 | -63.4 | 60.5 | -51 |
| **7** | 639.2 | -53.8 | 420.4 | -51 | 967.3 | -60.2 | 272.0 | -51 |
| **8** | 869.7 | -57.8 | 139.0 | -69 | 729.6 | -60.6 | 582.8 | -62.6 |
| **9** | 1043.1 | -76.2 | 102.8 | -65.8 | 807.4 | -57.4 | 489.0 | -61 |
| **10** | 1138.3 | -52.2 | 139.8 | -68.2 | 852.8 | -59.8 | 495.7 | -66.2 |
| **11** | 1411.9 | -57.8 | 373.2 | -51.4 | 1292.0 | -60.2 | 635.0 | -32.2 |
| **12** | 1546.8 | -60.2 | 613.6 | -63.8 | 1490.9 | -58.2 | 545.1 | -51 |
| **13** | 109.7 | -51.8 | 1012.0 | -70.2 | 1624.2 | -62.2 | 439.2 | -51.8 |
| **14** | 193.9 | -51 | 845.8 | -72.2 | 579.7 | -51.4 | 850.5 | -54.2 |
| **15** | 477.4 | -67.8 | 504.9 | -69.8 | 545.6 | -65 | 612.9 | -59.8 |
| **16** | 773.1 | -52.2 | 196.8 | -51 | 339.4 | -53 | 230.2 | -51 |
| **17** | 1085.5 | -67.8 | 39.9 | -51 | 294.1 | -51 | 43.8 | -51 |
| **18** | 646.7 | -63.8 | 512.4 | -58.6 | 397.3 | -51.8 | 557.1 | -51.8 |
| **19** | 710.8 | -51 | 355.1 | -66.6 | 507.0 | -51 | 552.3 | -58.6 |
| **20** | 778.4 | -51 | 237.0 | -56.2 | 533.9 | -60.6 | 414.5 | -51 |
| **21** | 681.7 | -59.8 | 645.7 | -75.8 | 322.0 | -67.4 | 518.9 | -57.4 |
| **22** | 927.0 | -62.6 | 755.0 | -70.6 | 15.5 | -54.2 | 394.8 | -60.2 |
| **23** | 1155.7 | -53.8 | 513.6 | -75 | 1225.6 | -60.2 | 482.2 | -63.8 |

Figure 3.7 shows the measurement points (Appendix B) and BTS locations in Okengwe Suburban environment.

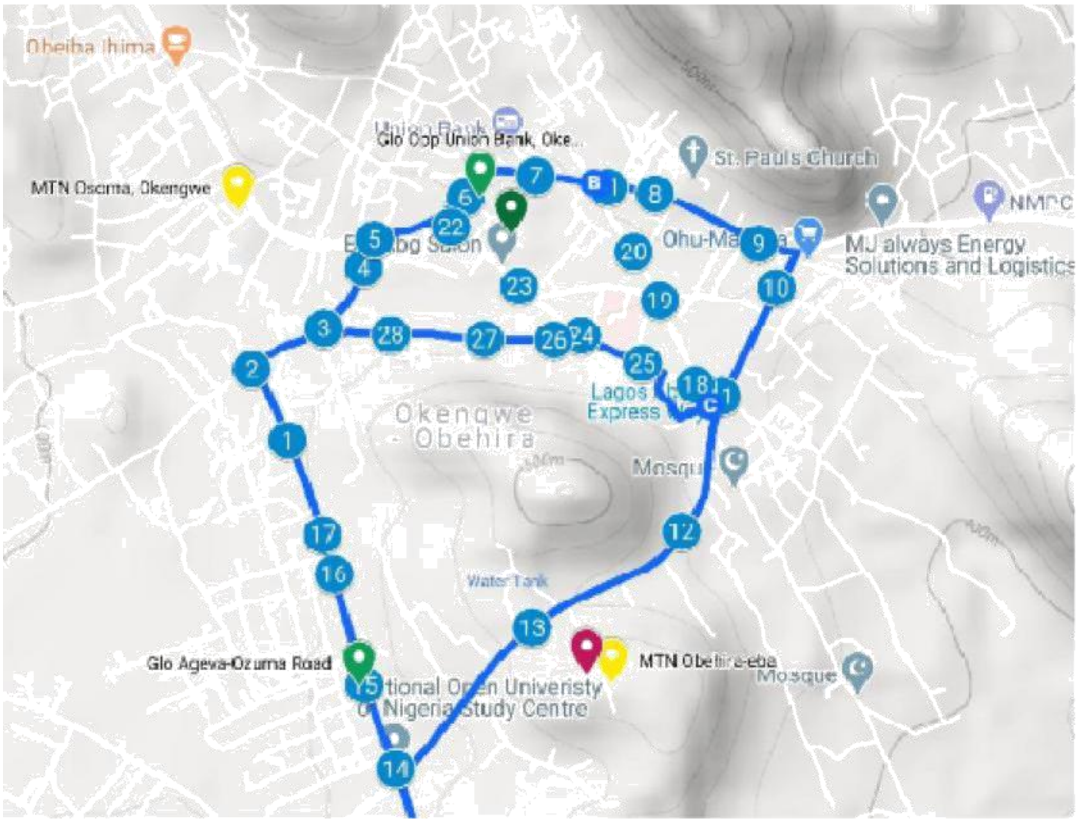


Figure 3. 7 Drive Test Routes in Okengwe Suburban Environment with Measurement Points and BTS Locations (Source: Google maps; Plotted: 10th February, 2020)

The average values of RSSI in dBm measured at each of the points in Figure 3.7 are shown in Table 3.4 for 3G Networks in the suburban environment.

Table 3.4 Average RSSI (dBm) of 3G Networks in Okengwe Suburban Environment

| | 9mobile 3G | | MTN 3G | | Glo 3G | | Airtel 3G | |
|---|---|---|---|---|---|---|---|---|
| **S/N** | **Distance (m)** | **$RSSI_{ave}$ (dBm)** | **Distance (m)** | **$RSSI_{ave}$ (dBm)** | **Distance (m)** | **$RSSI_{ave}$ (dBm)** | **Distance (m)** | **$RSSI_{ave}$ (dBm)** |
| **1** | 907.5 | -94.2 | 710.8 | -66.2 | 786.7 | -73.8 | 712.0 | -67 |
| **2** | 866.8 | -64.6 | 485.8 | -55.8 | 858.9 | -51.8 | 866.8 | -60.6 |
| **3** | 619.5 | -73.8 | 434.2 | -51 | 607.5 | -51 | 435.3 | -63 |
| **4** | 445.1 | -68.6 | 404.9 | -63.8 | 406.7 | -59.8 | 445.1 | -69 |
| **5** | 404.9 | -62.6 | 411.2 | -54.2 | 335.5 | -51 | 404.9 | -73.4 |
| **6** | 181.9 | -72.2 | 192.6 | -57.8 | 77.7 | -51 | 673.8 | -64.6 |
| **7** | 199.3 | -51.4 | 194.8 | -54.6 | 137.0 | -62.2 | 199.3 | -62.2 |
| **8** | 445.2 | -78.2 | 357.6 | -61.8 | 419.9 | -65.8 | 445.2 | -59 |
| **9** | 731.6 | -82.2 | 1424.6 | -64.2 | 841.6 | -46.2 | 2208.0 | -72.2 |
| **10** | 798.0 | -76.6 | 1243.5 | -58.6 | 917.0 | -70.2 | 798.0 | -73.4 |
| **11** | 2711.8 | -97.4 | 959.3 | -56.2 | 928.8 | -65.8 | 943.0 | -66.2 |
| **12** | 3013.2 | -93 | 520.3 | -74.2 | 1178.8 | -99.8 | 514.3 | -83.8 |
| **13** | 3542.1 | -106.2 | 541.4 | -77.8 | 541.4 | -85.8 | 295.1 | -87.4 |
| **14** | 2352.5 | -111.6 | 271.2 | -71.8 | 271.2 | -67.8 | 687.8 | -70.2 |
| **15** | 2094.0 | -109 | 14.3 | -87.8 | 14.3 | -51 | 1493.0 | -61.8 |
| **16** | 1157.7 | -111.4 | 1097.2 | -95.8 | 399.3 | -66.6 | 1141.3 | -63.8 |
| **17** | 1067.7 | -105 | 482.3 | -59.8 | 482.3 | -51.8 | 1015.6 | -57.4 |
| **18** | 2766.7 | -97.8 | 959.6 | -79.8 | 849.8 | -71.8 | 707.9 | -80.6 |
| **19** | 480.6 | -70.6 | 482.5 | -61.8 | 617.3 | -51 | 480.6 | -60.6 |
| **20** | 364.4 | -61.8 | 372.6 | -64.2 | 489.0 | -53.8 | 364.4 | -63 |
| **21** | 324.2 | -62.2 | 318.5 | -53.8 | 373.3 | -51 | 324.2 | -55.4 |
| **22** | 179.3 | -55.8 | 165.7 | -66.2 | 117.8 | -53.8 | 179.3 | -59 |
| **23** | 152.5 | -51 | 221.7 | -70.2 | 365.1 | -61.8 | 152.5 | -57 |
| **24** | 366.4 | -69.4 | 367.0 | -51 | 515.1 | -55.8 | 366.4 | -60.2 |
| **25** | 548.5 | -70.2 | 547.0 | -51 | 694.6 | -51 | 548.5 | -54.6 |
| **26** | 339.4 | -62.2 | 317.1 | -89.8 | 428.7 | -55 | 339.4 | -60.2 |
| **27** | 323.5 | -71.8 | 363.7 | -83.8 | 430.3 | -69.8 | 323.5 | -61.4 |
| **28** | 464.2 | -59 | 554.1 | -75.8 | 517.9 | -85.8 | 464.2 | -54.6 |

Similarly, the average values of RSSI in dBm measured for 2G Networks at each of the points in Figure 3.7 are shown in Table 3.5 for the suburban environment.

Table 3.5 Average RSSI (dBm) of 2G Networks in Okengwe Suburban Environment

| | 9mobile 2G | | MTN 2G | | Glo 2G | | Airtel 2G | |
|---|---|---|---|---|---|---|---|---|
| **S/N** | **Distance (m)** | **$RSSI_{ave}$ (dBm)** | **Distance (m)** | **$RSSI_{ave}$ (dBm)** | **Distance (m)** | **$RSSI_{ave}$ (dBm)** | **Distance (m)** | **$RSSI_{ave}$ (dBm)** |
| **1** | 1746.0 | -59 | 1182.7 | -65 | 936.9 | -74.6 | 1215.7 | -51.4 |
| **2** | 1928.0 | -56.2 | 873.4 | -60.2 | 858.9 | -51.8 | 1437.9 | -53.4 |
| **3** | 619.5 | -62.6 | 434.2 | -51 | 607.5 | -51 | 1385.0 | -56.2 |
| **4** | 445.1 | -57.8 | 404.9 | -70.2 | 406.7 | -61.8 | 1472.3 | -53.8 |
| **5** | 404.9 | -53 | 411.2 | -51 | 335.5 | -53.8 | 1535.7 | -52.2 |
| **6** | 181.9 | -51.4 | 192.6 | -51 | 77.7 | -51 | 1555.8 | -59 |
| **7** | 199.3 | -51 | 194.8 | -55.8 | 137.0 | -57.8 | 199.3 | -60.2 |
| **8** | 445.2 | -55.8 | 357.6 | -60.2 | 419.9 | -60.2 | 445.2 | -55.8 |
| **9** | 731.6 | -63.4 | 1424.6 | -57.8 | 3596.0 | -60.2 | 4538.0 | -74.2 |
| **10** | 798.0 | -62.6 | 1243.5 | -55.4 | 917.0 | -59.8 | 4491.9 | -66.2 |
| **11** | 790.0 | -84.6 | 959.3 | -51 | 928.8 | -69.8 | 4681.4 | -70.6 |
| **12** | 1032.1 | -77.8 | 520.3 | -63 | 1178.8 | -85.8 | 4865.9 | -65 |
| **13** | 1196.7 | -91.8 | 258.4 | -69.8 | 541.4 | -70.2 | 5360.2 | -69 |
| **14** | 1077.9 | -92.6 | 271.2 | -55.8 | 271.2 | -51.8 | 5864.1 | -73.8 |
| **15** | 1190.5 | -85.8 | 692.9 | -86.2 | 14.3 | -51 | 729.5 | -60.2 |
| **16** | 1421.6 | -84.6 | 875.2 | -87.8 | 399.3 | -53.4 | 889.1 | -55.8 |
| **17** | 1515.3 | -69 | 482.3 | -61 | 482.3 | -51 | 971.1 | -59 |
| **18** | 707.9 | -83 | 959.6 | -71.8 | 849.8 | -65.8 | 707.9 | -67.4 |
| **19** | 480.6 | -51.8 | 482.5 | -61 | 617.3 | -53.8 | 480.6 | -55 |
| **20** | 364.4 | -51 | 372.6 | -53.8 | 489.0 | -53.8 | 364.4 | -54.2 |
| **21** | 324.2 | -51.4 | 318.5 | -51 | 373.3 | -53.8 | 324.2 | -51.8 |
| **22** | 179.3 | -51 | 165.7 | -57.4 | 117.8 | -51 | 1480.7 | -51.8 |
| **23** | 152.5 | -51 | 221.7 | -60.2 | 365.1 | -69 | 152.5 | -55.8 |
| **24** | 366.4 | -52.6 | 367.0 | -53.8 | 515.1 | -56.2 | 366.4 | -59 |
| **25** | 548.5 | -55.8 | 547.0 | -51 | 694.6 | -53 | 548.5 | -51 |
| **26** | 339.4 | -51 | 317.1 | -84.2 | 428.7 | -78.6 | 339.4 | -53.4 |
| **27** | 323.5 | -63.8 | 363.7 | -80.2 | 430.3 | -69.4 | 323.5 | -53.8 |
| **28** | 464.2 | -55.8 | 554.1 | -72.2 | 517.9 | -70.2 | 464.2 | -52.6 |

Table 3.2 Average RSSI(dBm) of 2G Networks in Okengwe Suburban Area

Figure 3.8 shows the measurement points (Appendix C) and the BTS locations of the serving networks in Agasa/Upogoro rural environment.

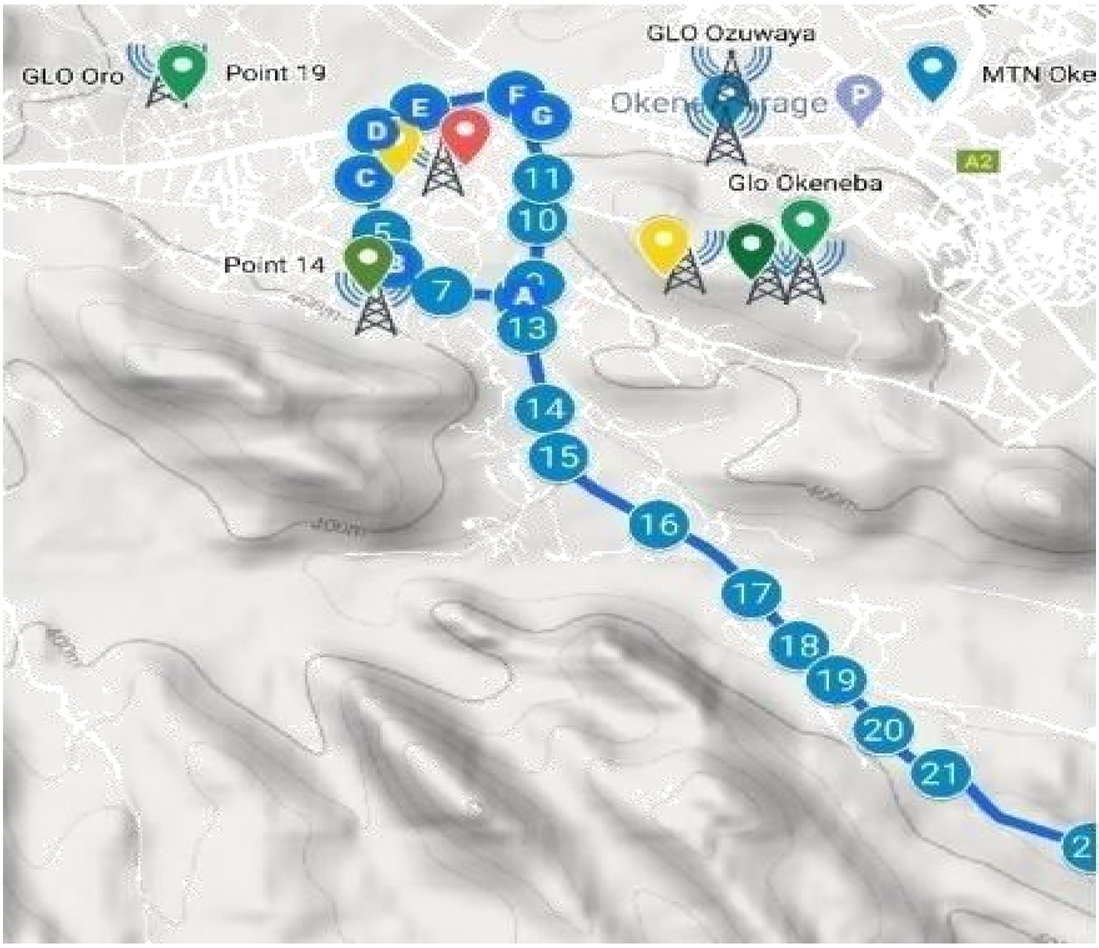


Figure 3. 8 Drive Test Routes in Agasa/Upogoro Rural Environment with Measurement Points and BTS Locations (Source: Google maps; Plotted: 10th February, 2020)

The average values of RSSI in dBm measured at each of the points in Figure 3.8 for Agasa/Upogoro Rural environment are shown in Table 3.6.

Table 3.6 Average RSSI (dBm) of 3G Networks in Agasa/Upogoro Rural Environment

| | **9mobile 3G** | | **MTN 3G** | | **Glo 3G** | | **Airtel 3G** | |
|---|---|---|---|---|---|---|---|---|
| **S/N** | **Distance (m)** | **$RSSI_{ave}$ (dBm)** | **Distance (m)** | **$RSSI_{ave}$ (dBm)** | **Distance (m)** | **$RSSI_{ave}$ (dBm)** | **Distance (m)** | **$RSSI_{ave}$ (dBm)** |
| **1** | 1123.3 | -87.8 | 593.0 | -60.6 | 1323.3 | -68.2 | 430.7 | -65.4 |
| **2** | 407.9 | -85.8 | 274.9 | -61.8 | 1012.7 | -63.8 | 282.7 | -68.2 |
| **3** | 812.8 | -80.6 | 127.8 | -69.8 | 853.1 | -65.8 | 295.6 | -82.6 |
| **4** | 593.6 | -63.8 | 335.3 | -71.8 | 898.8 | -81.8 | 307.0 | -83.8 |
| **5** | 332.6 | -61.8 | 1151.1 | -80.6 | 1107.1 | -84.2 | 402.7 | -72.6 |
| **6** | 199.7 | -66.2 | 4230.1 | -64.2 | 1236.3 | -68.2 | 508.2 | -67.8 |
| **7** | 260.1 | -60.2 | 962.6 | -55.4 | 1410.0 | -77 | 597.7 | -77.4 |
| **8** | 562.3 | -67.4 | 657.2 | -51.4 | 1095.3 | -87.8 | 698.1 | -86.2 |
| **9** | 610.0 | -73.8 | 579.4 | -61.8 | 1025.1 | -101.8 | 662.1 | -71 |
| **10** | 730.4 | -71.4 | 587.1 | -66.6 | 3402.3 | -99.4 | 445.1 | -58.6 |
| **11** | 867.7 | -68.6 | 4778.8 | -76.6 | 1501.3 | -92.2 | 383.0 | -57.4 |
| **12** | 447.4 | -69 | 709.2 | -65.4 | 760.7 | -37.8 | 436.4 | -56.6 |
| **13** | 586.1 | -70.2 | 699.9 | -61 | 1097.5 | -94.2 | 835.8 | -77.8 |
| **14** | 808.8 | -84.2 | 884.3 | -98.6 | 1187.9 | -95.8 | 1215.2 | -79 |
| **15** | 1176.0 | -69.8 | 1037.4 | -89.8 | 1275.7 | -80.2 | 1446.8 | -76.2 |
| **16** | 1254.7 | -82.6 | 1238.9 | -99.4 | 1309.5 | -92.2 | 1882.4 | -82.6 |
| **17** | 1972.8 | -96.6 | 2116.6 | -102.6 | 1523.9 | -103 | 2221.6 | -83 |
| **18** | 2272.1 | -92.6 | 6182.8 | -96.2 | 1786.6 | -101.8 | 1961.2 | -93.8 |
| **19** | 2488.9 | -76.6 | 2054.9 | -80.2 | 3815.6 | -89 | 1772.1 | -91.8 |
| **20** | 2779.4 | -77.8 | 2238.0 | -92.2 | 1452.4 | -93.8 | 1543.7 | -89.8 |
| **21** | 3078.4 | -89.4 | 2601.7 | -97.4 | 1254.2 | -90.2 | 1300.1 | -95.8 |
| **22** | 2973.7 | -100.2 | 1168.4 | -87.8 | 2873.4 | -91.8 | 767.3 | -82.2 |
| **23** | 3245.4 | -111.8 | 1087.7 | -96.2 | 2620.3 | -87.8 | 570.2 | -82.6 |
| **24** | 4323.8 | -108.2 | 1121.0 | -102.6 | 2306.5 | -96.6 | 522.5 | -84.2 |
| **25** | 3731.3 | -112.6 | 1274.9 | -88.6 | 2067.9 | -95.8 | 723.2 | -87.8 |
| **26** | 4000.0 | -103.4 | 1531.4 | -95.8 | 1756.2 | -79.8 | 946.9 | -90.6 |
| **27** | 4353.7 | -87.8 | 1842.1 | -99.4 | 1397.1 | -91.4 | 1274.9 | -92.2 |

The average values of RSSI in dBm measured at each of the points in Figure 3.8 for 2G Networks in Agasa/Upogoro Rural environment are shown in Table 3.7.

Table 3.7 Average RSSI (dBm) of 2G Networks in Agasa/Upogoro Rural Environment

| | 9mobile 2G | | MTN 2G | | Glo 2G | | Airtel 2G | |
|---|---|---|---|---|---|---|---|---|
| **S/N** | **Distance (m)** | **$RSSI_{ave}$ (dBm)** | **Distance (m)** | **$RSSI_{ave}$ (dBm)** | **Distance (m)** | **$RSSI_{ave}$ (dBm)** | **Distance (m)** | **$RSSI_{ave}$ (dBm)** |
| **1** | 1123.3 | -60.6 | 593.0 | -65.4 | 1323.3 | -55.8 | 430.7 | -51.8 |
| **2** | 942.4 | -70.2 | 274.9 | -60.6 | 1012.7 | -52.6 | 1168.4 | -64.2 |
| **3** | 812.8 | -73 | 127.8 | -65 | 853.1 | -56.6 | 295.6 | -70.2 |
| **4** | 593.6 | -57.4 | 335.3 | -61.4 | 898.8 | -59.8 | 307.0 | -69.4 |
| **5** | 332.6 | -51.8 | 587.9 | -73.4 | 1107.1 | -68.2 | 402.7 | -33.4 |
| **6** | 199.7 | -51 | 433.3 | -51.8 | 1236.3 | -53.8 | 508.2 | -51.8 |
| **7** | 1236.9 | -51.4 | 582.6 | -51.8 | 1410.0 | -66.2 | 597.7 | -67 |
| **8** | 562.3 | -63.8 | 794.7 | -57.4 | 1095.3 | -67.8 | 698.1 | -73.8 |
| **9** | 610.0 | -52.6 | 579.4 | -60.2 | 1025.1 | -76.2 | 662.1 | -61.8 |
| **10** | 730.4 | -61.4 | 587.1 | -54.2 | 1569.0 | -81.8 | 445.1 | -55 |
| **11** | 867.7 | -53.4 | 639.6 | -67.4 | 1501.3 | -65.4 | 383.0 | -51 |
| **12** | 447.4 | -69 | 709.2 | -59.4 | 760.6 | -51 | 702.8 | -53.8 |
| **13** | 947.7 | -64.2 | 699.9 | -61.8 | 1097.5 | -78.2 | 835.8 | -73.8 |
| **14** | 808.8 | -73 | 884.3 | -87.8 | 1187.9 | -77.8 | 1215.2 | -71.8 |
| **15** | 1176.0 | -65.8 | 1037.4 | -81 | 1275.7 | -70.2 | 1446.8 | -56.2 |
| **16** | 1491.0 | -61.8 | 1238.9 | -96.2 | 1309.5 | -67.8 | 1882.4 | -70.6 |
| **17** | 1972.8 | -66.2 | 1580.8 | -94.2 | 1746.0 | -80.2 | 2350.5 | -63.8 |
| **18** | 2272.1 | -72.2 | 2770.5 | -83.8 | 3626.0 | -78.6 | 2639.5 | -87.4 |
| **19** | 1938.1 | -51.8 | 2054.9 | -82.2 | 1926.1 | -70.2 | 2853.3 | -83.8 |
| **20** | 2779.4 | -70.2 | 2238.0 | -72.2 | 4008.8 | -74.2 | 3145.1 | -77.8 |
| **21** | 3078.4 | -81 | 2601.7 | -89.8 | 1250.6 | -75.8 | 2925.5 | -88.2 |
| **22** | 2973.7 | -89 | 1168.4 | -92.2 | 1165.2 | -71.8 | 3242.3 | -44.6 |
| **23** | 3245.4 | -97 | 1087.7 | -97.8 | 1183.1 | -82.2 | 3414.3 | -70.2 |
| **24** | 4323.8 | -91.8 | 1121.0 | -94.2 | 1322.1 | -79.4 | 3555.5 | -79 |
| **25** | 3731.3 | -90.2 | 1274.9 | -99 | 1518.5 | -87.8 | 3805.5 | -77.8 |
| **26** | 4000.0 | -87.8 | 1531.4 | -96.6 | 1806.8 | -67.4 | 4047.8 | -89.4 |
| **27** | 4353.7 | -66.2 | 1842.1 | -92.2 | 2142.7 | -76.2 | 4377.3 | -81.8 |

Typical parameters used for network analysis are given in Table 3.8.

Table 3.8 Network Parameters Used

| Network Type | BTS Power | BTS Antenna Height | MS Receiver Antenna Height |
|---|---|---|---|
| 2G | 40dB | 32m | 1.5m |
| 3G | 43dB | 30m | 1.5m |

## 3.6 Data Analysis

The models selected as reference models for this study were the Free Space model, the COST-231 model, the Hata model, the Egli model and the ECC-33 model. These models were chosen because they have the characteristics of adaptability to conditions different their original development conditions. They have been used by past researchers to predict path-loss in environments with various type of terrain and they performed well in some of the environments (Imoize and Oseni, 2019; Oudira *et al*., 2018; Shoewu *et al*., 2016).

**a. Measured Path-loss**

The collected data shown in the Tables 3.2 to 3.7 are used to compute the measured Path-loss ($PL_m$) at any measurement point is given by Lin and Maw (2018) as:

$$PL_m \text{ (dB)} = EIRP_t \text{ (dB}_\text{m}) - P_r(\text{dB}_\text{m}) \tag{3.2}$$

Where $EIRP_t$ is the effective isotropic radiated power of the BTS and $P_r$ is the received signal power.

**b. Calculation of Path-loss using Free Space Path-loss models**

The Free Space Path-loss was calculated using Orike et al. (2017) from:

$$P_{Lfs}\ (dB) = 32.44 + 20\log(f_c) + 20\log(d) \tag{3.3}$$

where $P_{Lfs}$ (dB) is the Free Space Path-loss in dB, $f_c$ is the signal carrier frequency in MHz and $d$ is the distance between the transmitter and the receiver in km.

**c. Calculation of Path-loss using Hata Path-loss models**

Hata model path-loss was calculated from:

$$P_L(\text{dB}) = 69.55 + 26.16 \log f_c - 13.82 \log h_t - a(h_r) + (44.9 - 6.55 \log h_t) \log d \tag{3.4}$$

where $a(h_r)$ is a correction factor for effective mobile antenna height (Zreikat and Dordevic, 2017).

For Okengwe Suburban and Agasa/Upogoro Rural areas, the receiver height correction factor used was:

$$a(h_r) = (1.1 \log f_c - 0.7)h_r - (1.56 \log f_c - 0.8) \text{ dB} \tag{3.5a}$$

and for Okene Central urban area:

$$a(h_r) = 3.2(\log 1.75h_r)^2 - 4.97 \text{ dB} \tag{3.5b}$$

**d. Calculation of Path-loss using COST-231 Path-loss models**

The equation used for calculating the COST-231 path-loss is given by Maloku *et al.* (2019) as:

$$P_L \text{ (dB)} = 46.3 + 33.9 \log f_c - 13.28 \log (h_t) - a(h_r) + (44.9 - 6.55 \log h_t)\log d + C_M \tag{3.6}$$

Where $a(h_r)$ is defined in equations (3.5a) and (3.5b) and

$C_M$ = 0 dB for all the three environments since the urban area is not a very large city.

**e. Calculation of Path-loss using Egli Path-loss models**

The Egli model equation used to calculate the path-loss is given by Okoro and Iwuji (2019) as:

$$P_{Legli} \text{ (dB)} = 20 \log f_c + P_0 + 76.3 \tag{3.7}$$

where $P_0 = 40 \log d - 20 \log_{10} h_t + 10 \log_{10} h_r$ (3.8)

**f. Calculation of Path-loss using ECC-33 Path-loss models**

The ECC-33 model path-loss was calculated from Imoize and Oseni (2019) as:

$$P_L = A_{fs} + A_{bm} - G_t - G_r \tag{3.9}$$

where $A_{fs} = 92.4 + 20 \log (d) + 20 \log (f)$ (3.10a)

$A_{bm}$: $= 20.41 + 9.83\log(d) + 7.894\log(f) + 9.56[\log(f)]^2$ (3.10b)

$G_t$: $= \log(h_t)(13.958 + 5.8[\log(d)]^2)$ (3.10c)

$G_r$: $= [42.57 + 13.7 \log(f)][\log(h_r) - 0.585]$ (3.10d)

**g. Tables of Results**

Equipped with the field measurements of RSSI, location data and the above equations for the various reference models, the stage was set for the computation of the path-loss at the 2G (1800MHz) and 3G (2100MHz) frequencies of each network in each of the environments. The computation was done using the Microsoft Excel spreadsheet. The tables of the results can be found in Appendices D to L.

### 3.7 RMSE of Calculated Path-loss

In order to determine the closeness of the predicted path-loss to the measured or actual path-loss, the statistical root mean square deviation (RMSD or RMSE) is calculated for each predicted path-loss data set for each network type in each environment and is given by Lin and Maw (2018):

$$RMSE = \sqrt{\sum_{i=1}^{n} \frac{[PL_m(d) - PL_r(d)]^2}{n}} \tag{3.11}$$

where $PL_m(d)$ = measured path loss (dB), $PL_r(d)$ = calculated path loss (dB) and $n$ = number of measured data points.

Since data was collected from the four available networks for this research, the average RMSE of each predicted model for the four networks were determined and used for the modeling. This gave a broader and better description of the actual path-loss of the environments as it covers every part of the environments.

# CHAPTER FOUR

## 4.0 RESULTS AND DISCUSSION

### 4.1 Measured Received Signal Strength Indicator (RSSI)

The variation of the RSSI (dBm) with distance (km) presented in Tables 3.2 to 3.7 are the raw field data in that order. The RSSI values were re-arranged in order of increasing distance and presented along with measured and calculated path-loss in Appendices D-L.

The rearranged RSSI-distance variation data in Appendices D-L are presented graphically in order to visually observe the pattern of the received signal strength variation with increasing distances away from the transmitting antenna.

#### 4.1.1 3G RSSI Variation in the Urban environment

Figures 4.1(a)-(d) show the variation of the RSSI with Receiver-Base Transceiver Station separation for 3G Networks in Okene Central Urban environment.

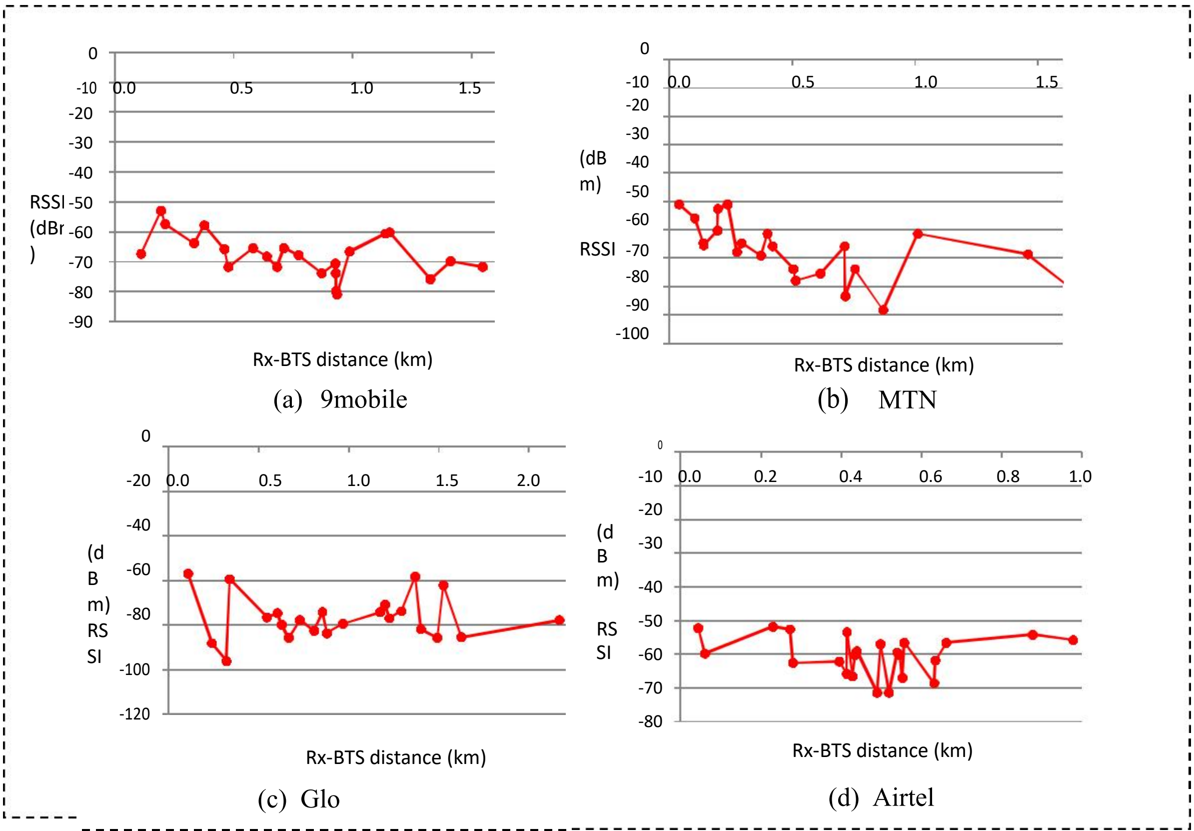


Figure 4. 1 RSSI Variation with Distance for 3G UMTS in the Urban Area

The level of irregularities in the graph pattern in Figure 4.1 and the low RSSI even at points close to the BTS are majorly the effect of the mountainous terrain. In addition, the Okene Central urban environment is also characterised by buildings of two to three storeys very close (some 5m to 8m) to the roads where measurements were taken. The shadowing effects of the buildings also contribute to the irregular shapes of the graphs. Density of population and vehicular penetration are high and also contibute to the high path-loss.

### 4.1.2 3G RSSI Variation in the Suburban environment

Figures 4.2(a)-(d) show the RSSI-distance relationship for 3G Networks in Okengwe Suburban environment.

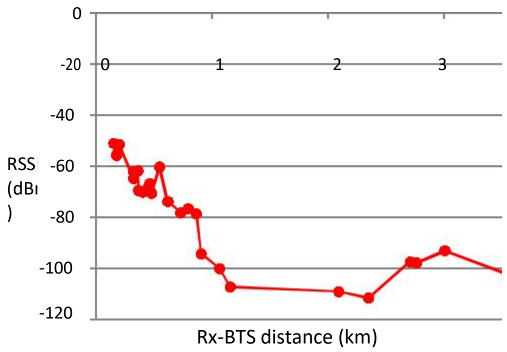


(a) 9mobile

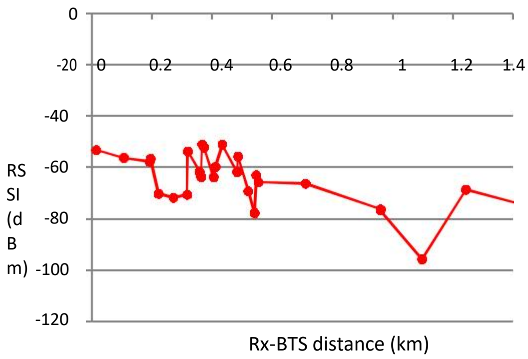


(b) MTN

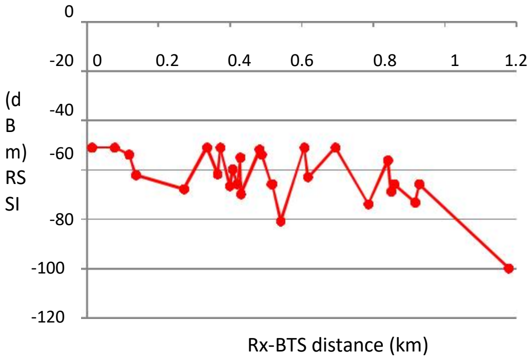


(c) Glo

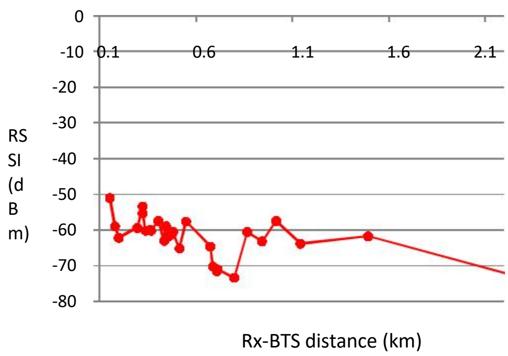


(d) Airtel

Figure 4. 2 RSSI Variation with Distance for 3G UMTS in the Suburban Area

The Okengwe suburban environment, unlike the Okene Central Urban area, is not characterised with buildings too close to the roads where signal measurements were captured. There is clearance of at least 15m to 20m between the buildings and the road. Hence the buildings do not contribute significantly to the signal path-loss experienced in this area. The mountains are the major factors. Vehicular penetration is not high and the population is moderate.

### 4.1.3 3G RSSI Variation in the Rural environment

Figures 4.3(a)-(d) show the variation of RSSI with 3G Networks in Agasa/Upogoro rural environment.

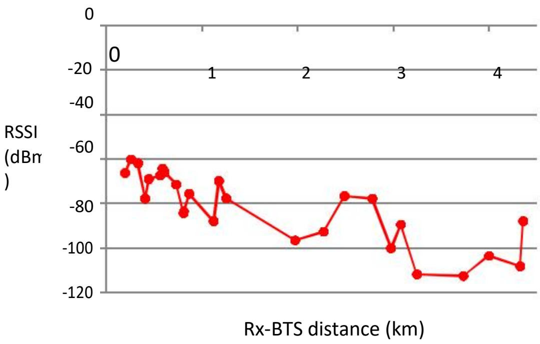


(a) 9mobile

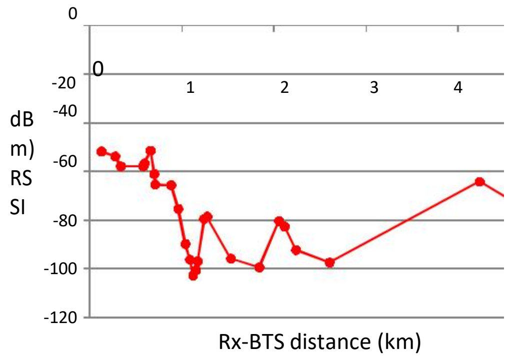


(b) MTN

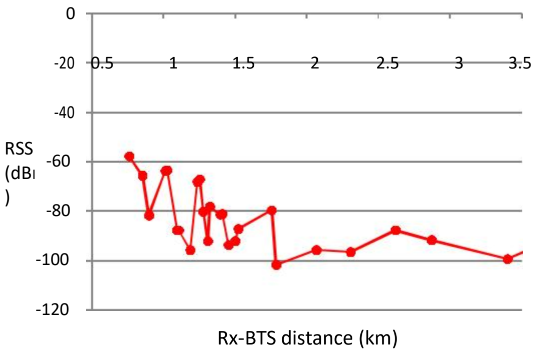


(c) Glo

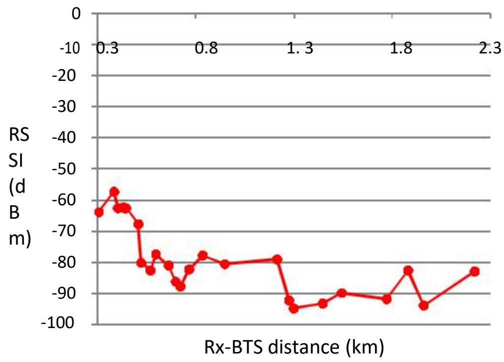


(d) Airtel

Figure 4. 3 RSSI Variation with Distance for 3G UMTS in the Rural Area

From Figure 4.3, it can be seen that the RSSI variation graphs (a) – (d) for the Agasa/ Upogoro environment follow a similar irregular pattern. The environment has a long stretch of road where measurements were taken (see Figure 3.9). The environment is fairly open, implying that there is good clearance between the buildings and the roads. The population is relatively lower than the suburban environment and the effect of vehicular penetration is very insignificant. The observed graph pattern is majorly a function of the hilly terrain. The signal level towards the far end is very low.

### 4.1.4 2G RSSI Variation in the Urban environment

The 2G received signal variation for Okene Central urban environment is shown in Figure 4.4.

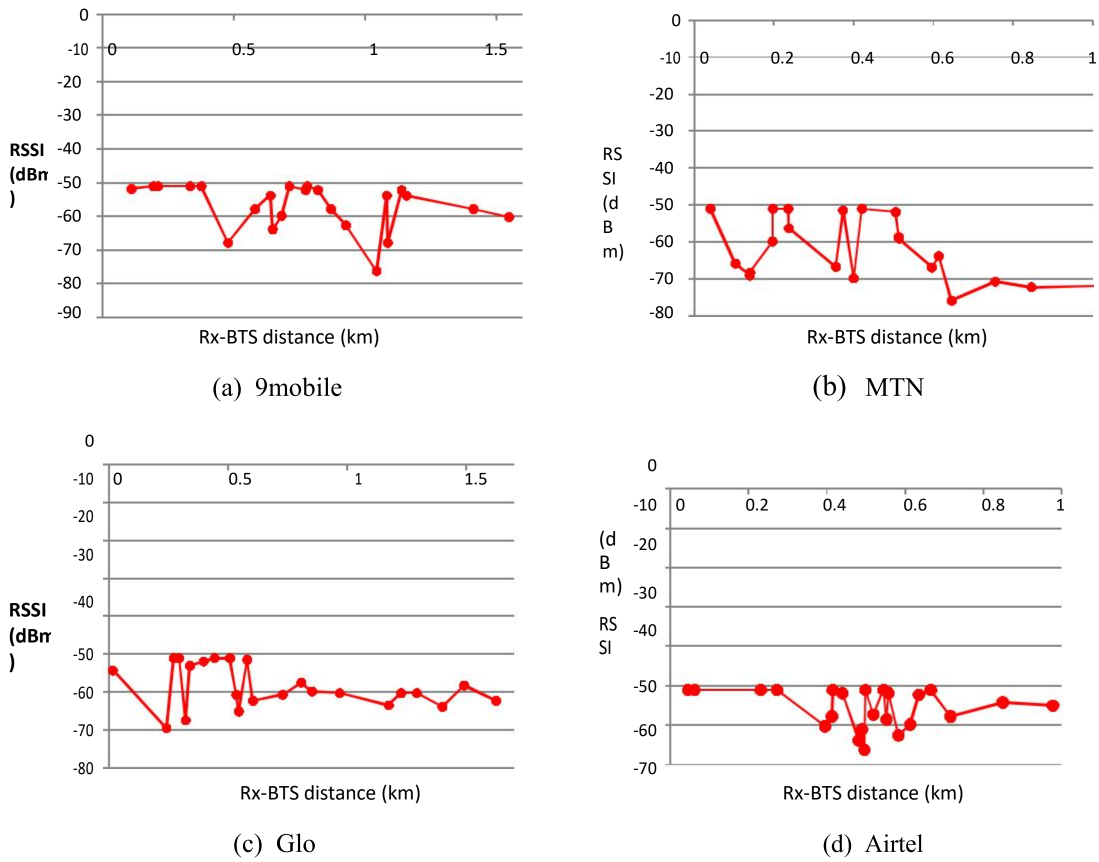


(a) 9mobile (b) MTN

(c) Glo (d) Airtel

Figure 4. 4 RSSI Variation with Distance for 2G EDGE in the Urban Area

The irregular pattern of the graphs in Figure 4.4 are relatively similar for the four Networks. 2G received signals are higher than the 3G because 2G transmission frequency is lower than 3G frequencies and signal losses increase with increasing frequencies. However, the irregular graph pattern is caused by the same factors explained in Section 4.1.1.

### 4.1.5 2G RSSI Variation in the Suburban environment

Figure 4.5(a)-(d) shows the variation pattern of received signal with distance at the 1800MHz frequency in the Suburban environment.

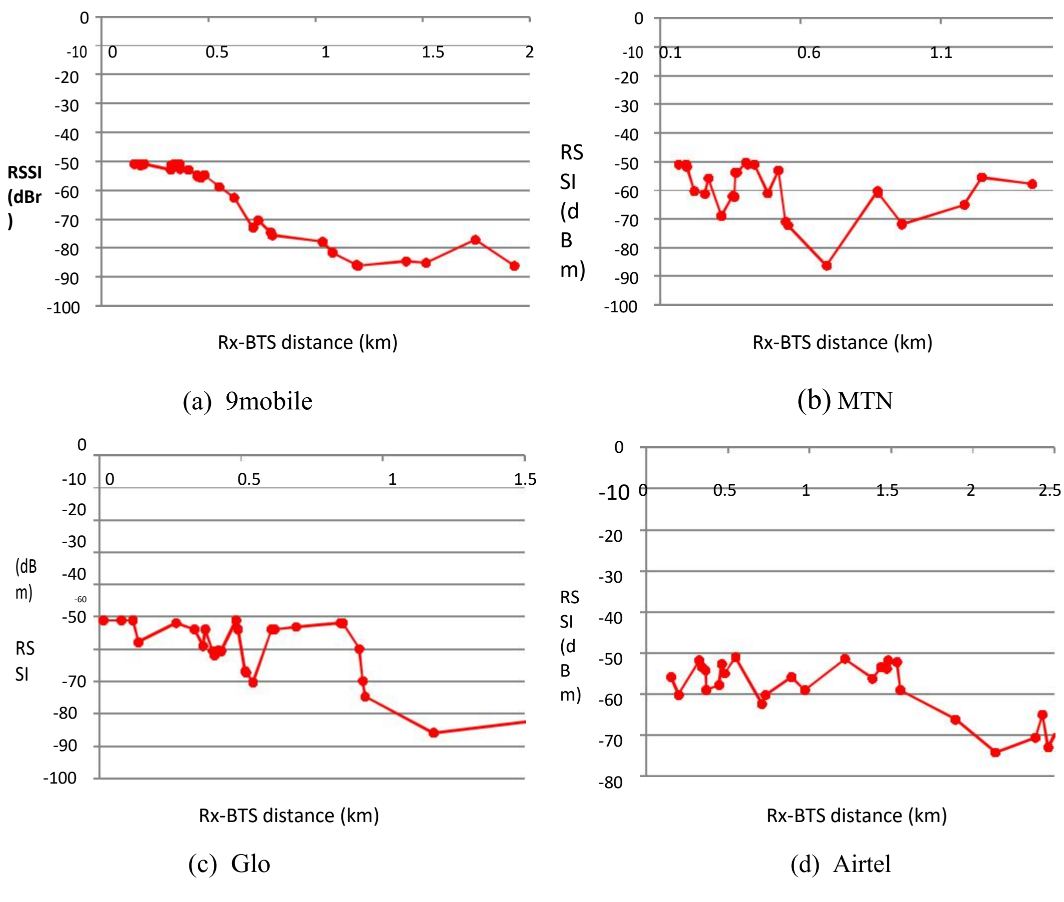


Figure 4.5 RSSI Variation with Distance for 2G EDGE in the Suburban Area

The pattern of the graphs in Figure 4.5 is irregular majorly because of the mountainous terrain as ealier explained in Section 4.1.2. The variation pattern of MTN is slightly different from the other three. This is because the MTN BTS is located on one of the mountains such that, at a distance greater than 1km, very high signal level can still be received at some points where the other path-loss factors are not significant.

### 4.1.6 2G RSSI Variation in the Rural environment

In Agasa/Upogoro Rural environment, the RSSI-Distance variation for the 2G Networks are as shown in the graphs (a)-(d) of Figure 4.6.

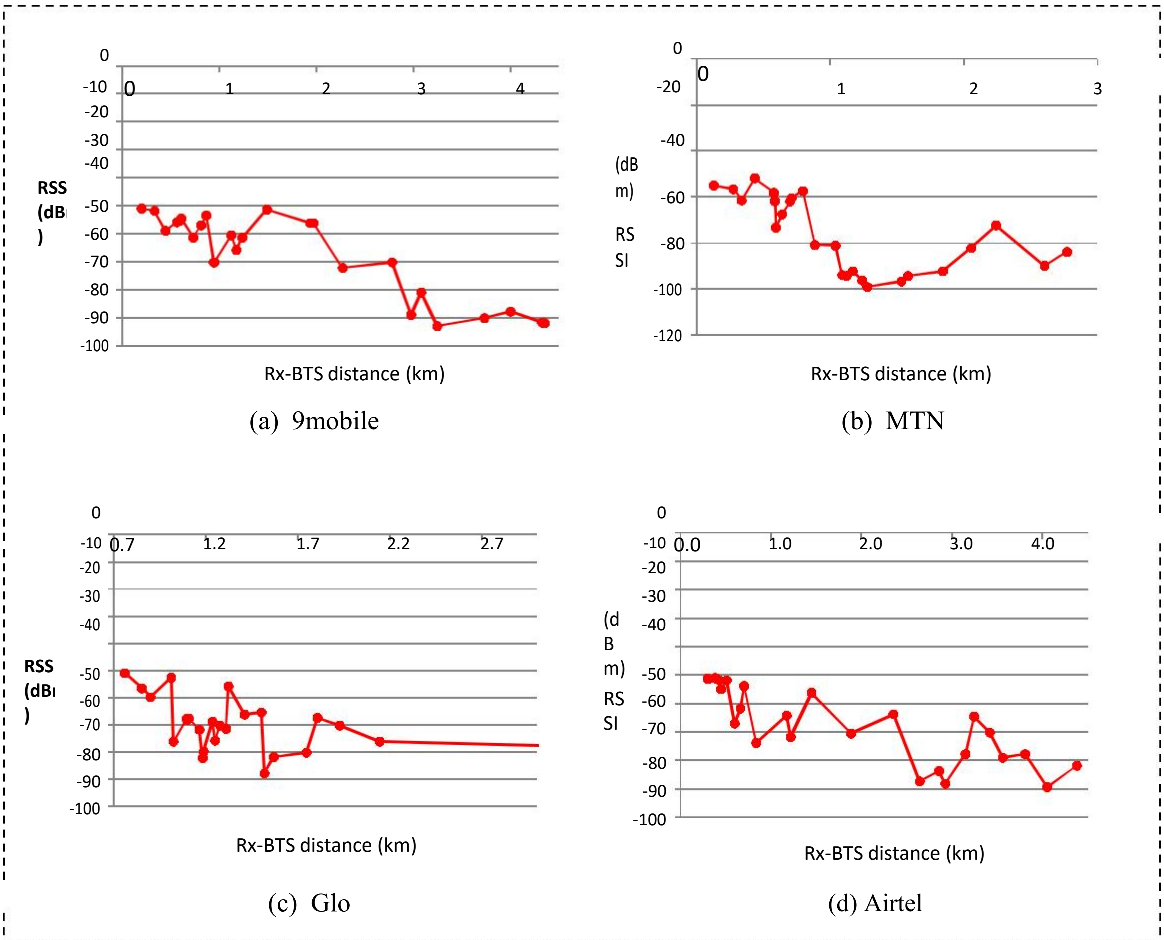


Figure 4.6 RSSI Variation with Distance for 2G EDGE in the Rural Area

The highly irregular graph pattern observed in Figure 4.6 for the Agasa/Upogoro Rural area indicates the irregular mountainous terrain as explained in Section 4.1.3. In addition, the more interior part of the environment is about 3km from any serving BTS resulting in very poor reception.

## 4.2 Measured and Calculated Path-loss

The values of measured Path-loss ($PL_m$) and the calculated path-loss for Free Space model ($PL_{fs}$), COST-231 model ($PL_{cost231}$), Hata model ($PL_{hata}$), Egli model ($PL_{egli}$) and ECC-33 model ($PL_{ecc33}$) are contained in Appendix D to L. Figures 4.7 to 4.12 are the graphical representation of the measured and calculated path-loss for all the Network Services and Network types in the three environments.

### 4.2.1 3G Networks Signal Path-loss in the Urban Area

Figure 4.7(a-d) shows the comparison between the reference models path-loss and the measured path-loss for 3G Networks (9mobile, MTN, Glo and Airtel) in the urban environment.

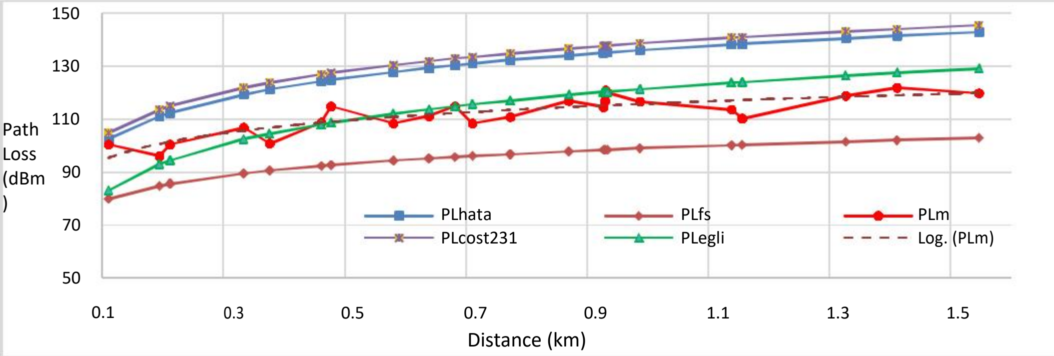


(a) 9mobile

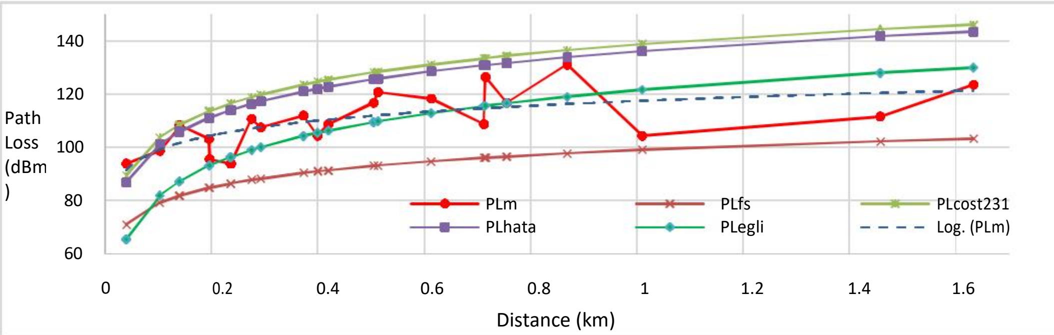


(b) MTN

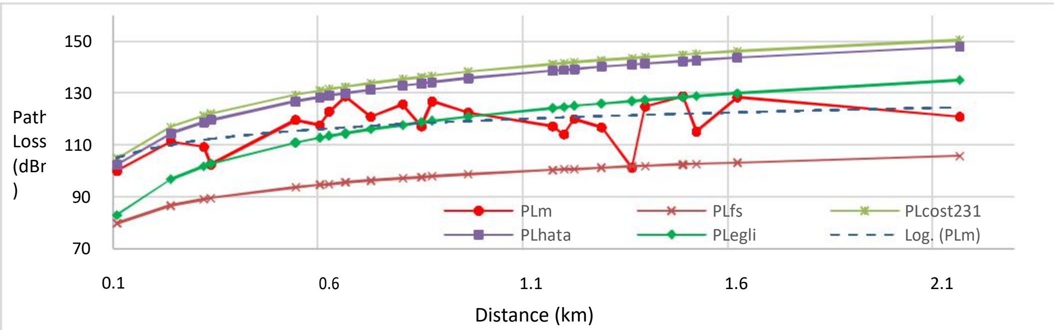


(c) Glo

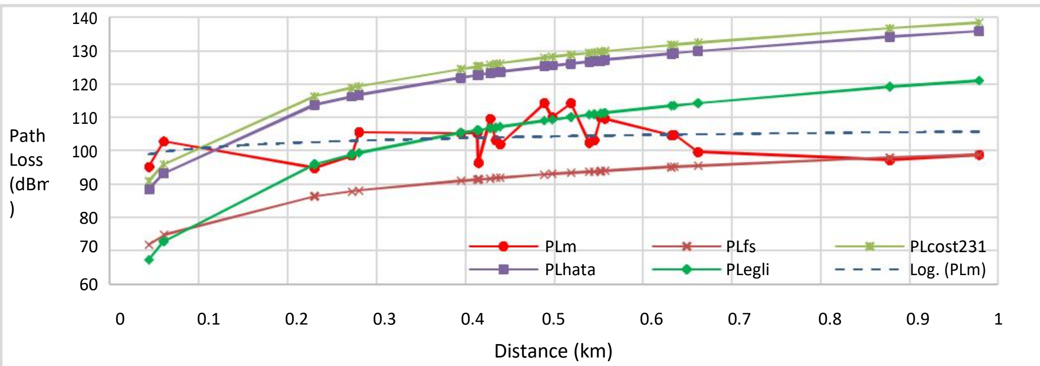


(d) Airtel

Figure 4.7 Measured and Calculated Path-loss for 3G Networks in the Urban Area

The path-loss graphs (a) – (d) of Figure 4.7 show that the Free Space model consistently under predicts the path-loss for the 3G Network in the urban environment. The Hata ($PL_{hata}$) and COST-231 ($PL_{cost231}$) models give path-loss predictions higher than the actual measurements in all of the graphs (a) – (d). The ECC-33 ($PL_{ecc33}$) model predictions are so

much greater than the actual measured path-loss that it could not be displayed in the graphs for the purpose of clarity. The over-prediction of the ECC-33 model can be seen in the path-loss tables in the Appendix D to I. The Egli model ($PL_{egli}$), in its original form,

exhibits a relatively better prediction than the rest. However, a better prediction model is possible after optimization of all the models than that of the Egli model in its original form.

The consistent pattern of the measured and calculated path-loss in the four graphs is an indication of the agreement between the measurement data from the four Networks serving the environment.

### 4.2.2 3G Networks Signal Path-loss in the Suburban Area

The measured and calculated path-loss for 3G signals in Okengwe Suburban environment is presented in the graphs (a) to (d) of Figure 4.8.

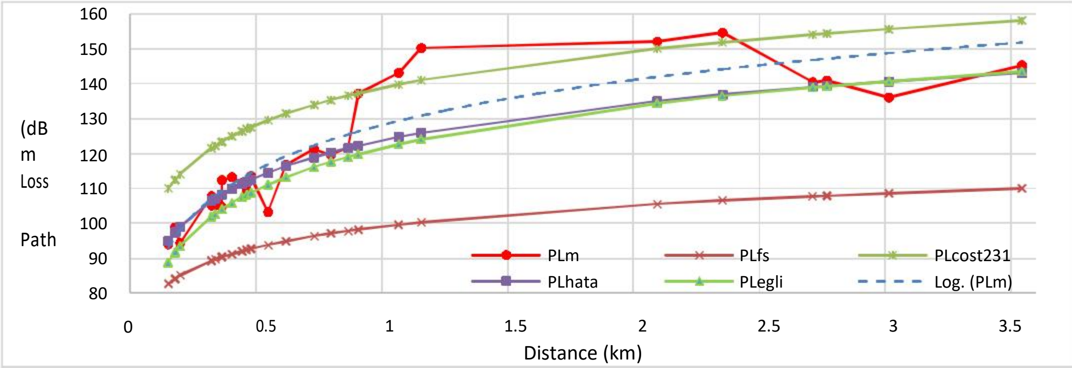


(a) 9mobile

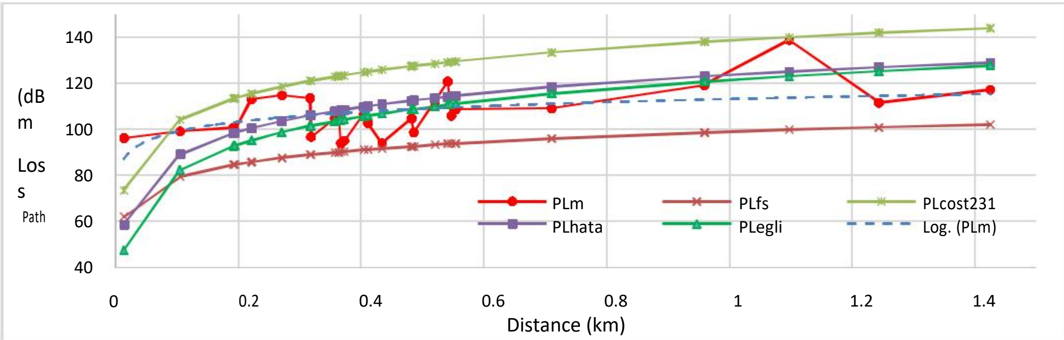


(b) MTN

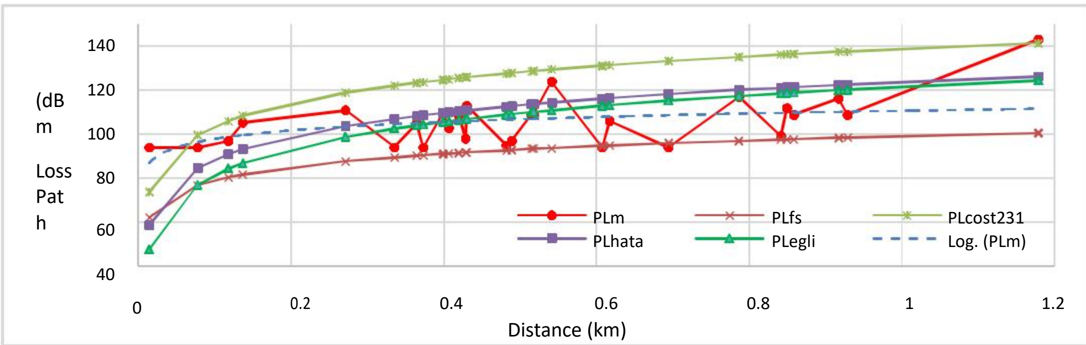


(c) Glo

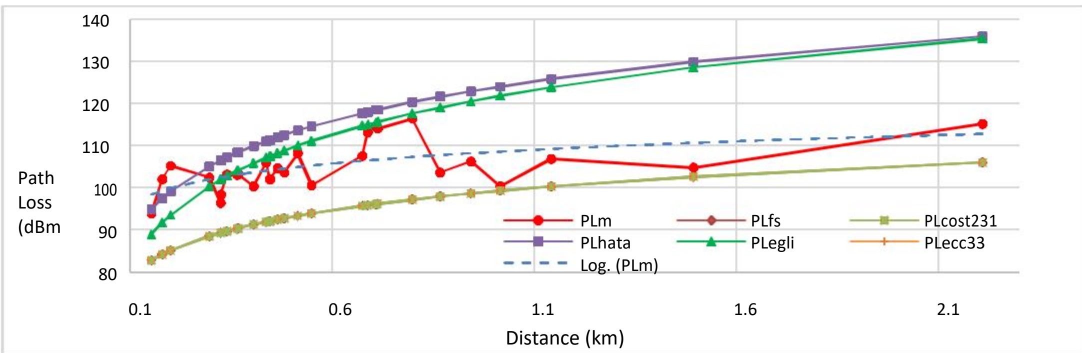


(d) Airtel

Figure 4.8 Measured and Calculated Path-loss for 3G Network in the Suburban Area

As shown in Figure 4.8, the Hata and Egli models in their original forms show high level of closeness to the measured path-loss. COST-231 and Free Space predictions show significant deviation from the measured path-loss.

### 4.2.3 3G Networks Signal Path-loss in the Rural Area

The measured and calculated path-loss for 3G signals in Agasa/Upogoro rural environment is presented in the graphs (a) to (d) of Figure 4.9.

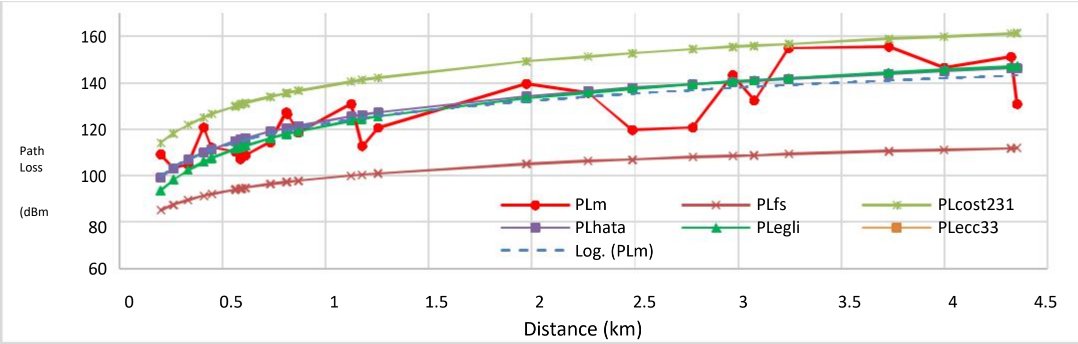


(a) 9mobile

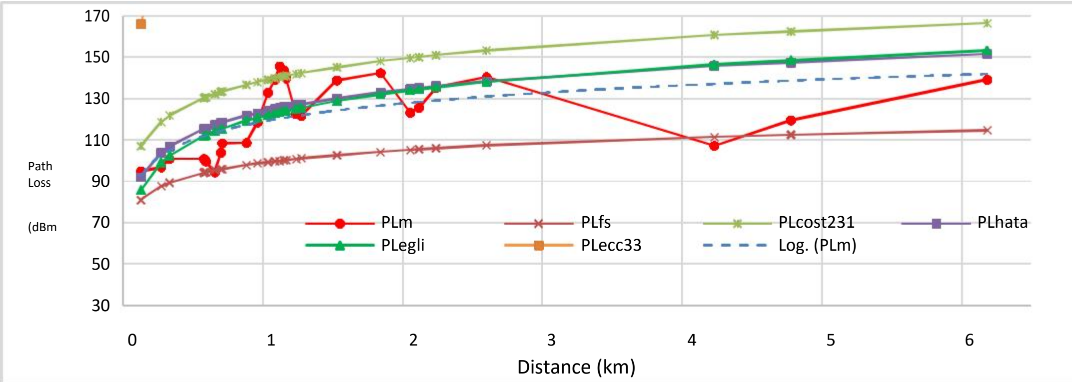


(b) MTN

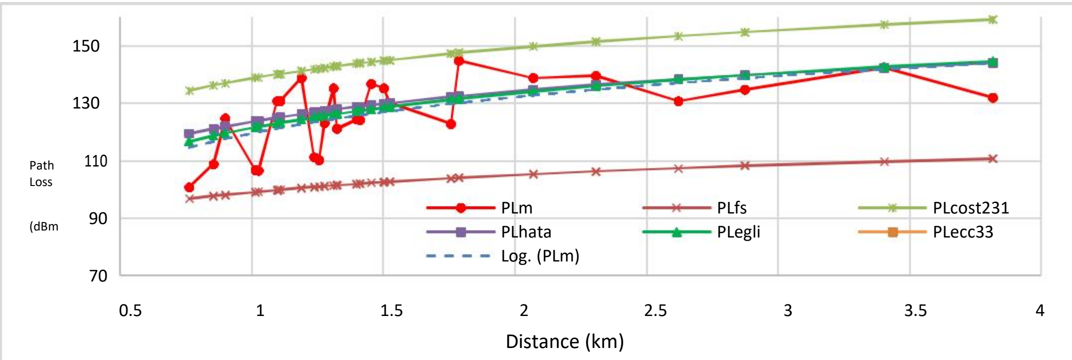


(c) Glo

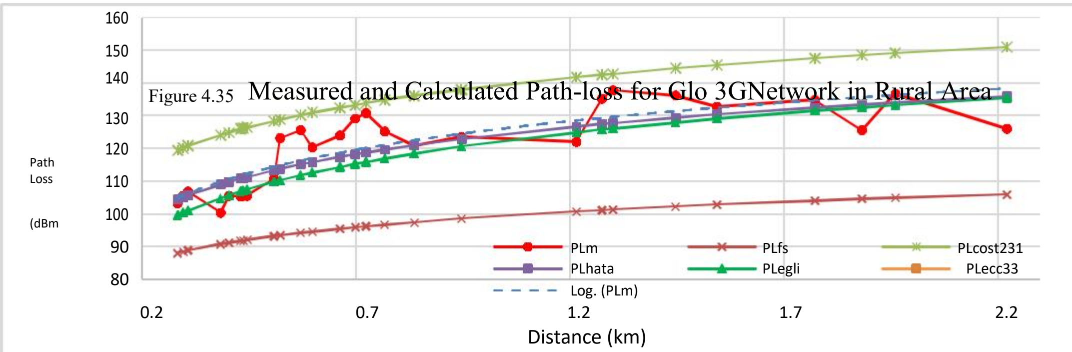


(d) Airtel

Figure 4. 9 Measured and Calculated Path-loss for 3G Networks in the Rural Area

Figure 4.9 shows that the Hata and Egli models prediction of path-loss in the rural area is closer to the actual values than the COST-231 and Free Space models. This is similar to the case of the surburban area. This could be because of the similarity in topography and other factors causing path-loss in the two environments.

### 4.2.4 2G Networks Signal Path-loss in the Urban Area

The measured and calculated path-loss for 2G signals in Okene Central urban environment is presented in the graphs (a) to (d) of Figure 4.10.

The graphs reveal that the COST-231 model consistently over-predicts the path-loss for the urban area at 2G 1800MHz frequencies. The Free Space model and Hata model slightly under-predict and over-predict the path-loss respectively.

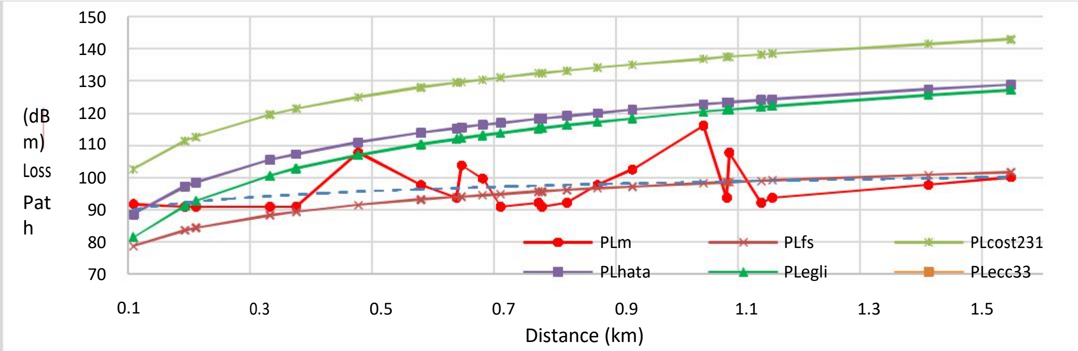


(a) 9mobile

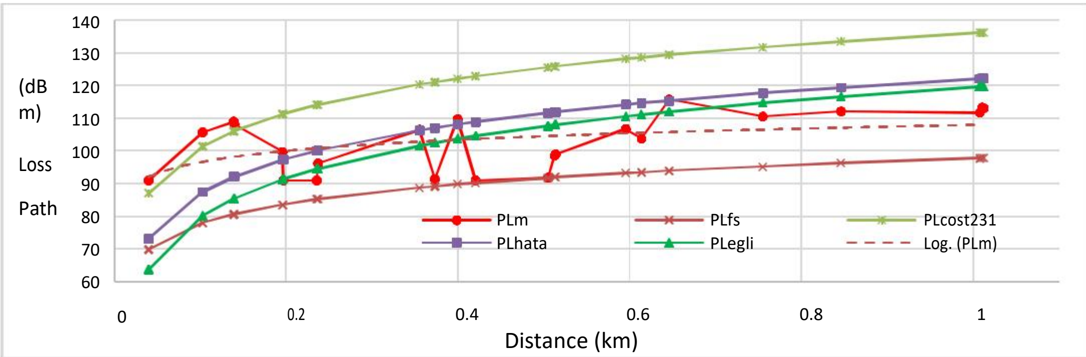


(b) MTN

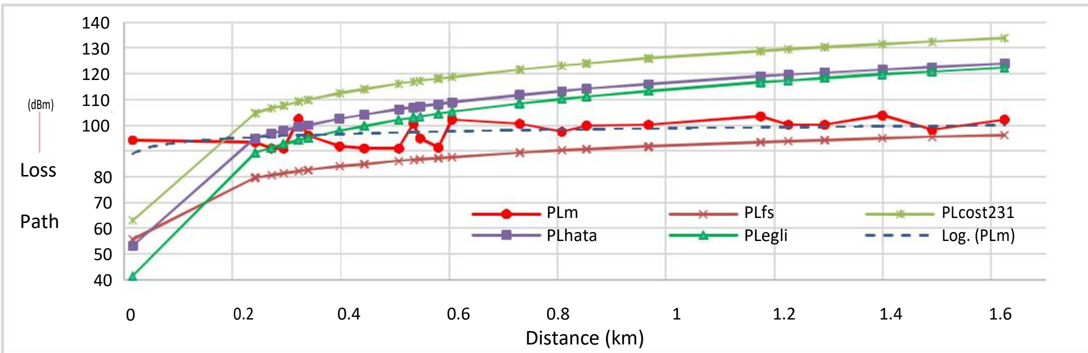


(c) Glo

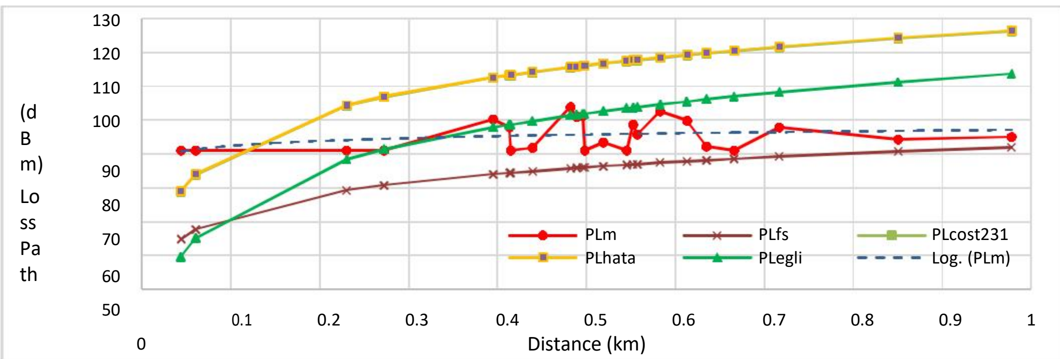


(d) Airtel

Figure 4.10 Measured and Calculated Path-loss for 2G Networks in the Urban Area

However, the Egli model consistently gives a path-loss prediction that is close to the measured path-loss as observed in Figure 4.10.

### 4.2.5 2G Networks Signal Path-loss in the Suburban Area

The measured and calculated path-loss for 2G signals in Okengwe suburban environment is presented in the graphs (a) to (d) of Figure 4.11.

Similar to the 2G urban environment case, the COST-231 model consistently over-predicts the path-loss for the suburban area at 2G (1800MHz) frequencies. The Free Space model under-predicts the path-loss. The level of predictions by the Hata and Egli models is close to the measured path-loss and the precision is high too.

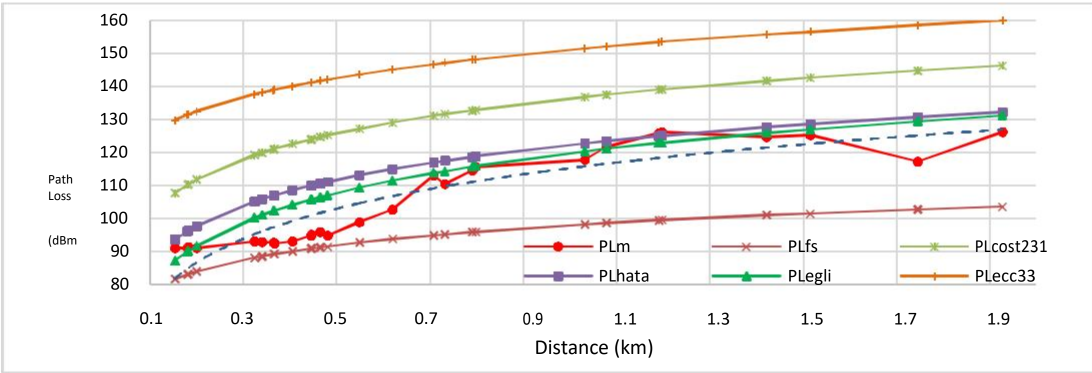


(a) 9mobile

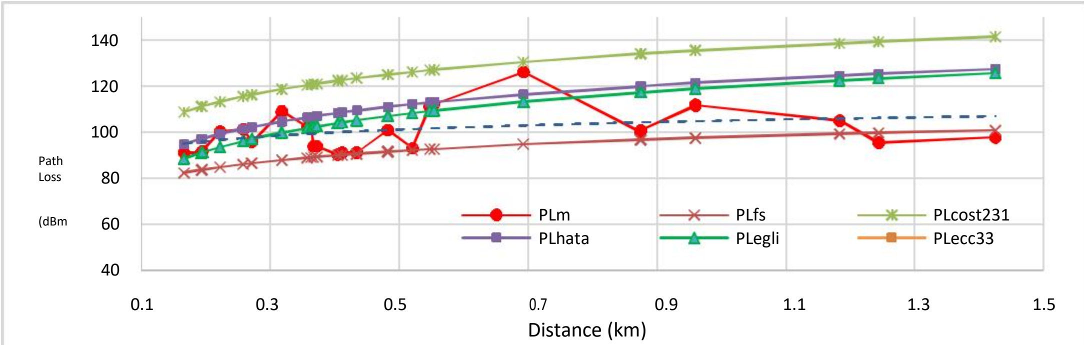


(b) MTN

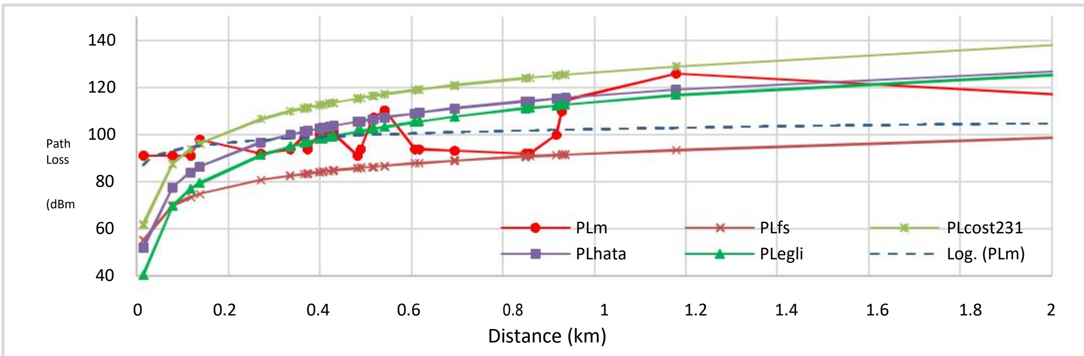


(c) Glo

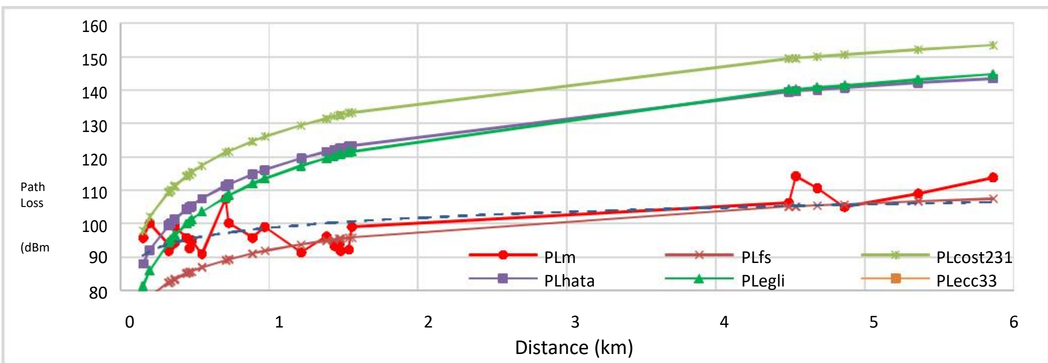


(d) Airtel

Figure 4.11 Measured and Calculated Path-loss for 2G Networks in the Suburban Area

### 4.2.6 2G Networks Signal Path-loss in the Rural Area

The measured and calculated path-loss for 2G signals in Agasa/Upogoro rural environment is presented in the graphs (a) to (d) of Figure 4.12.

In all the four graphs, the COST-231 model and Free Space model consistently over-predicts and under-predicts the path-loss respectively for the rural area at 2G 1800MHz frequencies. None of the models exhibit closeness in path-loss prediction to the measured path-loss. The predictions by the Hata and Egli models are close to each other. This shows that none of the models can give a reasonable prediction in this environment without modification.

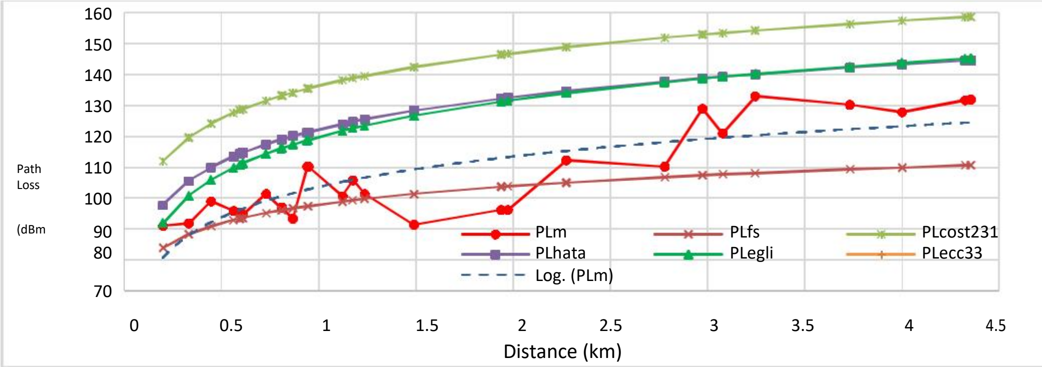


(a) 9mobile

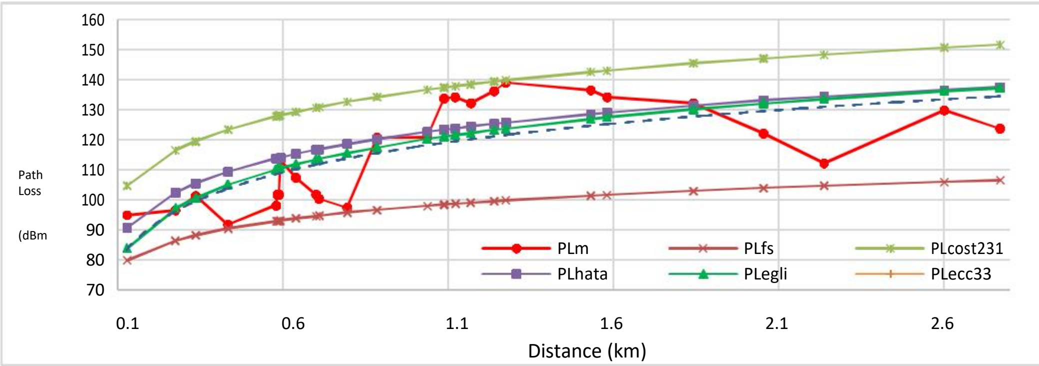


(b) MTN

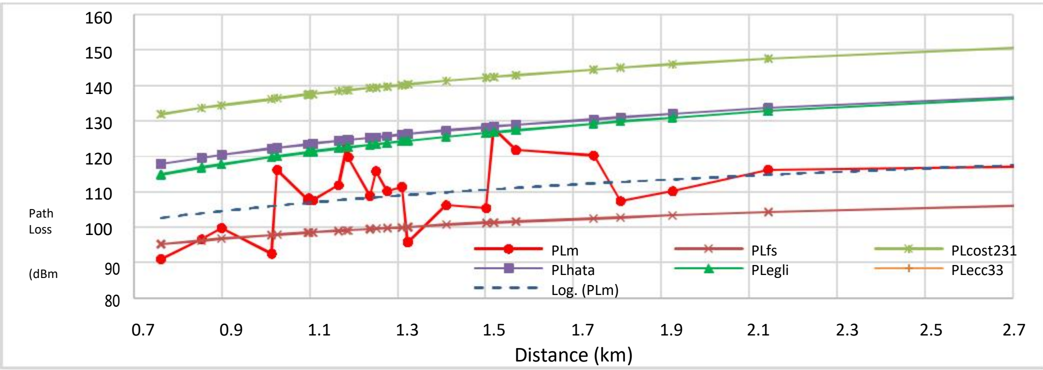


(c)()Glo

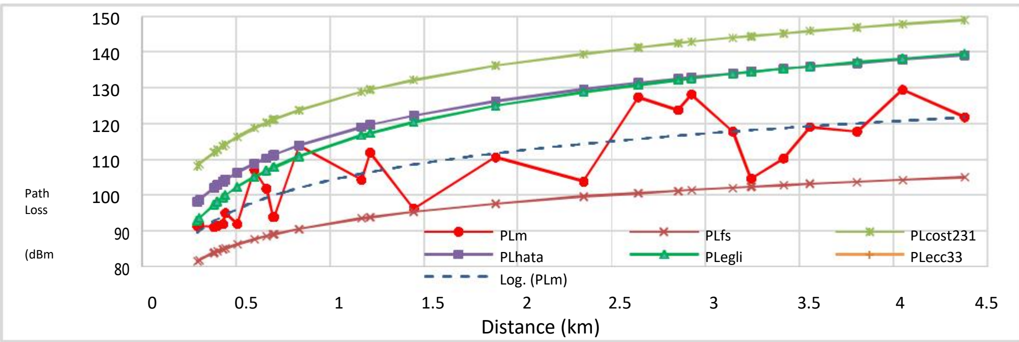


(d) Airtel

Figure 4.12 Measured and Calculated Path-loss for 2G Network in the Rural Area

## 4.3 Validation of Calculated Path-loss/RMSE Values

Sections 4.2 and 4.3 present the graphs for visual assessment of the nature of received signal strength and the path-loss in the three environments. The empirical analysis was done by calculating the RMSE of each path-loss model for each network and network type and for each environment using equation (3.11).

Since the measured signal strengths of four different networks whose cells spread over each of the areas are being used, it is most appropriate that the average of the four RMSE values is employed in the evaluation and modeling process. This is in contrast to several other studies in which only one network is considered in arriving at the optimal models (Shoewu *et al.*, 2016; Worgu *et al.*, 2017).

The average RMSE value ($RMSE_{ave}$) of each reference path-loss model was calculated by:

$$RMSE_{ave} = \frac{1}{n}\sum_{i=1}^{n} RMSE_i \qquad (4.1)$$

where $RMSEi$ is the RMSE of the $i$ th Network.

### 4.3.1 RMSE Values of Path Loss Models for Urban Environment

The RMSE of the reference models for 3G and 2G are shown in Tables 4.1 and 4.2 respectively for the four Networks in the urban environment. The Tables also present the average RMSE of each of the models which is calculated using equation (4.1).

Table 4.1 RMSE Values of Path Loss Models for 3G Networks Urban Environment

| | Network | FS | COST-231 | Hata | Egli | ECC-33 |
|---|---|---|---|---|---|---|
| 1 | **9mobile 3G** | 16.91 | 20.95 | 18.49 | 6.80 | 154.29 |
| 2 | **MTN 3G** | 20.55 | 16.99 | 14.98 | 12.29 | 126.85 |
| 3 | **Glo 3G** | 22.01 | 19.66 | 17.46 | 10.25 | 163.77 |
| 4 | **Airtel 3G** | 14.51 | 23.58 | 21.30 | 12.18 | 133.17 |
| | **Average RMSE** | **18.50** | **20.30** | **18.06** | **10.38** | **144.52** |

Table 4.1 shows that the Egli model in its original form has an average RMSE of 10.38dBm which is the least of the five models. This shows that it will perform better in path-loss prediction in this environment than the others as observed also from Section 4.2.1 and Figure 4.7(a-d). ECC-33 model deviates widely from measured path-loss by a very wide margin of 144.52dBm. Hence it cannot be employed for path-loss prediction in this environment in the 3G (2100MHz) frequency.

Table 4.2 RMSE Values of Path Loss Models for 2G Networks in Urban Environment

| | Network | FS | COST-231 | Hata | Egli | ECC-33 |
|---|---|---|---|---|---|---|
| 1 | **9mobile 2G** | 7.52 | 34.29 | 21.10 | 18.76 | 164.77 |
| 2 | **MTN 2G** | 16.14 | 21.03 | 11.81 | 12.57 | 126.90 |
| 3 | **Glo 2G** | 12.69 | 23.66 | 16.25 | 15.93 | 160.30 |
| 4 | **Airtel 2G** | 12.48 | 20.74 | 20.89 | 12.26 | 141.17 |
| | **Average RMSE** | **12.21** | **24.93** | **17.51** | **14.88** | **148.29** |

Table 4.2 shows that Free Space model gives the least RMSE of 12.21dBm in the 2G 1800MHz frequency in the urban environment. But Free Space model is not feasible since the environment under investigation consists of other sources of path-loss also. The ECC-33 model again deviates widely with a RMSE of 148.28dBm. The rest of Egli model, Hata model and COST-231 model have average RMSEs of 14.88dBm, 17.51dBm and 24.93dBm respectively.

### 4.3.2 RMSE Values of Path Loss Models for Suburban Environment

The RMSE of the reference models for 3G and 2G networks are shown in Tables 4.3 and 4.4 respectively for the four networks in the urban environment. The tables also present the average RMSE of each of the models.

Table 4.3 RMSE Values of Path Loss Models for 3G Networks Suburban Environment

| | Network | FS | COST-231 | Hata | Egli | ECC-33 |
|---|---|---|---|---|---|---|
| 1 | **9mobile 3G** | 27.32 | 14.47 | 8.45 | 9.54 | 163.29 |
| 2 | **MTN 3G** | 18.70 | 20.48 | 11.69 | 12.99 | 131.40 |
| 3 | **Glo 3G** | 17.58 | 23.30 | 13.73 | 14.35 | 135.55 |
| 4 | **Airtel 3G** | 12.51 | 24.99 | 11.51 | 9.96 | 146.74 |
| | **Average RMSE** | **19.03** | **20.81** | **11.35** | **11.71** | **144.25** |

From Table 4.3, the RMSE of 3G network for the suburban environment shows Hata model with the least deviation of 11.35dBm, closely followed by Egli model with an average RMSE of 11.71dBm. Free Space model, COST-231 model and ECC-33 model give wider deviations of 19.03dBm, 20.81dBm and 144.25dBm respectively.

Table 4.4 RMSE Values of Path Loss Models for 2G Networks in Suburban Environment

| | Network | FS | COST-231 | Hata | Egli | ECC-33 |
|---|---|---|---|---|---|---|
| 1 | **9mobile 2G** | 14.66 | 23.24 | 10.11 | 7.08 | 139.88 |
| 2 | **MTN 2G** | 12.61 | 25.70 | 13.77 | 11.93 | 139.48 |
| 3 | **Glo 2G** | 17.10 | 20.73 | 14.89 | 15.92 | 145.62 |
| 4 | **Airtel 2G** | 9.61 | 30.36 | 21.70 | 20.95 | 203.18 |
| | **Average RMSE** | **13.50** | **25.01** | **15.12** | **13.97** | **157.04** |

The model with the least average RMSE, from Table 4.4, is the Free Space model with average RMSE of 13.50dBm and followed closely by Egli model with deviation of 13.97dBm. Hata model also gave an RMSE of 15.12 which is close to the first two.

COST-231 model average path-loss is 25.01dBm while ECC-33 model consistently gives an unacceptably wide deviation of 157.04dBm.

### 4.3.3 RMSE Values of Path Loss Models for Rural Environment

The RMSE values of reference path-loss models for the rural environment is presented in Tables 4.5 and 4.6 for 3G and 2G networks respectively.

Table 4.5 RMSE Values of Path Loss Models for 3G Networks in Rural Environment

| | Network | FS | COST231 | Hata | Egli | ECC33 |
|---|---|---|---|---|---|---|
| 1 | **9mobile 3G** | 26.2 | 18.7 | 8.92 | 9.26 | 188.36 |
| 2 | **MTN 3G** | 24.65 | 24.35 | 14.72 | 14.53 | 187.84 |
| 3 | **Glo 3G** | 26.21 | 20.32 | 9.87 | 9.48 | 193.55 |
| 4 | **Airtel 3G** | 25.38 | 15.11 | 6.55 | 7.67 | 154.34 |
| | **Average RMSE** | **25.61** | **19.62** | **10.02** | **10.24** | **181.02** |

The two models with the lowest average RMSEs shown in Table 4.5 are Hata model and Egli model with 10.02dBm and 10.24dBm respectively. COST-231 and Free Space came next with values of 19.62dBm and 25.61dBm respectively. ECC-33 has an average RMSE of 181.02dBm in the rural environment at 3G 2100MHz frequency.

Table 4.6 RMSE Values of Path Loss Models for 2G Networks in Rural Environment

| | Network | FS | COST231 | Hata | Egli | ECC33 |
|---|---|---|---|---|---|---|
| 1 | **9mobile 2G** | 11.82 | 34.14 | 20.68 | 19.12 | 204.07 |
| 2 | **MTN 2G** | 22.25 | 21.45 | 11.52 | 10.68 | 166.09 |
| 3 | **Glo 2G** | 12.46 | 32.42 | 19.26 | 17.75 | 199.43 |
| 4 | **Airtel 2G** | 14.75 | 24.37 | 15.22 | 13.94 | 205.29 |
| | **Average RMSE** | **15.32** | **28.1** | **16.67** | **15.37** | **193.72** |

The average RMSEs of reference path-loss models in the rural environment at the 2G 1800MHz is shown in Table 4.6. Although the deviations are generally high, the least deviation is exhibited by the Free Space model followed closely by the Egli model with values of 15.32dBm and 15.37dBm respectively. Hata model followed the first two closely with deviation of 16.67dBm. The widest deviation was exhibited by the ECC-33 model with the value of 193.72dBm.

### 4.3.4 Summary of average RMSE Values for all Environments

The summary of the average RMSE values extracted from Tables 4.1 to 4.6 is presented in Tables 4.7 and 4.8 for the 3G Network and 2G Network respectively.

Table 4.7 Average RMSE for 3G Network

| | | FS | COST231 | Hata | Egli | ECC33 |
|---|---|---|---|---|---|---|
| 1 | **Urban** | 18.50 | 20.30 | 18.06 | 10.38 | 144.52 |
| 2 | **Suburban** | 19.03 | 20.81 | 11.35 | 11.71 | 144.25 |
| 3 | **Rural** | 25.61 | 19.62 | 10.02 | 10.24 | 181.02 |

Table 4.8 Average RMSE for 2G Networks

| | | FS | COST231 | Hata | Egli | ECC33 |
|---|---|---|---|---|---|---|
| 1 | **Urban** | 12.21 | 24.93 | 17.51 | 14.88 | 148.29 |
| 2 | **Suburban** | 13.50 | 25.01 | 15.12 | 13.97 | 157.04 |
| 3 | **Rural** | 15.32 | 28.10 | 16.67 | 15.37 | 193.72 |

Except for the Free Space model, all the models show increasing deviation from actual path-loss with decreasing frequency from 3G 2100MHz to 2G 1800MHz. This shows that none of the models can predict the path-loss of the mountainous environment accurately at 1800MHz frequency without modification.

## 4.4 Modeling

Obtaining an accurate and suitable path-loss model is achieved either by modeling or by modifying existing models (Popoola *et al.,* 2018; Worgu *et al*., 2017). The process of developing models suitable for the various environments in Okene land, which is the aim of this research, is by modifying existing path-loss models that were employed as reference models.

Having studied their performances in the various environments for 2G and 3G Networks, it has been observed that ECC-33 model consistently predicts path-loss values with excessive deviation from the measured path-loss. This is most likely because it was developed for frequencies above 3000MHz. It is therefore not suitable for modification for optimization in any of the environments under investigation. The Free Space model also does not qualify for consideration because it is not realistic. Having disqualified the Free Space and the ECC-33 models, the rest of COST-231 model, Hata model and Egli model are presented for modification to achieve optimal path-loss models for each of the environments.

### 4.4.1 The Modification Process

The average RMSE value for each model was used to modify the model by adding and subtraction the average RMSE value to and from its original equation. For instance, in the 3G Network, for the urban environment (Table 4.7), the average RMSE of ±18.06 of the un-modified Hata model was added to and subtracted from the Hata model equation so that the modified Hata model, $PL_{mod\text{-}hata}$, is:

$$PL_{mod\text{-}hata}(dB) = PL_{hata}(dB) \pm 18.06 \qquad (4.2)$$

The two evolving models are:

$$PL_{mod\text{-}hata}^{+} = 87.61 + 26.16\log f_c - 13.82\log h_t - a(h_r) + (44.9 - 6.55\log h_t)\log d \qquad (4.3)$$

and

$$PL_{mod\text{-}hata}^{-} = 51.49 + 26.16\log f_c - 13.82\log h_t - a(h_r) + (44.9 - 6.55\log h_t)\log d \qquad (4.4)$$

Equations (4.3) and (4.4) are then used to predict new path-loss values at 3G 2100MHz for the four Networks (9mobile, MTN, Glo and Airtel) in the urban environment. The RMSEs of the new path-loss values are computed and the new average RMSE determined. Finally, the new average RMSEs are compared with the former average RMSE to determine the model with the least average RMSE.

The process in equations (4.2) to (4.4) is repeated for the COST-231 and the Egli models for the four networks in the three environments. The computations were done using Microsoft Excel Spreadsheet.

The average RMSE of the modified models and those of the original models were compared (Figures 4.13 to 4.18). The model with the lowest average RMSE value is selected as the best performance path-loss prediction model for that network type in that environment.

### 4.4.2 Modification Results

The results of the processes in Section 4.5.1 are presented in the bar charts of Figures 4.13 to 4.18. The bar charts compare the average RMSEs of the modified models of the COST-231, Hata and Egli models with those of the un-modified models for the environment. The model with the least average RMSE is the optimal model for the environment.

### 4.4.3 Path-loss Model Optimization for 3G 2100MHz:

The path-loss models optimization at the 3G frequencies for the three environments follows the procedure explained in details below.

#### i. Urban Environment:

The average RMSE for the modified and un-modified models in the urban environment at 3G frequencies is shown in Figure 4.13. The chart indicates that the COST-231 model, with the average RMSE of 20.30dBm subtracted from it, gives the least average RMSE of 9.39dBm.

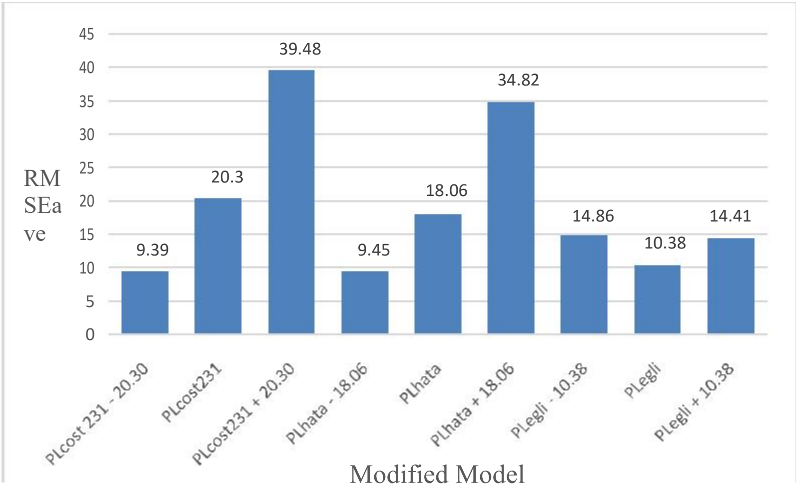


Figure 4.13 Urban 3G UMTS Model RMSE

Therefore, the optimal model for 3G in the urban environment is obtained by subtracting 20.30 from the COST-231 model. Thus the modified COST-231, $PL_{mod\text{-}cost231}$, is:

$$PL_{mod\text{-}cost231} = (46.3 - 20.3) + 33.9\log f_c - 13.28\log(h_t) - a(h_r) + (44.9 - 6.55\log h_t)\log d + C_M \quad (4.5)$$

and the optimal model for 3G in the urban environment, $PL_{opt\text{-}urban3G}$, therefore is:

$$PL_{opt\text{-}urban3G} = 26.0 + 33.9\log f_c - 13.28\log(h_t) - a(h_r) + (44.9 - 6.55\log h_t)\log d + C_M \quad (4.6)$$

**ii. Suburban Environment:**

Figure 4.14 presents the average RMSE values for the modified and un-modified models in the suburban environment at 3G frequencies. The chart shows that the COST-231 model, with the average RMSE of 20.81dBm subtracted from it, gives the least average RMSE value of 11.28dBm.

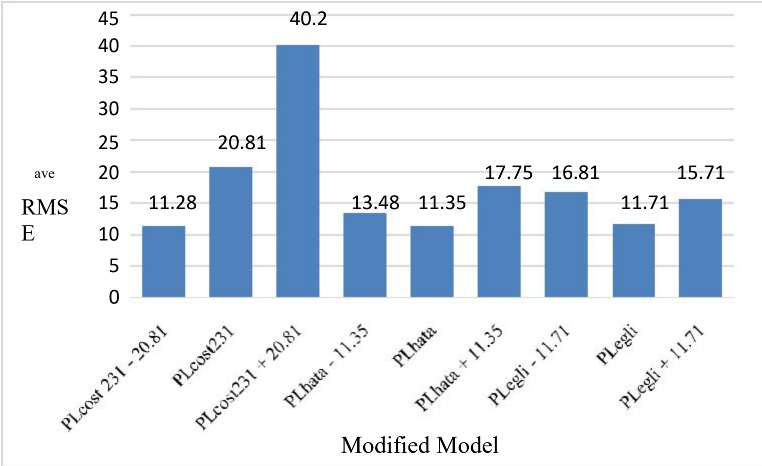


Figure 4.14 Suburban 3G UMTS Model RMSE

Therefore, the optimal model for 3G in the suburban environment is obtained by subtracting 20.81 from the COST-231 model. The modified model is:

$$PL_{mod\text{-}cost231} = (46.30 - 20.81) + 33.9\log f_c - 13.28\log(h_t) - a(h_r) + (44.9 - 6.55\log h_t)\log d + C_M \qquad (4.7)$$

$$PL_{opt\text{-}suburban3G} = 25.49 + 33.9\log f_c - 13.28\log(h_t) - a(h_r) + (44.9 - 6.55\log h_t)\log d + C_M \qquad (4.8)$$

### iii. Rural Environment:

Figure 4.15 shows the average RMSE values for the modified and un-modified models in the rural environment at 3G frequencies. It can be seen from the chart that Hata model in its original form gives an average RMSE of 10.02dBm for 3G Networks in the rural environment which is lower than the average RMSE of any of the modified models.

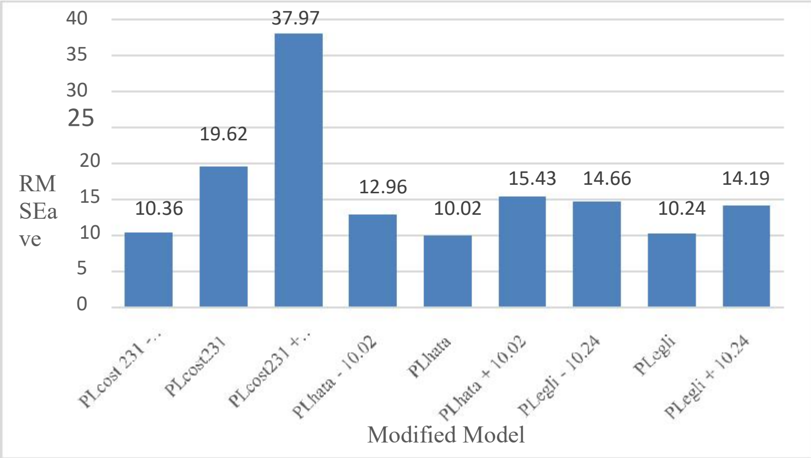


Figure 4.15 Rural 3G UMTS Model RMSE

Therefore, the original Hata model is selected as the best path-loss model for the rural environment at 3G frequencies so that:

$$PL_{opt\text{-}rural3G} = PL_{hata} = 69.55 + 26.16\log f_c - 13.82\log(h_t) - a(h_r) + (44.9 - 6.55\log h_t)\log d \qquad (4.9)$$

### 4.4.4 Path-loss Model Optimization for 2G (1800MHz)

The optimization process in section 4.4.3 is followed to obtain the optimal models at the 2G frequencies for all the three environments.

#### i. Urban Environment:

Figure 4.16 presents the average RMSE values for the modified and un-modified models in the urban environment at 2G frequencies. The chart shows that the COST-231 model, with the average RMSE of 24.93dBm subtracted from it, gives the least average RMSE of 12.99dBm.

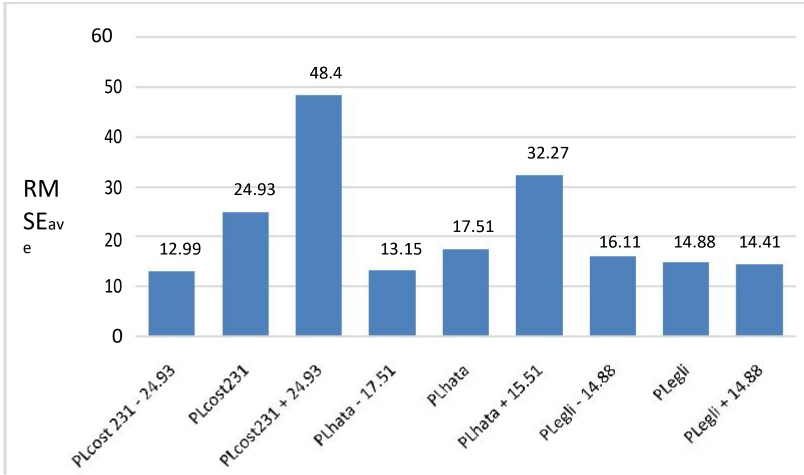


Figure 4.16 Urban 2G UMTS Model RMSE

Therefore the optimal model for 2G path-loss prediction in the urban environment is obtained by subtracting 24.93 from the COST-231 model:

$$PL_{mod\text{-}cost231} = (46.30 - 24.93) + 33.9\log f_c - 13.28\log(h_t) - a(h_r) + (44.9 - 6.55\log h_t)\log d + C_M \quad (4.10)$$

$$PL_{opt\text{-}urban2G} = 21.37 + 33.9\log f_c - 13.28\log(h_t) - a(h_r) + (44.9 - 6.55\log h_t)\log d + C_M \quad (4.11)$$

**ii. Suburban Environment:**

Figure 4.17 show the average RMSE values for the modified and un-modified models in the suburban environment at 2G frequencies. The chart shows that the COST-231 model, with the average RMSE of 25.01dBm subtracted from it, gives the least average RMSE of 11.60dBm.

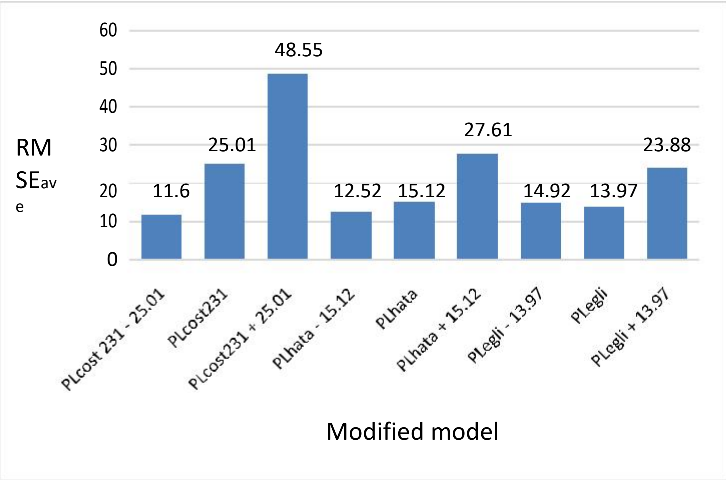


Figure 4.17 Suburban 2G UMTS Model RMSE

Therefore, the optimal model for 2G path-loss prediction in the suburban environment was obtained by subtracting 25.01 from the COST-231 model as follows:

$$PL_{mod\text{-}cost231} = (46.3 - 25.01) + 33.9\log f_c - 13.28\log(h_t) - a(h_r) + (44.9 - 6.55\log h_t)\log d + C_M \quad (4.12)$$

$$PL_{opt\text{-}suburban2G} = 21.29 + 33.9\log f_c - 13.28\log(h_t) - a(h_r) + (44.9 - 6.55\log h_t)\log d + C_M \quad (4.13)$$

### iii. Rural Environment:

Figure 4.18 show the average RMSE values for the modified and un-modified models in the suburban environment at 2G frequencies. The bar chart shows the Hata model, with the average RMSE of 16.67dBm subtracted from it, gives the least average RMSE of 10.34dBm.

Therefore, the optimal model for 2G in the rural environment is obtained by subtracting 16.67 from the Hata model:

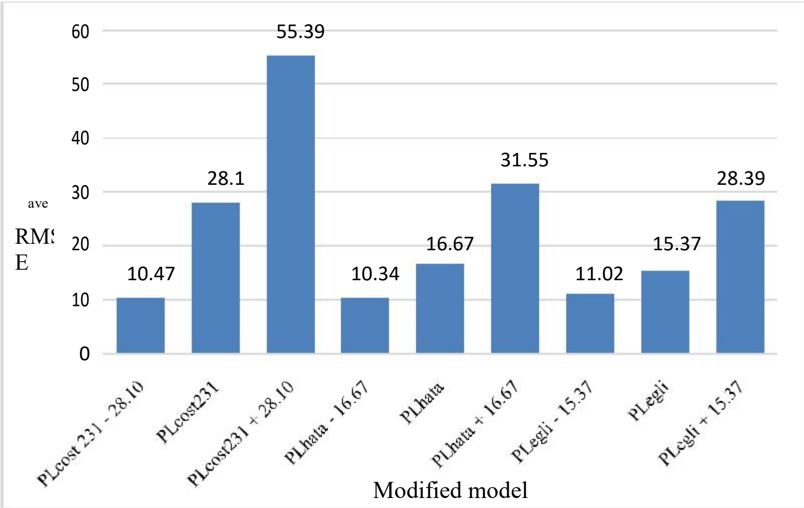


Figure 4.18 Rural 2G UMTS Model RMSE

$$PL_{opt\text{-}hata} = (69.55 - 16.67) + 26.16\log f_c - 13.82\log(h_t) - a(h_r) + (44.9 - 6.55\log h_t)\log d \tag{4.14}$$

$$PL_{opt\text{-}rural3G} = 52.88 + 26.16\log f_c - 13.82\log(h_t) - a(h_r) + (44.9 - 6.55\log h_t)\log d \tag{4.15}$$

## 4.5 Summary of Optimized Path-loss models:

The optimal models for the environments are presented in the following equations:

For 3G network:

*i.* Urban Environment,

$$PL_{opt\text{-}urban3G} = 26.0 + 33.9\log f_c - 13.28\log(h_t) - a(h_r) + (44.9 - 6.55\log h_t)\log d + C_M \tag{4.16}$$

*ii.* Suburban Environment,

$$PL_{opt\text{-}suburban3G} = 26.0 + 33.9\log f_c - 13.28\log(h_t) - a(h_r) + (44.9 - 6.55\log h_t)\log d + C_M \tag{4.17}$$

*iii.* Rural Environment,

$$PL_{opt\text{-}rural3G} = PL_{hata} = 69.55 + 26.16\log f_c - 13.82\log(h_t) - a(h_r) + (44.9 - 6.55\log h_t)\log d \quad (4.18)$$

For 2G Network:

*iv.* Urban Environment,

$$PL_{opt\text{-}urban2G} = 21.37 + 33.9\log f_c - 13.28\log(h_t) - a(h_r) + (44.9 - 6.55\log h_t)\log d + C_M \quad (4.19)$$

*v.* Suburban Environment,

$$PL_{opt\text{-}suburban2G} = 21.29 + 33.9\log f_c - 13.28\log(h_t) - a(h_r) + (44.9 - 6.55\log h_t)\log d + C_M \quad (4.20)$$

*vi.* Rural Environment,

$$PL_{opt\text{-}rural3G} = 52.88 + 26.16\log f_c - 13.82\log(h_t) - a(h_r) + (44.9 - 6.55\log h_t)\log d \quad (4.21)$$

Generally, the optimal Path-loss models for the urban and suburban environments were obtained by modifying the COST-231 model for 3G and 2G networks while the Hata model was modified to obtain the optimal models for the rural environment at 3G and 2G frequencies. This shows that Hata model and COST-231 model, which is an extension of Hata model, are flexible for adaptation to various types of environments.

## 4.6 Performance evaluation

The optimized Path-loss Prediction models for the three environments in Okene Area of Kogi State have been obtained by the modification of existing models. In order to evaluate the performance of these new optimal models, the average RMSE values of the optimal models are compared with those of the reference models to determine the percentage by which each of the reference models was improved by the optimal models.

The percentage improvement of the new models compared with each of the reference models was determined from the relation:

$$\text{Performance over } PL_{ref} = \frac{\text{Average RMSE of } PL_{ref} - \text{Average RMSE of } PL_{opt}}{\text{Average RMSE of } PL_{ref}} \times 100\% \qquad (4.22)$$

where $PL_{opt}$ is the optimal Path-loss model and $PL_{ref}$ is the reference model.

### 4.6.1. Urban environment Optimized model performance

Figures 4.19(a) and (b) show the comparison between the average RMSEs of the optimal model and the reference models for 3G Network and 2G Network respectively in the urban environment.

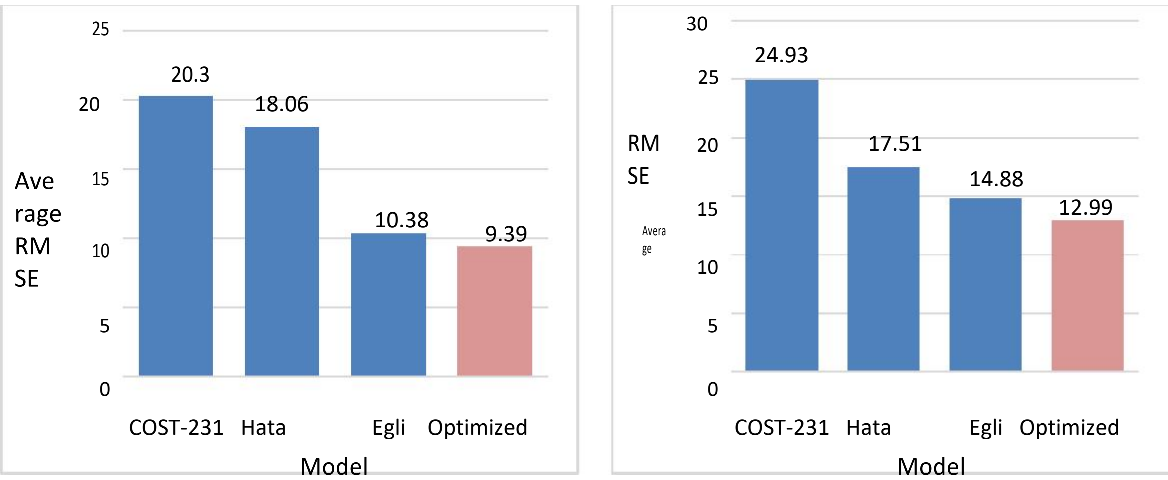


(a) 3G UMTS (b) 2G EDGE

Figure 4.19 Optimized Model Compared with Reference Models for Urban Area

From Figure 4.19(a), using equation (4.22), the performance of 3G $PL_{opt\text{-}urban}$ with respect to each of the reference models is calculated as follows:

$$\text{COST-231} = \frac{20.30 - 9.39}{20.30} \times 100\% = 53.74\% \qquad (4.23)$$

$$\text{Hata} = \frac{18.06 - 9.39}{18.06} \times 100\% = 48.01\% \qquad (4.24)$$

$$\text{Egli} = \frac{10.38 - 9.39}{10.38} \times 100\% = 9.54\% \quad (4.25)$$

From Figure 4.19(b), the 2G optimal model performance is calculated for each reference model as follows:

$$\text{COST-231} = \frac{24.93 - 12.99}{24.93} \times 100\% = 47.89\% \quad (4.26)$$

$$\text{Hata} = \frac{17.51 - 12.99}{17.51} \times 100\% = 25.81\% \quad (4.27)$$

$$\text{Egli} = \frac{14.88 - 12.99}{14.88} \times 100\% = 12.70\% \quad (4.28)$$

### 4.6.2 Suburban environment optimal models performance

Figure 4.20(a) and Figure 4.20(b) show the comparison between the average RMSEs of optimal models and the reference models for 3G network and 2G network respectively in the suburban environment.

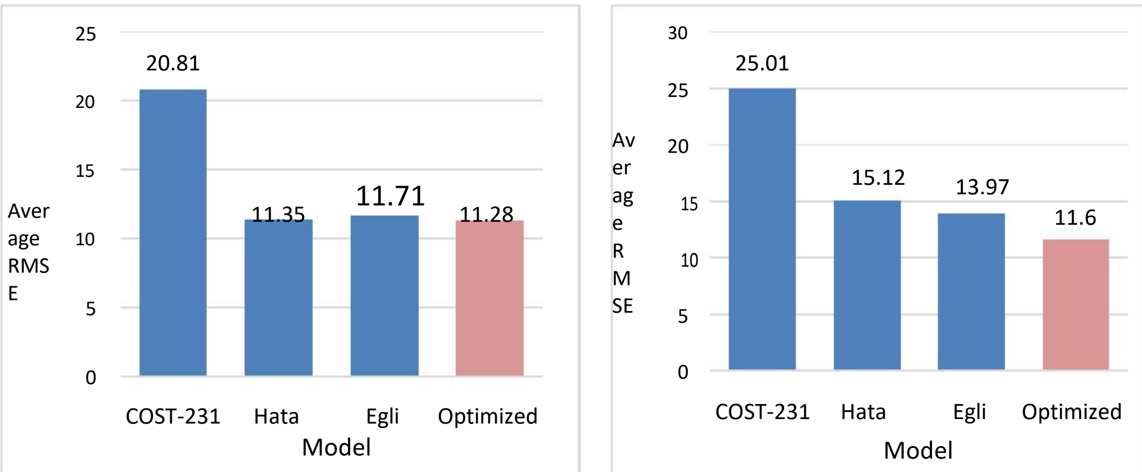


(a) 3G UMTS (b) 2G EDGE

Figure 4.20 Optimal Models Compared with Reference Models for Suburban Area

From Figure 4.20(a), using equation (4.22), the performance of 3G $PL_{opt\text{-}suburban}$ with respect to each of the reference models is calculated as follows:

$$\text{COST-231} = \frac{20.81-11.28}{20.81} \times 100\% = 45.80\% \quad (4.29)$$

$$\text{Hata} = \frac{11.35-11.28}{11.35} \times 100\% = 0.62\% \quad (4.30)$$

$$\text{Egli} = \frac{11.71-11.28}{11.71} \times 100\% = 3.67\% \quad (4.31)$$

From Figure 4.20(b), the 2G optimal model performance for suburban environment is calculated for each reference model as follows:

$$\text{COST-231} = \frac{25.01-11.60}{25.01} \times 100\% = 53.62\% \quad (4.32)$$

$$\text{Hata} = \frac{15.12-11.60}{15.12} \times 100\% = 23.28\% \quad (4.33)$$

$$\text{Egli} = \frac{13.97-11.60}{13.97} \times 100\% = 16.96\% \quad (4.34)$$

### 4.6.3 Rural environment optimal model performance

Figures 4.21(a) and (b) show the comparison between the average RMSEs of the optimal models and the reference models for 3G Network and 2G Network respectively in the suburban environment.

As explained earlier, it can be seen from Figure 4.21(a) that the Hata model, in its original form, gives the optimal path-loss prediction for the 3G network in the rural environment than the adjusted COST-231 model. Therefore, no improvement in performance can be calculated for the optimal Path-loss model at 3G for the rural environment.

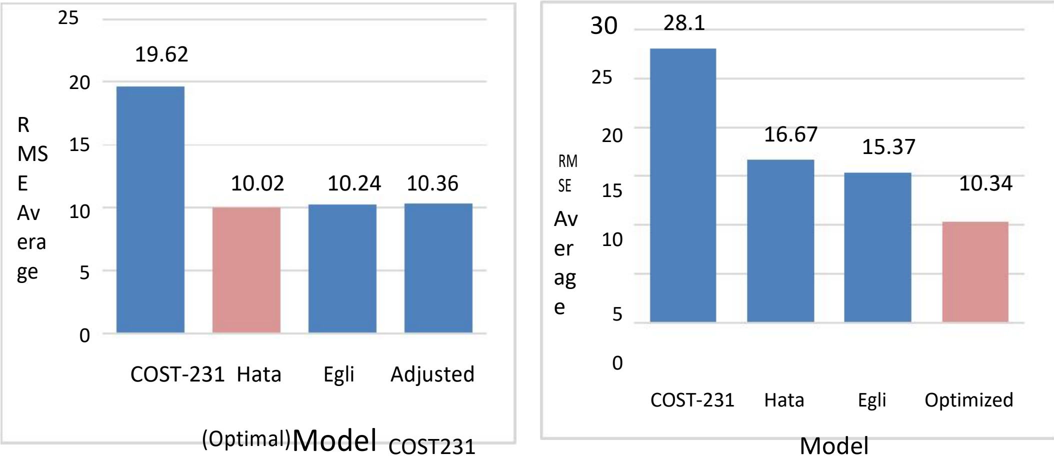


(a) 3G UMTS

(b) 2G EDGE

Figure 4. 21 Optimal Models Compared with Reference Models for Rural Area

From Figure 4.21(b), using equation (4.22), the optimal model performance for 2G in the rural environment is calculated for each reference model as follows:

$$\text{COST-231} = \frac{28.10 - 10.34}{28.10} \times 100\% = 63.20\% \qquad (4.35)$$

$$\text{Hata} = \frac{16.67 - 10.34}{16.67} \times 100\% = 37.97\% \qquad (4.36)$$

$$\text{Egli} = \frac{15.37 - 10.34}{15.37} \times 100\% = 32.73\% \qquad (4.37)$$

### 4.6.4 Performance evaluation summary

The percentage improvement in performance of the new optimal Path-loss prediction models over the reference COST-231, Hata and Egli models for each environment is summarized in Table 4.9.

The percentage improvement in predictability of the optimal models over each of the reference models was determined using equation (4.22). Results show that there are improvements of varying degrees of the optimal models over the reference models.

Table 4.9 Percentage Improvement of the Optimal Models over the Reference Models

| S/N | Environment type | Network type | Improvement over COST-231 model | Improvement over Hata model | Improvement over Egli model |
|---|---|---|---|---|---|
| 1 | **Urban** | 3G | 53.74% | 48.01% | 9.54% |
| 2 | **Urban** | 2G | 47.89% | 25.81% | 12.70% |
| 3 | **Suburban** | 3G | 45.80% | 0.62% | 3.67% |
| 4 | **Suburban** | 2G | 53.62% | 23.28% | 16.96% |
| 5 | **Rural** | 3G | - | - | - |
| 6 | **Rural** | 2G | 63.20% | 37.97% | 32.73% |

## 4.7 Findings

The irregular patterns of the RSSI-distance graphs are evidences of the poor network signal reception in Okene area. The remote part of the Agasa/Upogoro rural environment has no BTS location (see Figure 3.9). Hence, the reception there is extremely poor as they can only receive signals from some kilometers away, coupled with the obstructions from the mountains. Having observed the features of the environments, it is clear that the mountains are the major cause of path-loss in Okene area and consequently the cause of poor signal reception.

Location of some BTSs on top of the mountains did not solve the problem as seen in Okengwe where an MTN BTS was situated at Otutudakene which is some 490m above sea level but poor signal is received some 300m away at 424m above sea level. Booster stations at low altitudes via microwave link will make good signals available to the subscribers. Infrastructure sharing, especially cell towers, are recommended for effective service delivery to obstructed areas.

# 5.0 CONCLUSION AND RECOMMENDATIONS

## 5.1 Conclusion

This aim of this research was to develop path-loss models suitable for path-loss prediction in a mountainous environment with Okene in Kogi State, Nigeria, as a case study. The first step by which the aim was achieved was the use of virtual maze GPS software to obtain geographical location of base stations and measurement points along the drive test routes. Cellmapper and Network Cell Info Lite were used to capture and record the 2G (1800MHz) and 3G (2100MHz) received signal strength (RSS) of 9mobile, Airtel, MTN and Glo networks at the measurement points. The cell identification digit (CID) of each serving network cell was also captured. The geographical location data was used to determine the distance between the transmitting cells and the receiver. The received signal strength was used to calculate the measured path-loss. Five reference models – Free Space, Hata, COST-231, Egli and ECC-33 – were used to calculate the path-loss for the four networks. Graphical comparison of the calculated path-loss and the measured path-loss showed that the ECC-33 model path-loss deviated from the measured path-loss by a very wide margin. This could be because the ECC-33 was originally developed from the Okumura model for frequency range of 3.0GHz to 3.5GHz. The deviation of the path-loss prediction of each of the models from the measured path-loss was determined using the root mean square error (RMSE) regression metrics. The average of the RMSEs of the four networks was determined for each of the reference models and used to modify the models. However, the free space model prediction was found unrealistic while the ECC-33 model prediction deviated too widely for modification. Hence they were dropped out of the modification process. The Egli model showed good performance with the least average RMSE before modification, but the performance dropped after modification.

The COST-231 model was found suitable for modification to obtain the optimal Path-loss models for 3G UMTS (2100MHz) and 2G EDGE (1800MHz) frequencies in the urban and suburban environments. The average RMSE of the optimal models obtained were 9.39dBm for 3G and 12.88dBm for 2G networks in the urban area; and 11.28dBm for 3G and 11.60dBm for 2G networks in the suburban area. However, for 3G network in the rural environment, the original Hata model was found to give the least average RMSE of 10.02dBm among all the models even after modification; while the modified Hata model gives an optimal Path-loss model with an average RMSE of 10.34 for 2G network in the rural area.

The optimal models show various percentages of performance improvement over the reference Hata, COST-231 and Egli models in each of the environments. In the urban environment, the optimal models show percentage improvement of 53.74% at 3G and 47.89% at 2G over the reference COST-231 model. The suburban optimal models improved the path-loss prediction performance by 45.80% for 3G and 53.62% for 2G over the reference COST-231 model. In the rural environment, the performance of the optimal model at 2G is 37.97% over the reference Hata model.

The effect of mountains on RF signal propagation has been explored in this study. Mountainous environments suffer excessive signal path-loss due to shadowing effect. This reflected in the received signal measured on the field. In summary, it can be concluded that the poor signal reception in many parts of Okene in Kogi State of Nigeria is as a result of high path-loss due mainly to the irregular terrain.

## 5.2 Recommendations

The field data used in this work was collected for a period of two months. It is recommended that future research in this area be extended to data collection of, at least, six months to one year in order to obtain more accurate models. It is also recommended that a single path-loss model should be developed for the mountainous area with correction factors for each propagation environment in the area.

# REFERENCES


Abiodun, C. I., Azi, S. O., Ojo, J. S., & Akinyemi, P. (2017). Assessment of Path Loss Prediction Models for Wireless Propagation Channels at L-Band Frequency over Different Micro-Cellular Environments of Ekiti State, Southwestern Nigeria. *World Academy of Science, Engineering and Technology International Journal of Electronics and Communication Engineering, 11*(10), 1103-1109.

Akujobi, E., Nosiri, O., & Uzoechi, L. (2016). Path Loss Characterization of 3G Wireless Signal for Urban and Sub-urban Environments in Port Harcourt City, Nigeria. *International Research Journal of Engineering and Technology (IRJET), 3*(03), 16-32.

Anggraeni, M. E., & Dwiyanti, N. (2018). Performance Analysis of Empirical Path Loss Models for UHF TV Broadcast on Mountainous Area. *2018 International Electronics Symposium on Engineering Technology and Applications (IES-ETA)*, 247-252.

Bakare, B. I., Ekanem, I. A., & Allen, I. O. (2017). Appraisal of Global System for Mobile Communication (GSM) In Nigeria. *American Journal of Engineering Research (AJER), Volume-6,* (Issue-6), pp-97-102.

Cavalcanti, B. J., Cavalcante, G. A., Mendonça, L. M. d., Cantanhede, G. M., de Oliveira, M. M. M., & D'Assunção, A. G. (2017). A Hybrid Path Loss Prediction Model based on Artificial Neural Networks using Empirical Models for LTE and LTE-A at 800 MHz and 2600 MHz. *Journal of Microwaves, Optoelectronics and Electromagnetic Applications, Vol. 16*(No. 3), 708-722.

Dijkstra, L., Poelman, H., & Veneri, P. (2019). The EU-OECD definition of a functional urban area. *OECD Regional Development Working Papers, OECD Publishing, Paris, 2019*(11). doi:https://doi.org/10.1787/d58cb34d-en

Ebhota, V. C., Isabona, J., & Srivastava, V. M. (2018). Modelling Simulation and Analysis of signal path loss for 4G network planning. *Journal of Engineering and Applied Sciences, 13*(7), 1907-1918.

Eichie, J. O., Oyedum, O. D., Ajewole, M. O., & Aibinu, A. M. (2017). Comparative analysis of basic models and artificial neural network based model for path loss prediction. *Progress In Electromagnetics Research, 61*, 133-146.

Elechi, P., & Otasowie, P. O. (2016). Path loss prediction model for GSM fixed wireless access. *European Journal of Engineering Research and Science, EJERS, Vol. 1*(Issue 1), pp 1-4.

Emurotu, J. E., & Habib, L. O. (2019). Assessment of some water quality of Obuburu River, Okene, Kogi State, Nigeria. *Journal of Applied Sciences and Environmental Management, 23*(11), 1995-2002.

Famoriji, J., & Olasoji, Y. (2013). Development of a Radiowave Propagation Model for Hilly Areas. *International Journal of Electronics Communication and Computer Engineering, 4*(2), 536-539.

Hoomod, H. K., Al-Mejibli, I., & Jabboory, A. I. (2018). Analyzing Study of Path loss Propagation Models in Wireless Communications at 0.8 GHz. *Journal of Physics: Conference Series, 1003*(1), pp 1-9. doi:10.1088/1742-6596/1003/1/012028

Ibhaze, A. E., Imoize, A. L., Ajose, S. O., John, S. N., Ndujiuba, C. U., & Idachaba, F. E. (2017). An empirical propagation model for path loss prediction at 2100MHz in a dense urban environment. *Indian Journal of Science and Technology, 10*(5), 1-9.

Imoize, A., & Oseni, A. (2019). Investigation and pathloss modeling of fourth generation long term evolution network along major highways in Lagos Nigeria. *Ife Journal of Science, 21*(1), 39-60.

Isabona, J., Konyeha, C., Chinule, C., & Isaiah, G. (2013). Radio field strength propagation data and pathloss calculation methods in UMTS network. *Advances in Physics Theories and Applications, 21*, 54-68.

Jawad, H. M., Jawad, A. M., Nordin, R., Gharghan, S. K., Abdullah, N. F., Ismail, M., & Abu-AlShaeer, M. J. (2019). Accurate Empirical Path-Loss Model Based on Particle Swarm Optimization for Wireless Sensor Networks in Smart Agriculture. *IEEE Sensors Journal, 20*(1), 552-561. doi:10.1109/JSEN.2019.2940186

Lasisi, H., Adediran, Y. A., & Ayodele, A. A. (2017). Development of Propagation Path Loss Prediction Model for Mobile Communications Network Deployment in Osogbo, Nigeria. *European Journal of Engineering, 2*(11), 13-17.

Lee, C., & Park, S. (2018). Diffraction Loss Prediction of Multiple Edges Using Bullington Method with Neural Network in Mountainous Areas. *International Journal of Antennas and Propagation*, 2018, 2011-2010. doi:https://doi.org/10.1155/2018/8737594

Lin, K. Z., & Maw, M. M. (2018). Empirical Outdoor Propagation Model for Sub-Urban: A Case Study Patheingyi Township in MANDALAY. *Joint International Conference on Science, Technology and Innovation, Mandalay by IEEE, 2*(575.11), 360-364.

Maloku, H., Fazliu, Z. L., Sela, E., & Ibrani, M. (2019). Path Loss Model Fitting for TV Bands based on Experimental Measurements for Urban Environments in Kosovo. *2019 42nd International Convention on Information and Communication Technology, Electronics and Microelectronics (MIPRO)*, 480-485.

Mohamed, I. (2018). Path-Loss Estimation for Wireless Cellular Networks Using Okumura/Hata Model. *Science Journal of Circuits, Systems and Signal Processing, 7*(1), 20-27.

Mollel, M. S., & Kisangiri, M. (2014). An overview of various propagation model for mobile communication. *Proceedings of the 2nd Pan African International Conference on Science, Computing and Telecommunications (PACT 2014), Arusha, Tanzania,*, 148-153.

Musefiu, A., Tonga, A. D., & Jafaru, I. (2017). Determination of Path Loss of GSM Signal in Kazaure Town. *International Journal Of Electrical, Electronics And Data Communication, 5*(5), 24-27.

Okoro, R., & Iwuji, P. (2019). Investigation of GSM Signal Strength in Rural Communities in the South-Eastern Region of Nigeria. *European Scientific Journal, 15*(15), 140 - 152.

Oluwafemi, I. B., Femijemilohun, O. J., Oluwasola, S.-L., & Owolabi, I. E. (2018). Investigation of Error Bounds of Empirical Path Loss Models at UHF Band in Ondo State, Nigeria. *ARPN Journal of Engineering and Applied Sciences, 13*(9), 1-10.

Omorogiuwa, O., & Edeko, F. (2009). Investigation and Modeling of Power Received at 1800 MHz in a Mountainous Terrain: Case Study of Igarra in Edo State, Ajaokuta and Okene in Kogi State, Nigeria. *International Journal of electrical and power engineering, 3*(3), 129-135.

Onuu, M. U., & Usanga, E. M. (2017). Path Loss Prediction for Some GSM Networks for Akwa Ibom State, Nigeria. *Global Journal of Research In Engineering, 17*(2), 27-39.

Orike, S., Elechi, P., & Ekanem, I. A. (2017). Assessment and Modeling of GSM Signal Propagation in Uyo, Nigeria. *European Journal of Engineering Research and Science, 2*(11), 49-58.

Oudira, H., Diouane, L., & Garah, M. (2018). Empirical Path Loss Models Optimization for Mobile Communication. *2018 IEEE 5th International Congress on Information Science and Technology (CIST)*, 443-448.

Popoola, S. I., Adetiba, E., Atayero, A. A., Faruk, N., Calafate, C. T., & Yuen, C. (2018). Optimal Model for Path Loss Predictions using Feed-forward Neural Networks. *Cogent Engineering, 5*(1). doi:10.1080/23311916.2018.1444345

Popoola, S. I., Atayero, A. A., Arausi, O. D., & Matthews, V. O. (2018). Path Loss Dataset for Modeling Radio Wave Propagation in Smart Campus Environment. *Data in Brief 17 (2018) 1062–1073, 17*, 1062-1073.

Popoola, S. I., Atayero, A. A., Faruk, N., Calafate, C. T., Olawoyin, L. A., & Matthews, V. O. (2017). Standard Propagation Model Tuning for Path Loss Predictions in Built-Up Environments. *International Conference on Computational Science and Its Applications*, 363-375.

Popoola, S. I., Atayero, A. A., & Popoola, O. A. J. D. i. b. (2018). Comparative Assessment of Data obtained using Empirical Models for Path loss Predictions in a University Campus Environment. *Data in brief, 18*, 380-393. doi:org/10.1016/j.dib.2018.03.040

Rahul, R., Bansal, B., & Kapoor, R. (2019). Performance Analysis of Empirical Radio Propagation Models in Wireless Cellular Networks. *World Scientific News, 121*, 40-46.

Rappaport, T. S. (2005). *Wireless Communications: Principles and Practice* (Vol. 2): Prentice Hall PTR , New Jersey.

Shoewu, O., Salau, N., Ogunlewe, A., & Oborkhale, L. (2016). Path Loss Measurement and Modeling for Lagos State G.S.M Environments. *Review of Computer Engineering Research, 3*(4), 69-81. doi:10.18488/journal.76/2016.3.4/76.4.69.81

Surajudeen-Bakinde, N. T., Faruk, N., Popoola, S. I., Salman, M. A., Oloyede, A. A., Olawoyin, L. A., & Calafate, C. T. (2018). Path loss predictions for multi-transmitter radio propagation in VHF bands using Adaptive Neuro-Fuzzy Inference System. *International Journal of Engineering Science Technology,, 21*(4), 679-691.

Tarkaa, N. S., Agbo, V. A., & Oglegba, S. O. (2017). Radio Propagation Path-loss Analysis for an Operative GSM Network. *The International Journal of Engineering and Science (IJES), 6*(9), 53-67.

Tonga, D. A., Umar, S., & Uhaiburo, J. (2019). Path Loss Propagation Model Prediction for GSM Mobile Networks in Nigeria. *International Journal of Latest Engineering Science (IJLES), 2*(6), 40-46.

Wang, W., Jost, T., & Raulefs, R. (2017). A Semi-Deterministic Path Loss Model for In-Harbor LoS and NLoS Environment. *IEEE Transactions on Antennas and Propagation, 65*(12), 7399-7404.

Worgu, S., Ajumo, S. G., & Odu, N. N. (2017). Comparative Evaluation of the Pathloss Prediction Performance Hata-Okumura Pathloss Model for Urban, Suburban and Rural Areas. *International Journal of Systems Science and Applied Mathematics, 2*(1), 42-50.

Zreikat, A., & Dordevic, M. (2017). Performance Analysis of Path loss Prediction Models in Wireless Mobile Networks in Different Propagation Environments. *Proceedings of the 3rd World Congress on Electrical Engineering and Computer Systems and Science*. doi:10.11159/vmw17.103

# APPENDICES

## APPENDIX A

Table I: Received Signal Strength Measurement Locations in Okene Urban area

| S/N | Receiver Location Address | Latitude | Longitude | Altitude (m) |
|---|---|---|---|---|
| **1** | Open field, Lagos rd, Okene | 7.551721 | 6.224818 | 395 |
| **2** | Saw Mill, Okene | 7.552367 | 6.227635 | 393 |
| **3** | PHCN Business Office, Okene | 7.554391 | 6.228554 | 383 |
| **4** | New Mr Biggs, Okene | 7.556571 | 6.229579 | 378 |
| **5** | Isah Abdullahi Estate, Lafia Street | 7.556675 | 6.231043 | 381 |
| **6** | First Bank, Lafia Street | 7.554945 | 6.232487 | 393 |
| **7** | YAS Photos, Lafia Street | 7.553012 | 6.234323 | 405 |
| **8** | LG Treasury Department, Lafia Street | 7.550554 | 6.236468 | 410 |
| **9** | Post Office, Okene | 7.550528 | 6.237347 | 415 |
| **10** | Unity Bank, Itakpe Road, Okene | 7.552211 | 6.238272 | 410 |
| **11** | General Hospital, Okene | 7.554918 | 6.238775 | 418 |
| **12** | MANR Zonal Office, Govt House Road, Okene | 7.556987 | 6.237576 | 413 |
| **13** | Solardad College, Okene | 7.559026 | 6.232717 | 411 |
| **14** | UBA Bank, Govt House Road, Okene | 7.557936 | 6.230324 | 398 |
| **15** | Iruvucheba Road junction, Round-about | 7.551385 | 6.224698 | 396 |
| **16** | Ali Omeiza Clinic Junction, Iruvucheba, Okene | 7.550411 | 6.228062 | 410 |
| **17** | Former Microfinance Bank, Iruvucheba | 7.550048 | 6.230461 | 415 |
| **18** | Ozuwaya junction, Iruvucheba | 7.550079 | 6.232875 | 410 |
| **19** | Idozumi round-about, | 7.550257 | 6.234185 | 412 |
| **20** | Idozumi junction, Lafia Street | 7.551996 | 6.235119 | 396 |
| **21** | Mosque, Ozuwaya Street | 7.550429 | 6.232738 | 409 |
| **22** | Beside GLO BTS, Ozuwaya Street | 7.552657 | 6.230406 | 390 |
| **23** | Kekere Hotel, Ozuwaya Street, Okene | 7.554518 | 6.229177 | 386 |

# APPENDIX B

Table II: Received Signal Strength Measurement Locations in Okengwe Suburban area

| S/N | Receiver Location Address | Latitude | Longitude | Altitude(m) |
|---|---|---|---|---|
| **1** | By Adeoye junction, Ozuma-Ageva Rd | 7.542867 | 6.187792 | 437 |
| **2** | Ageva Junction, Ozuma | 7.544827 | 6.186826 | 434 |
| **3** | Asuwe Lodge, Ozuma | 7.545956 | 6.188762 | 424 |
| **4** | Asuwe Shopping Complex, Ozuma | 7.547611 | 6.189833 | 427 |
| **5** | Ozuma junction, Ihima-Adavi Road, Okengwe | 7.548405 | 6.190104 | 432 |
| **6** | Sharp Image Photo studio, Okengwe | 7.549561 | 6.192547 | 437 |
| **7** | Charity Hospital junction, Okengwe | 7.550141 | 6.194433 | 440 |
| **8** | St Paul's Shopping Complex, Okengwe | 7.549656 | 6.197635 | 448 |
| **9** | Central Mosque, Okengwe | 7.548299 | 6.200412 | 444 |
| **10** | Ayede Cinema, Obehira | 7.547066 | 6.200876 | 445 |
| **11** | Chairman Junction, Obehira | 7.544084 | 6.199414 | 449 |
| **12** | Ohugeri market, Obehira | 7.540362 | 6.198333 | 461 |
| **13** | Otutu-Idakene, Obehira | 7.537723 | 6.194337 | 484 |
| **14** | Ogori junction, Obehira-Ageva | 7.533827 | 6.190677 | 447 |
| **15** | By Glo BTS, Ageva-Ozuma Road | 7.536134 | 6.189853 | 453 |
| **16** | Inozi junction, Ageva-Ozuma Road | 7.539188 | 6.189022 | 443 |
| **17** | By former LMC Principal's house, Ageva Ozuma Rd | 7.540279 | 6.188724 | 440 |
| **18** | Makaranta-Ohuda junction, Obehira | 7.544406 | 6.198719 | 464 |
| **19** | General Hospital Junction, Ohuda road | 7.546716 | 6.197761 | 451 |
| **20** | Atuna Arts, Ohuda-Obehira Road, Okengwe | 7.548062 | 6.197057 | 446 |
| **21** | Utohuda, Obehira Junction, Okengwe | 7.549841 | 6.196373 | 451 |
| **22** | Makaranta Junction, Alh Saka place, Okengwe | 7.548737 | 6.192173 | 437 |
| **23** | Utabo, Makaranta Road, Okengwe | 7.547117 | 6.193996 | 440 |
| **24** | Eikoku Junction, Makaranta Road, Okengwe | 7.545753 | 6.195656 | 442 |
| **25** | I.N.A Primary School, Okengwe | 7.544985 | 6.197298 | 455 |
| **26** | Ogembe family house, Eikoku, Okengwe | 7.545636 | 6.194919 | 452 |
| **27** | C.A.C. No.2, Eikoku, Okengwe | 7.545651 | 6.193057 | 448 |
| **28** | Eikoku Primary School, Okengwe | 7.545788 | 6.190551 | 444 |

## APPENDIX C

Table III: Received Signal Strength Measurement Locations in Agasa/Upogoro rural area

| S/N | Receiver Location Address | Latitude | Longitude | Altitude (m) |
|---|---|---|---|---|
| 1 | Iruvochinomi/Ege Junction, Agasa | 7.551954 | 6.222969 | 400 |
| 2 | BIGR Filling Station, Agasa | 7.551419 | 6.219609 | 396 |
| 3 | Deeper Life Church, Agasa junction | 7.550385 | 6.218135 | 386 |
| 4 | PHCN Substation area, by MTN BTS, Agasa | 7.548399 | 6.217714 | 401 |
| 5 | Greater Tomorrow Nursery/Primary School, Agasa | 7.546059 | 6.218313 | 408 |
| 6 | Oro junction, Agasa | 7.544757 | 6.218743 | 412 |
| 7 | Last Bend before Upogoro road | 7.543635 | 6.220399 | 404 |
| 8 | Oro junction, Upogoro road, Agasa | 7.543365 | 6.223201 | 403 |
| 9 | Gospel Assembly Church, Agasa | 7.543936 | 6.223573 | 412 |
| 10 | Talabi Medical Centre, Agasa | 7.546632 | 6.223678 | 424 |
| 11 | Okeneba junction, Agasa | 7.548411 | 6.223852 | 428 |
| 12 | Agasa junction round about | 7.551042 | 6.223817 | 404 |
| 13 | By Distribution Transformer, Agasa | 7.542063 | 6.223326 | 401 |
| 14 | Agasa-uvete | 7.538646 | 6.223928 | 397 |
| 15 | Agasa Cemetry | 7.536604 | 6.224388 | 388 |
| 16 | Govt Day Sec School, Anyava, Agasa | 7.533754 | 6.227831 | 373 |
| 17 | Agasa-Upogoro border | 7.530803 | 6.231032 | 366 |
| 18 | Catholic Church, Upogoro | 7.528599 | 6.232655 | 370 |
| 19 | Upogoro Mosque | 7.527132 | 6.233956 | 385 |
| 20 | Royal Highness Palace, Upogoro | 7.525023 | 6.235548 | 393 |
| 21 | Water tank, Upogoro | 7.523178 | 6.237525 | 405 |
| 22 | Upogoro New settlement entry | 7.520044 | 6.242725 | 354 |
| 23 | Bottom of hill, Upogoro new settlement | 7.518737 | 6.245609 | 338 |
| 24 | Level 1, Upogoro New layout | 7.517835 | 6.247945 | 330 |
| 25 | Bend, New layout, Upogoro | 7.515837 | 6.249351 | 324 |
| 26 | High Tension Crossing, New layout, Upogoro | 7.513991 | 6.250972 | 316 |
| 27 | Far end Upogoro New layout | 7.511463 | 6.252941 | 313 |

APPENDIX D

Table IV: 9mobile 3G UMTS Measured and Predicted Path Loss for Okene Central Urban Area

| S/N | d (km) | RSSI (dBm) | $PL_m$ (dBm) | $PL_{fspl}$ (dBm) | $PL_{cost231}$ (dBm) | $PL_{hata}$ (dBm) | $PL_{egli}$ (dBm) | $PL_{ecc33}$ (dBm) |
|---|---|---|---|---|---|---|---|---|
| **1** | 0.1097 | -57.4 | 100.4 | 79.9 | 104.9 | 102.4 | 83.1 | 158.5 |
| **2** | 0.1939 | -53 | 96 | 84.8 | 113.6 | 111.1 | 93 | 187.4 |
| **3** | 0.2116 | -57.4 | 100.4 | 85.6 | 115 | 112.4 | 94.5 | 192.1 |
| **4** | 0.3328 | -63.8 | 106.8 | 89.5 | 121.9 | 119.3 | 102.4 | 217.9 |
| **5** | 0.376 | -57.8 | 100.8 | 90.6 | 123.8 | 121.2 | 104.5 | 225.3 |
| **6** | 0.4612 | -65.8 | 108.8 | 92.3 | 126.9 | 124.3 | 108 | 237.9 |
| **7** | 0.4774 | -71.8 | 114.8 | 92.7 | 127.5 | 124.9 | 108.6 | 240 |
| **8** | 0.5804 | -65.4 | 108.4 | 94.3 | 130.4 | 127.8 | 112 | 252.6 |
| **9** | 0.6392 | -68.2 | 111.2 | 95.2 | 131.9 | 129.3 | 113.7 | 258.9 |
| **10** | 0.6817 | -71.8 | 114.8 | 95.7 | 132.9 | 130.3 | 114.8 | 263.2 |
| **11** | 0.7108 | -65.4 | 108.4 | 96.1 | 133.5 | 131 | 115.6 | 266 |
| **12** | 0.7731 | -67.8 | 110.8 | 96.8 | 134.8 | 132.3 | 117 | 271.7 |
| **13** | 0.8697 | -73.8 | 116.8 | 97.9 | 136.6 | 134.1 | 119.1 | 279.8 |
| **14** | 0.927 | -71.6 | 114.6 | 98.4 | 137.6 | 135 | 120.2 | 284.2 |
| **15** | 0.9294 | -73.8 | 116.8 | 98.4 | 137.6 | 135.1 | 120.2 | 284.4 |
| **16** | 0.9306 | -79.8 | 120.8 | 98.5 | 137.7 | 135.1 | 120.2 | 284.5 |
| **17** | 0.9338 | -77 | 120 | 98.5 | 137.7 | 135.1 | 120.3 | 284.8 |
| **18** | 0.9871 | -73.6 | 116.6 | 99 | 138.6 | 136 | 121.3 | 288.7 |
| **19** | 1.1383 | -70.6 | 113.6 | 100.2 | 140.8 | 138.2 | 123.7 | 298.9 |
| **20** | 1.1557 | -67.2 | 110.2 | 100.3 | 141 | 138.4 | 124 | 299.9 |
| **21** | 1.3271 | -75.8 | 118.8 | 101.5 | 143.1 | 140.5 | 126.4 | 310.1 |
| **22** | 1.4119 | -78.8 | 121.8 | 102.1 | 144 | 141.5 | 127.5 | 314.7 |
| **23** | 1.5468 | -76.8 | 119.8 | 102.9 | 145.4 | 142.9 | 129.1 | 321.5 |
| | | | **RMSE =** | **16.91** | **20.95** | **18.49** | **6.80** | **154.29** |

APPENDIX E

Table V: MTN 2G EDGE Measured and Predicted Path Loss for Okene Central Urban Area

| S/N | d (km) | RSSI (dBm) | $PL_m$ (dBm) | $PL_{fspl}$ (dBm) | $PL_{cost231}$ (dBm) | $PL_{hata}$ (dBm) | $PL_{egli}$ (dBm) | $PL_{ecc33}$ (dBm) |
|---|---|---|---|---|---|---|---|---|
| **1** | 0.0399 | -51 | 91 | 69.8 | 87.1 | 73.1 | 63.7 | 114.6 |
| **2** | 0.1028 | -65.8 | 105.8 | 78 | 101.5 | 87.5 | 80.1 | 153.5 |
| **3** | 0.139 | -69 | 109 | 80.6 | 106.1 | 92.1 | 85.3 | 167.9 |
| **4** | 0.1398 | -68.2 | 108.2 | 80.7 | 106.2 | 92.1 | 85.4 | 168.1 |
| **5** | 0.1956 | -59.8 | 99.8 | 83.6 | 111.3 | 97.3 | 91.3 | 185.2 |
| **6** | 0.1968 | -51 | 91 | 83.6 | 111.4 | 97.4 | 91.4 | 185.5 |
| **7** | 0.2356 | -51 | 91 | 85.2 | 114.1 | 100.1 | 94.5 | 195.1 |
| **8** | 0.237 | -56.2 | 96.2 | 85.3 | 114.2 | 100.2 | 94.6 | 195.4 |
| **9** | 0.3551 | -66.6 | 106.6 | 88.8 | 120.4 | 106.3 | 101.6 | 218.2 |
| **10** | 0.3732 | -51.4 | 91.4 | 89.2 | 121.1 | 107.1 | 102.5 | 221.2 |
| **11** | 0.3995 | -69.8 | 109.8 | 89.8 | 122.2 | 108.1 | 103.7 | 225.2 |
| **12** | 0.4204 | -51 | 91 | 90.2 | 123 | 108.9 | 104.6 | 228.3 |
| **13** | 0.5049 | -51.8 | 91.8 | 91.8 | 125.7 | 111.7 | 107.7 | 239.4 |
| **14** | 0.5124 | -58.6 | 98.6 | 92 | 126 | 111.9 | 108 | 240.4 |
| **15** | 0.5136 | -59 | 99 | 92 | 126 | 112 | 108 | 240.5 |
| **16** | 0.5955 | -66.8 | 106.8 | 93.3 | 128.3 | 114.2 | 110.6 | 249.8 |
| **17** | 0.6136 | -63.8 | 103.8 | 93.5 | 128.7 | 114.7 | 111.1 | 251.7 |
| **18** | 0.6457 | -75.8 | 115.8 | 94 | 129.5 | 115.4 | 112 | 255 |
| **19** | 0.755 | -70.6 | 110.6 | 95.3 | 131.9 | 117.8 | 114.7 | 265.2 |
| **20** | 0.8458 | -72.2 | 112.2 | 96.3 | 133.6 | 119.5 | 116.7 | 272.8 |
| **21** | 1.0075 | -71.8 | 111.8 | 97.8 | 136.3 | 122.2 | 119.8 | 284.7 |
| **22** | 1.0102 | -73.4 | 113.4 | 97.9 | 136.3 | 122.3 | 119.8 | 284.9 |
| **23** | 1.012 | -73.2 | 113.2 | 97.9 | 136.3 | 122.3 | 119.8 | 285 |
| | | | **RMSE =** | **16.14** | **21.03** | **11.81** | **12.57** | **126.90** |

APPENDIX F

Table VI: Glo 3G UMTS Measured and Predicted Path Loss for Okengwe Suburban Area

| S/N | d (km) | RSSI (dBm) | $PL_m$ (dBm) | $PL_{fspl}$ (dBm) | $PL_{cost231}$ (dBm) | $PL_{hata}$ (dBm) | $PL_{egli}$ (dBm) | $PL_{ecc33}$ (dBm) |
|---|---|---|---|---|---|---|---|---|
| **1** | 0.0143 | -51 | 94 | 62.1 | 73.7 | 58.7 | 47.6 | 82.8 |
| **2** | 0.0777 | -51 | 94 | 76.8 | 99.6 | 84.6 | 77 | 142.6 |
| **3** | 0.1178 | -53.8 | 96.8 | 80.4 | 105.9 | 90.9 | 84.3 | 161.9 |
| **4** | 0.137 | -62.2 | 105.2 | 81.8 | 108.3 | 93.2 | 86.9 | 169.3 |
| **5** | 0.2712 | -67.8 | 110.8 | 87.7 | 118.7 | 103.7 | 98.8 | 206 |
| **6** | 0.3355 | -51 | 94 | 89.5 | 122 | 106.9 | 102.5 | 218.4 |
| **7** | 0.3651 | -61.8 | 104.8 | 90.3 | 123.3 | 108.2 | 103.9 | 223.5 |
| **8** | 0.3733 | -51 | 94 | 90.5 | 123.6 | 108.6 | 104.3 | 224.8 |
| **9** | 0.3993 | -66.6 | 109.6 | 91 | 124.6 | 109.6 | 105.5 | 228.9 |
| **10** | 0.4067 | -59.8 | 102.8 | 91.2 | 124.9 | 109.9 | 105.8 | 230 |
| **11** | 0.4199 | -65.8 | 108.8 | 91.5 | 125.4 | 110.4 | 106.4 | 232 |
| **12** | 0.4287 | -55 | 98 | 91.7 | 125.7 | 110.7 | 106.7 | 233.3 |
| **13** | 0.4303 | -69.8 | 112.8 | 91.7 | 125.8 | 110.8 | 106.8 | 233.5 |
| **14** | 0.4823 | -51.8 | 94.8 | 92.7 | 127.5 | 112.5 | 108.8 | 240.7 |
| **15** | 0.489 | -53.8 | 96.8 | 92.8 | 127.7 | 112.7 | 109 | 241.6 |
| **16** | 0.5151 | -65.8 | 108.8 | 93.3 | 128.5 | 113.5 | 109.9 | 244.9 |
| **17** | 0.5179 | -65.8 | 108.8 | 93.3 | 128.6 | 113.6 | 110 | 245.2 |
| **18** | 0.5414 | -80.8 | 123.8 | 93.7 | 129.3 | 114.3 | 110.8 | 248.1 |
| **19** | 0.6075 | -51 | 94 | 94.7 | 131 | 116 | 112.8 | 255.6 |
| **20** | 0.6173 | -63 | 106 | 94.8 | 131.3 | 116.3 | 113.1 | 256.6 |
| **21** | 0.6946 | -51 | 94 | 95.9 | 133.1 | 118.1 | 115.1 | 264.4 |
| **22** | 0.7867 | -73.8 | 116.8 | 96.9 | 135 | 120 | 117.3 | 272.9 |
| **23** | 0.8416 | -56.2 | 99.2 | 97.5 | 136 | 121 | 118.4 | 277.5 |
| **24** | 0.8498 | -68.8 | 111.8 | 97.6 | 136.2 | 121.2 | 118.6 | 278.2 |
| **25** | 0.8589 | -65.8 | 108.8 | 97.7 | 136.3 | 121.3 | 118.8 | 278.9 |
| **26** | 0.917 | -73.2 | 116.2 | 98.3 | 137.3 | 122.3 | 119.9 | 283.5 |
| **27** | 0.9288 | -65.8 | 108.8 | 98.4 | 137.5 | 122.5 | 120.1 | 284.4 |
| **28** | 1.1788 | -99.8 | 142.8 | 100.4 | 141.2 | 126.2 | 124.3 | 301.4 |
| | | | **RMSE =** | **17.58** | **23.30** | **13.73** | **14.35** | **135.55** |

APPENDIX G

Table VII: Airtel 2G EDGE Measured and Predicted Path Loss for Okengwe Suburban Area

| S/N | d (km) | RSSI (dBm) | $PL_m$ (dBm) | $PL_{fspl}$ (dBm) | $PL_{cost231}$ (dBm) | $PL_{hata}$ (dBm) | $PL_{egli}$ (dBm) | $PL_{ecc33}$ (dBm) |
|---|---|---|---|---|---|---|---|---|
| **1** | 0.1525 | -55.8 | 95.8 | 75.8 | 97.9 | 88 | 81.3 | 173.6 |
| **2** | 0.1993 | -60.2 | 100.2 | 78.1 | 102 | 92.1 | 85.9 | 187.3 |
| **3** | 0.3235 | -51.8 | 93.8 | 82.3 | 109.4 | 99.4 | 94.3 | 214 |
| **4** | 0.3242 | -51.8 | 91.8 | 82.3 | 109.4 | 99.5 | 94.4 | 214.1 |
| **5** | 0.3394 | -53.4 | 93.4 | 82.7 | 110.1 | 100.1 | 95.2 | 216.8 |
| **6** | 0.3644 | -54.2 | 94.2 | 83.3 | 111.2 | 101.2 | 96.4 | 220.9 |
| **7** | 0.3664 | -59 | 99 | 83.4 | 111.2 | 101.3 | 96.5 | 221.3 |
| **8** | 0.4452 | -57.8 | 95.8 | 85.1 | 114.2 | 104.3 | 99.9 | 232.9 |
| **9** | 0.4642 | -52.6 | 92.6 | 85.4 | 114.8 | 104.9 | 100.6 | 235.5 |
| **10** | 0.4806 | -55 | 95 | 85.7 | 115.4 | 105.4 | 101.2 | 237.6 |
| **11** | 0.5485 | -51 | 91 | 86.9 | 117.4 | 107.5 | 103.5 | 245.8 |
| **12** | 0.7079 | -62.4 | 107.4 | 89.1 | 121.3 | 111.3 | 107.9 | 262.2 |
| **13** | 0.7295 | -60.2 | 100.2 | 89.3 | 121.7 | 111.8 | 108.5 | 264.1 |
| **14** | 0.8891 | -55.8 | 95.8 | 91.1 | 124.7 | 114.8 | 111.9 | 277.3 |
| **15** | 0.9711 | -59 | 99 | 91.8 | 126.1 | 116.1 | 113.4 | 283.3 |
| **16** | 1.2157 | -51.4 | 91.4 | 93.8 | 129.5 | 119.6 | 117.3 | 299 |
| **17** | 1.385 | -56.2 | 96.2 | 94.9 | 131.5 | 121.6 | 119.6 | 308.3 |
| **18** | 1.4379 | -53.4 | 93.4 | 95.2 | 132.1 | 122.1 | 120.2 | 311.1 |
| **19** | 1.4723 | -53.8 | 93.8 | 95.4 | 132.4 | 122.5 | 120.7 | 312.8 |
| **20** | 1.4807 | -51.8 | 91.8 | 95.5 | 132.5 | 122.6 | 120.8 | 313.2 |
| **21** | 1.5357 | -52.2 | 92.2 | 95.8 | 133.1 | 123.1 | 121.4 | 315.9 |
| **22** | 1.5558 | -59 | 99 | 95.9 | 133.3 | 123.3 | 121.6 | 316.8 |
| **23** | 4.4919 | -66.2 | 106.2 | 105.2 | 149.4 | 139.5 | 140.1 | 400.3 |
| **24** | 4.538 | -74.2 | 114.2 | 105.2 | 149.5 | 139.6 | 140.2 | 401.1 |
| **25** | 4.6814 | -70.6 | 110.6 | 105.5 | 150 | 140.1 | 140.8 | 403.8 |
| **26** | 4.8659 | -65 | 105 | 105.8 | 150.6 | 140.7 | 141.4 | 407 |
| **27** | 5.3602 | -69 | 109 | 106.7 | 152.1 | 142.2 | 143.1 | 415.3 |
| **28** | 5.8641 | -73.8 | 113.8 | 107.5 | 153.5 | 143.5 | 144.7 | 423.1 |
| | | | **RMSE =** | **9.61** | **30.36** | **21.70** | **20.95** | **203.18** |

APPENDIX H

Table VIII: MTN 3G UMTS Measured and Predicted Path Loss for Agasa/Upogoro Rural Area

| S/N | d (km) | RSSI (dBm) | $PL_m$ (dBm) | $PL_{fspl}$ (dBm) | $PL_{cost231}$ (dBm) | $PL_{hata}$ (dBm) | $PL_{egli}$ (dBm) | $PL_{ecc33}$ (dBm) |
|---|---|---|---|---|---|---|---|---|
| **1** | 0.1278 | -51.8 | 94.8 | 81.1 | 107.1 | 92.1 | 85.7 | 165.9 |
| **2** | 0.2749 | -53.8 | 96.8 | 87.8 | 118.8 | 103.9 | 99 | 206.8 |
| **3** | 0.3353 | -57.8 | 100.8 | 89.5 | 121.9 | 106.9 | 102.4 | 218.4 |
| **4** | 0.5794 | -57.8 | 100.8 | 94.3 | 130.3 | 115.3 | 111.9 | 252.5 |
| **5** | 0.5871 | -57.6 | 100.6 | 94.4 | 130.5 | 115.5 | 112.2 | 253.3 |
| **6** | 0.593 | -56.6 | 99.6 | 94.5 | 130.6 | 115.6 | 112.3 | 254 |
| **7** | 0.6572 | -51.4 | 94.4 | 95.4 | 132.2 | 117.2 | 114.1 | 260.8 |
| **8** | 0.6999 | -61 | 104 | 95.9 | 133.2 | 118.2 | 115.2 | 265 |
| **9** | 0.7092 | -65.4 | 108.4 | 96 | 133.4 | 118.4 | 115.4 | 265.8 |
| **10** | 0.8843 | -65.6 | 108.6 | 97.9 | 136.7 | 121.8 | 119.3 | 280.9 |
| **11** | 0.9626 | -75.4 | 118.4 | 98.7 | 138 | 123 | 120.7 | 286.9 |
| **12** | 1.0374 | -89.8 | 132.8 | 99.3 | 139.2 | 124.2 | 122 | 292.2 |
| **13** | 1.0877 | -96.2 | 139.2 | 99.7 | 139.9 | 124.9 | 122.9 | 295.6 |
| **14** | 1.121 | -102.6 | 145.6 | 100 | 140.4 | 125.4 | 123.4 | 297.7 |
| **15** | 1.1511 | -100.6 | 143.6 | 100.2 | 140.8 | 125.8 | 123.9 | 299.7 |
| **16** | 1.1684 | -96.8 | 139.8 | 100.3 | 141 | 126 | 124.1 | 300.7 |
| **17** | 1.2389 | -79.4 | 122.4 | 100.8 | 141.9 | 126.9 | 125.1 | 305 |
| **18** | 1.2749 | -78.6 | 121.6 | 101.1 | 142.3 | 127.3 | 125.6 | 307.1 |
| **19** | 1.5314 | -95.8 | 138.8 | 102.7 | 145.2 | 130.2 | 128.8 | 320.7 |
| **20** | 1.8421 | -99.4 | 142.4 | 104.3 | 148 | 133 | 132 | 334.8 |
| **21** | 2.0549 | -80.2 | 123.2 | 105.2 | 149.6 | 134.6 | 133.9 | 343.3 |
| **22** | 2.1166 | -82.6 | 125.6 | 105.5 | 150.1 | 135.1 | 134.4 | 345.7 |
| **23** | 2.238 | -92.2 | 135.2 | 106 | 151 | 136 | 135.4 | 350.1 |
| **24** | 2.6017 | -97.4 | 140.4 | 107.3 | 153.2 | 138.2 | 138 | 362.1 |
| **25** | 4.2301 | -64.2 | 107.2 | 111.5 | 160.7 | 145.7 | 146.4 | 402.7 |
| **26** | 4.7788 | -76.6 | 119.6 | 112.6 | 162.5 | 147.5 | 148.6 | 413.2 |
| **27** | 6.1828 | -96.2 | 139.2 | 114.8 | 166.5 | 151.5 | 153.1 | 436.1 |
| | | | **RMSE =** | **24.65** | **24.35** | **14.72** | **14.53** | **187.84** |

APPENDIX I

Table IX: 9mobile 2G EDGE Measured and Predicted Path Loss for Agasa/Upogoro Rural Area

| S/N | d (km) | RSSI (dBm) | $PL_m$ (dBm) | $PL_{fspl}$ (dBm) | $PL_{cost231}$ (dBm) | $PL_{hata}$ (dBm) | $PL_{egli}$ (dBm) | $PL_{ecc33}$ (dBm) |
|---|---|---|---|---|---|---|---|---|
| **1** | 0.1997 | -51 | 91 | 83.9 | 111.9 | 97.7 | 91.8 | 186.3 |
| **2** | 0.3326 | -51.8 | 91.8 | 88.3 | 119.6 | 105.5 | 100.6 | 214.4 |
| **3** | 0.4474 | -59 | 99 | 90.9 | 124.2 | 110 | 105.8 | 232 |
| **4** | 0.5623 | -55.8 | 95.8 | 92.9 | 127.6 | 113.5 | 109.8 | 246.2 |
| **5** | 0.5936 | -55.4 | 95.4 | 93.4 | 128.5 | 114.3 | 110.7 | 249.6 |
| **6** | 0.61 | -54.6 | 94.6 | 93.6 | 128.9 | 114.7 | 111.2 | 251.3 |
| **7** | 0.7304 | -61.4 | 101.4 | 95.2 | 131.6 | 117.4 | 114.3 | 263 |
| **8** | 0.8088 | -57 | 97 | 96.1 | 133.2 | 119 | 116.1 | 269.8 |
| **9** | 0.8128 | -57 | 97 | 96.1 | 133.2 | 119.1 | 116.2 | 270.1 |
| **10** | 0.8677 | -53.4 | 93.4 | 96.7 | 134.2 | 120.1 | 117.3 | 274.5 |
| **11** | 0.9424 | -70.2 | 110.2 | 97.4 | 135.5 | 121.3 | 118.7 | 280.1 |
| **12** | 0.9477 | -70.2 | 110.2 | 97.4 | 135.6 | 121.4 | 118.8 | 280.5 |
| **13** | 1.1233 | -60.6 | 100.6 | 98.9 | 138.2 | 124 | 121.8 | 292.2 |
| **14** | 1.176 | -65.8 | 105.8 | 99.3 | 138.9 | 124.7 | 122.6 | 295.5 |
| **15** | 1.2369 | -61.4 | 101.4 | 99.8 | 139.6 | 125.5 | 123.5 | 299 |
| **16** | 1.491 | -51.4 | 91.4 | 101.4 | 142.5 | 128.3 | 126.7 | 312.5 |
| **17** | 1.9381 | -56.2 | 96.2 | 103.7 | 146.5 | 132.3 | 131.3 | 332 |
| **18** | 1.9728 | -56.2 | 96.2 | 103.8 | 146.7 | 132.6 | 131.6 | 333.3 |
| **19** | 2.2721 | -72.2 | 112.2 | 105 | 148.9 | 134.7 | 134 | 344.1 |
| **20** | 2.7794 | -70.2 | 110.2 | 106.8 | 152 | 137.8 | 137.5 | 359.9 |
| **21** | 2.9737 | -89 | 129 | 107.4 | 153 | 138.8 | 138.7 | 365.3 |
| **22** | 3.0784 | -81 | 121 | 107.7 | 153.5 | 139.3 | 139.3 | 368 |
| **23** | 3.2454 | -93 | 133 | 108.1 | 154.3 | 140.1 | 140.2 | 372.3 |
| **24** | 3.7313 | -90.2 | 130.2 | 109.3 | 156.4 | 142.3 | 142.6 | 383.7 |
| **25** | 4.0000 | -87.8 | 127.8 | 109.9 | 157.5 | 143.3 | 143.8 | 389.4 |
| **26** | 4.3238 | -91.8 | 131.8 | 110.6 | 158.7 | 144.5 | 145.2 | 395.9 |
| **27** | 4.3537 | -92 | 132 | 110.7 | 158.8 | 144.6 | 145.3 | 396.5 |
| | | | **RMSE =** | **11.82** | **34.14** | **20.68** | **19.12** | **204.07** |